UNIVERSIDADE FEDERAL DE PERNAMBUCO

CENTRO DE CIÊNCIAS BIOLÓGICAS

REDE NORDESTE DE BIOTECNOLOGIA - RENORBIO

Tese de Doutorado

CONTRIBUIÇÃO DE NANOMATERIAIS NO DESENVOLVIMENTO DE BIOSSENSORES PARA DIAGNÓSTICO DA INFECÇÃO AGUDA DO DENGUE

MIZIA MARIA SABOIA DA SILVA

Recife-PE

2014

MIZIA MARIA SABOIA DA SILVA

CONTRIBUIÇÃO DE NANOMATERIAIS NO DESENVOLVIMENTO DE BIOSSENSORES PARA DIAGNÓSTICO DA INFECÇÃO AGUDA DO DENGUE

Tese apresentada ao Programa de Pós-Graduação em Biotecnologia da Rede Nordeste de Biotecnologia, Universidade Federal de Pernambuco, como parte dos requisitos exigidos para obtenção do título de Doutor em Biotecnologia.

Orientadora: Profa. Dra. Rosa Amália Fireman Dutra

Recife-PE

2014

Catalogação na Fonte:
Bibliotecário Bruno Márcio Gouveia, CRB-4/1788

Silva, Mizia Maria Saboia
Contribuição de nanomateriais no desenvolvimento de biossensores para diagnósticos da infecção aguda do dengue / Mizia Maria Saboia Silva. – Recife: O Autor, 2014.

115 folhas: il.
Orientador: Rosa Amália Fireman Dutra
Tese (doutorado) – Universidade Federal de Pernambuco. Centro de Ciências Biológicas. Pós-graduação em Biotecnologia da rede Nordeste de Biotecnologia, 2014.
Inclui bibliografia

1. Dengue I. Dutra, Rosa Amália Fireman (orient.) II. Título.

616.91852 CDD (22.ed.) UFPE/CCB-2014-136

MIZIA MARIA SABOIA DA SILVA

CONTRIBUIÇÃO DE NANOMATERIAIS NO DESENVOLVIMENTO DE BIOSSENSORES PARA DIAGNÓSTICO DA INFECÇÃO AGUDA DO DENGUE

APROVADA EM 10/03/2014

Banca examinadora:

Profa. Dra. Rosa Amália Fireman Dutra/UFPE (Presidente e Orientador)

Profa. Dra.Maria Tereza dos Santos correia/UFPE (Titular Interno)

Profa. Dra. Maria de Mascena Diniz Maia/UFRPE (Titular Externo)

Profa. Dra. Patrícia Maria Guedes Paiva/UFPE (Titular Externo)

Dra. Alessandra Batista de Mattos/CETENE (Titular Externo)

Recife-PE

2014

Dedico este trabalho

Aos meus pais, Severino e Celeste e irmãs Merielle e Michelline

Pelo amor, atenção e carinho recebidos diariamente

Amo vocês!

AGRADECIMENTOS

Agradeço em primeiro lugar a Deus pela oportunidade e possibilidade de realização deste trabalho.

À minha orientadora Profª. Drª. Rosa Dutra, por toda paciência e ensinamentos partilhados ao longo desse período.

À professora Marilia Goulart pela confiança e atenção dada ao longo do doutorado.

Aos meus pais, Severino e Celeste e minhas irmãs Michelline e Merielle pelo carinho, amor, paciência e conforto nas horas mais difíceis.

As minhas amigas Priscila, Maria Helena, Paula e Carol pela amizade verdadeira. Vocês foram fundamentais.

Aos amigos, Bárbara, Tatianny, Alessandra, Igor, Joilson, Sergio e Erika pelo apoio, e pelos momentos de risos e descontração.

A todos do Laboratório de Engenharia Biomédica - LEB (UFPE), e Pós-Graduação Rede Nordeste de Biotecnologia - RENORBIO que contribuíram para a minha formação.

À Coordenação de Aperfeiçoamento de Pessoal de Nível Superior – CAPES, pelo suporte financeiro.

“A maior recompensa para o trabalho do homem não é o que ele ganha com isso, mas o que ele se torna com isso”

John Ruskin

SUMÁRIO

RESUMO

O diagnóstico laboratorial da Dengue é fundamental para determinar os cuidados clínicos com o paciente, apoiar os programas de vigilância epidemiológica, pesquisar formulação de vacinas e também para a detecção precoce de uma possível epidemia. A proteína não estrutural 1 (NS1) do vírus Dengue é um marcador utilizado durante a fase aguda da enfermidade e tem sido proposto para o diagnóstico da doença. Atualmente, para diagnóstico da NS1 são usados os ensaios imunoenzimáticos e testes imunocromatográficos. Os imunossensores são dispositivos bioanalíticos que convertem a resposta da interação antígeno-anticorpo em um sinal elétrico, passível de quantificação. Recentemente, a contribuição de nanomateriais a estes dispositivos tem possibilitado aumento na reprodutibilidade e alcance de baixos limites de detecção tornando os imunossensores ferramentas promissoras para diagnóstico clínico. Nesta tese foram desenvolvidos dois imunosensores a base de nanomaterias para a detecção NS1, um marcador importante na infeção aguda da dengue. O primeiro imunossensor, constituído por um eletrodo de carbono vítreo (ECV), foi baseado no uso nanotubos de carbono de parede múltiplas carboxilados (NTCPMs-COOH) recoberto por um filme formado por deposição do Hidrocloreto de Polialilamina (PAH). Anticorpos anti-NS1 foram imobilizados de modo orientado via grupos aminos do PAH. De acordo com os resultados, o imunossensor desenvolvido exibiu uma faixa linear variando entre 0,1 µg mL^{-1} e 2,5 µg mL^{-1} de NS1, faixa clínica para diagnóstico precoce na fase aguda da doença. Uma boa correlação foi encontrada entre a concentração de NS1 e a mudança da corrente, mostrando um bom limite de detecção (0.035 µg mL^{-1}). O segundo imunossensor foi baseado em eletrodos impressos usando a transdução eletroquímica, visando o desenvolvimento de testes *point-of-care*. Os eletrodos impressos foram fabricados com um composto de tinta de carbono-Tiofeno seguidos por um filme de nanopartículas de ouro revestidas com proteína A (AuNP-PtnA) que orientaram a imobilização dos anticorpos anti-NS1. Um imunoensaio direto foi realizado, no qual a captura específica da NS1 foi avaliada através das reações da uma sonda redox com a superfície do eletrodo. De acordo com os resultados, foi observado que o uso do tiofeno na tinta de carbono aumentou significativamente a sensibilidade do eletrodo em 70% em relação ao eletrodo sem modificação. A curva de calibração do sensor mostrou uma faixa de resposta linear entre 0.05 – 0.6 µg mL^{-1} de NS1 e um limite de detecção de 0.015 µg mL^{-1}. Os imunossensores propostos apresentam-se como tecnologias inovadoras ainda não disponíveis no mercado de sensores. Ambos imunossesores apresentaram o uso combinado de tecnologias eletroquímicas com nanomateriais que contribuiu para uniformização da plataforma sensora, melhorara da estabilidade e reprodutibilidade dos eletrodos.

Palavras-chave: Imunossensor, Nanomaterias, Degue, NS1

ABSTRACT

Laboratory diagnosis of dengue is fundamental in determining clinical patient care, supporting epidemiological surveillance programs, researching the formulation of vaccines, and also for early detection of possible epidemics. Currently, commercial kits are available for serological diagnosis of dengue, although their high cost represents an onerous financial burden for developing countries. The nonstructural protein 1 (NS1) of the dengue virus can be used as a marker during the acute phase of the illness and it has been proposed for diagnosis of the disease. Immunosensors associated with nanomaterials have emerged as a tool with high sensitivity and specificity. In this thesis, two different immunosensors based on nanomaterials were developed for the detection of the acute form of dengue infection, using anti-NS1 antibodies. The first immunosensor was based on a modification made up of the multi-walled carbon nanotube (MWNT), carboxylates, and the polyallylamine hydrochloride (PAH) polymer, for immobilization oriented from the anti-NS1, using a glassy carbon electrode (GCE) as the working electrode. In this immunosensor, the anti-NS1 was immobilized on the surface via amino groups of the PAH. According to the results, the developed immunosensor exhibited a linear range varying from 0.1 µg mL^{-1} to 2.5 µg mL^{-1} of NS1, which is well-known in the clinical setting for early diagnosis of the acute phase of the disease. A good correlation was found between the concentration of NS1 and the change in the current, and a good detection limit (0.035 µg mL^{-1}) was demonstrated. The second immunosensor was based on printed electrodes using electrochemical transduction, the aim being to develop point-of-care testing. The printed electrodes were fabricated with an ink compound of carbon and thiophene, followed by a film of gold nanoparticles coated with protein A (AuNP-PtnA) which oriented the immobilization of the antibodies (anti-NS1). A direct immunoassay was performed and the specific capture of the NS1 was assessed through the reactions of a redox probe with the electrode surface. In accordance with the results, it was observed that the use of thiophene in the carbon ink significantly increased the sensitivity of the probe — 70% compared to an unmodified electrode. The calibration curve of the sensor showed a linear response range between 0.05 and 0.6 µg mL^{-1} of NS1, and a detection limit of 0.015 µg mL^{-1}. The proposed immunosensors are presented as an innovative technology that is not yet available in the sensor market. The combined use of these technologies with nanomaterials contributed to the standardization of the sensor platform and the improved stability and reproducibility of the electrodes.

Keywords: immunosensor, nanomaterials, dengue, NS1

LISTA DE FIGURAS

LISTA DE TABELAS

LISTA DE ABREVIATURAS

Anti-NS1 - anticorpo NS1

AuNP-PtnA - Nanopartículas de ouro proteína A

CNTs - Carbon nanotubes

DENV – Vírus da dengue;

ECV - Eletrodo de carbono vítreo;

E – Potencial;

$E_{1/2}$ - Potenciais de meia onda;

Ep2 - Pico de meia altura;

EDC – *N*-etil-*N´*-(3-dimetilaminopropil) carbodiimida;

EIs - Eletrodos impressos;

ELISA – Enzyme-Linked Immunoabsorbent Assay, do inglês Ensaio Imunoenzimático;

E_{pa} – Potencial de pico anódico;

E_{pc} – Potencial de pico catódico;

EQM – Eletrodo quimicamente modificado;

ER - Eletrodo de Referencia;

ET - Eletrodo de Trabalho;

FCD - Febre clássica da dengue;

FHD – Febre hemorrágica da dengue;

FTIR – Espectroscopia no infravermelho por transformada de Fourier

GCE – Glassy Carbon electrode

IgG ou IgM – Imunoglobulina G ou M, respectivamente;

Ipc – Corrente de picos catódico;

Ipa – Corrente de pico anódico;

MAC-ELISA – Ensaio imunoenzimático para captura de anticorpos IgM;

NTC - Nanotubos de carbono

NTCMP – Nanotubos de carbono de múltiplas parede;

NTCUP - Nanotubos de carbono de única parede;

NS1 – Proteína não-estrutural 1;

OMS - Organização mundial de Saúde;

PAH - Hidrocloreto de Polialilamina;

RDTs - rapid diagnostic tests

RT-PCR – Reação da Transcriptase Reversa seguida de Reação em Cadeia da Polimerase;

SCD – Síndrome do Choque da Dengue;

SEM – Microscopia eletrônica de varredura;

SPE - Screen Printing Elelctrode;

Thiophene-SPE - thiophene-modified screen printed carbon electrode

Δi – Variação de corrente;

VC – Voltametria cíclica;

1 INTRODUÇÃO

Dengue é uma doença infecciosa, não contagiosa, causada por um por um vírus que recebe o nome de DENV (Dengue Vírus) Trata-se de uma enfermidade de notificação compulsória (BRASIL, 2011), caracterizada por epidemias sazonais podendo apresentar, como ocorre atualmente no Brasil, comportamento endêmico com aumento da incidência em períodos chuvosos. A dengue é uma arbovirose humana (doença viral transmitida ao homem por vetores artrópodes) que pode ser causada por quatro vírus diferentes (DENV-1, DENV-2, DENV-3 e DENV-4) (HALSTEAD, 2007) no qual os quatro sorotipos são capazes de provocar infecção (POLONI, 2009; MACHADO et al., 2013). A Dengue é considerada hoje um dos principais problemas de saúde pública no mundo. Segundo a Organização Mundial da Saúde (OMS) (WHO, 2012), 50 a 100 milhões de pessoas são infectadas anualmente em mais de 100 países. Cerca de 550 mil doentes necessitam de hospitalização e 20 mil morrem em consequência da dengue (SEABRA; MENDONÇA, 2011). Uma vez que, até agora, não existem vacinas licenciadas ou terapias específicas para dengue, o manejo do paciente depende de um diagnóstico precoce e de um tratamento adequado (FELIX et al., 2012). O diagnóstico da Dengue é difícil quando baseado exclusivamente em aspectos clínicos, tendo em vista os sintomas poderem ser confundidos com outras doenças infecciosas.

Basicamente, o diagnóstico laboratorial da dengue pode ser feito pelo isolamento do vírus, pela detecção do genoma viral, pela detecção de antígenos virais e sorologia (IgG e IgM). Embora mais sensíveis e precisos, os testes moleculares possuem custo mais elevado e necessitam de laboratórios especializados, razão pela qual os testes sorológicos são os mais utilizados na rotina (Blacksell et al., 2008). No entanto os testes com anticorpos IgM e IgG somente resultarão positivo após vários dias, (GUZMAN et al., 2010).

Nas últimas décadas estudos demonstram que a proteína não estrutural 1 (NS1) do DENV é um importante marcador precoce, encontrada nos 4 sorotipos do DENV e está correlacionada à replicação viral (MACHADO et al., 2013). A NS1 é detectada em soros de pacientes em fase aguda da doença (infecção primária e secundária (YOUNG et al., 2000; ALCON et al., 2002a; KORAKA et al., 2002; KUMARASAMY et al., 2007; FRY et al., 2011).

Ensaios imunoenzimáticos e imunocromatográficos para a detecção da proteína viral NS1 estão disponíveis no mercado (ALCON et al., 2002a). No entanto, diante da necessidade da realização de métodos de diagnósticos mais práticos e de custo reduzido, os biossensores destacam-se, pois, combinando características desejadas, podem ser desenvolvidos para operarem em serviços descentralizados. Além disso, comparados aos testes imunocromatográficos para NS1 (ZAINAH et al., 2009a), eles têm a vantagem de poder fornecer resultados quantitativos, além de requererem amostras de pequenos volumes, na ordem de poucos microlitros. Deste modo, visando à minimização de tempo e custo busca-se novas alternativas para o diagnóstico.

Biossensores vêm demonstrando ser um dos mais atrativos métodos analíticos no ramo da detecção química, bioquímica e imunológica (HE et al., 2007; ZHU et al., 2007). Embora grandes avanços tenham sido alcançados com sensores confiáveis para a determinação segura da glicose e demais metabólitos baseados na reação enzima-substrato, no campo dos biossensores de afinidade (imunossensores e sensores moleculares) os progressos têm sido desafiadores devido à dificuldade em se alcançar os desejáveis limites de detecção, estabilidade e seletividade confiáveis (FENG et al., 2003). No intuito de superar estas dificuldades, o uso nanomateriais em dispositivos eletrônicos vem sendo estudados. Em particular, nanomateriais como nanopartículas de ouro, nanopartículas magnéticas, pontos quânticos, silícios porosos, nanotubos de carbono (NTCs) e nanobastões de ouro vêm sendo utilizados para construção de biossensores (KANG et al., 2007). A importância destes nanomateriais nos dispositivos analíticos já está completamente reconhecida e demonstra melhorar consideravelmente a sensibilidade e especificidade na detecção de biomoléculas (HE et al., 2007).

Uma grande variedade de eletrodos tem sido usada como suporte de imobilização em imunossensores eletroquímicos. Dentre estes, a tecnologia de eletrodos impressos (EIs) é considerada como promissora, pois pode ser comercializada em larga escala com vantagens atrativas, como miniaturização, (BERGAMINI; ZANONI, 2005). A tecnologia de EIs é baseada na deposição de diferentes tipos de tintas sobre substratos inertes, sendo bastante adequada

para produção em massa de dispositivos portáteis (WANG et al., 2008). Com o intuito de aperfeiçoar esses dispositivos, a modificação dos EIs com nanomateriais tem sido bastante estudada (FANJUL-BOLADO et al., 2009). Isso posto, o presente estudo teve como objetivo desenvolver biossensores a base de nanomaterias para a detecção da infecção aguda do dengue empregando anticorpos anti-NS1 a fim de criar medidas que levem ao tratamento adequado da doença através do diagnóstico de casos agudos e/ou recentes de Dengue.

2.REVISÃO DE LITERATURA

2.1 A dengue

A Dengue é uma das principais preocupações da saúde pública nas regiões tropicais e subtropicais do mundo (WHO, 2012). É uma infecção viral aguda de importância global em termos de morbidade e mortalidade, transmitida por artrópodes, principalmente o mosquito *Aedes aegypti*, infectado por um dos quatro sorotipos do vírus Dengue (DENV) (DENV-1, DENV-2, DENV-3, DENV-4), que vem se espalhando rapidamente, com um aumento de 30 vezes na taxa global nos últimos 50 anos (figura 1). Durante o século XIX, era considerada uma doença esporádica que causava epidemias com longos intervalos, refletindo, a lentidão dos sistemas de transporte que limitava o deslocamento das pessoas naquela época. Hoje, a Dengue figura como a mais importante arbovirose humana (DEEN et al., 2006).

Figura 1: Número de casos de Dengue notificados à OMS, anualmente entre 1955-2010.

Fonte: (WHO, 2012). Adaptado pela autora.

A OMS estima que de 50 a 100 milhões de novas infecções ocorrem anualmente em mais de 100 países endêmicos (WHO, 2012) (Figura 2),

400.000 casos de febre hemorrágica da dengue (FHD) e 22.000 mortes, principalmente de crianças, (MACIEL, I. J., SIQUEIRA JÚNIOR, J. B., & MARTELLI, 2008), e estima-se que cada caso de atendimento ambulatorial ou hospitalar pode custar cerca de U$ 514-1394 (SUAYA et al., 2009), afetando frequentemente as populações mais pobres. Os verdadeiros números são provavelmente muito piores, já que as notificações nem sempre são documentadas (SUAYA et al., 2007; BEATTY et al., 2011).

Figura 2: Distribuição mundial do risco de Dengue (determinação da condição de risco com base em relatórios combinados da OMS, os EUA Centers for Disease Control and Prevention, Gideon on-line, ProMED, DengueMap, Eurosurveillance e literatura

Áreas de Risco, Dengue

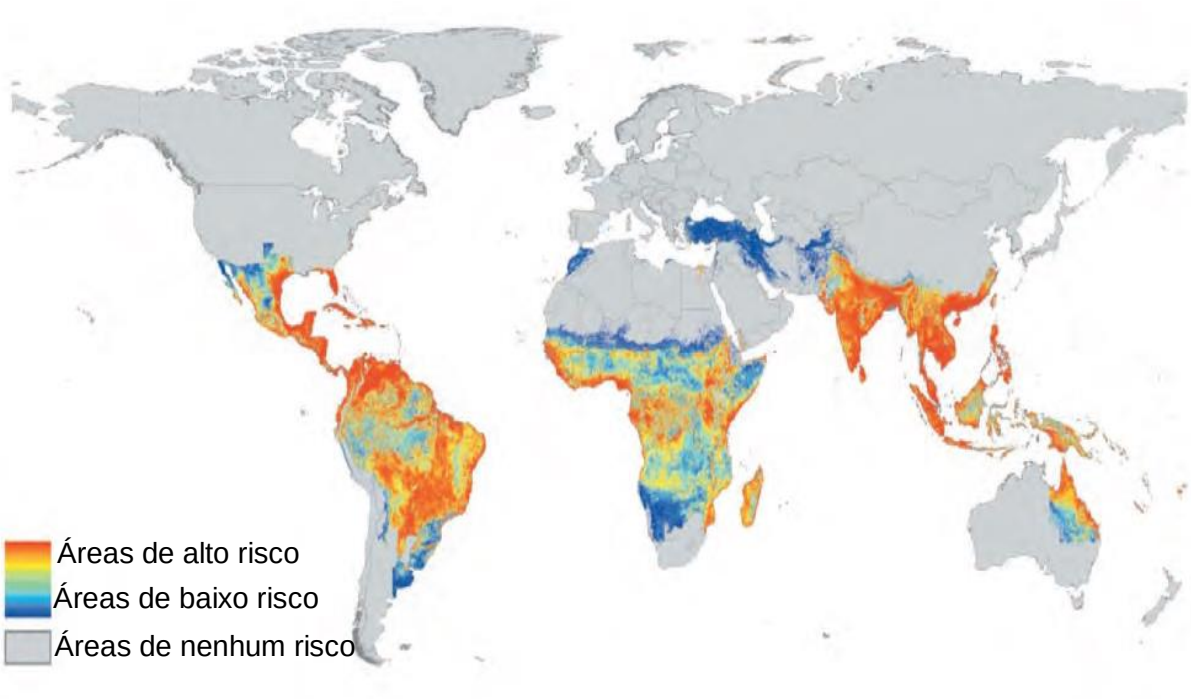

Fonte: (SIMMONS et al., 2012). Traduzido pela autora.

O indivíduo picado pelo mosquito transmissor da dengue passa por um período de incubação do vírus que varia entre 3 e 7 dias. Infecções primárias, ou seja, no primeiro contato do organismo com o patógeno, podem não apresentar manifestações claras ou apenas uma febre indiferenciada. A doença cursa de forma assintomática ou com quadro clinico que varia desde uma febre indiferenciada e autolimitada, passando pela febre clássica da dengue (FCD), até quadros graves de febre hemorrágica da dengue (FHD) e Síndrome do Choque da Dengue (SCD) (SAM et al., 2013). Esta forma grave esta intimamente relacionada à reinfecção e, por isso é de grande importância clínica e epidemiológica conhecer os sorotipos circulantes e evitar a co-circulação de mais um sorotipo através de medidas de combate ao vetor, já que até o presente momento não há vacinas disponíveis. O desafio atual das autoridades sanitárias nacionais e internacionais é reverter a tendência de aumento das epidemias, bem como o aumento da incidência de Dengue hemorrágica (BARRETO, M. L., & TEIXEIRA, 2008).

Figura 3: Tipos de manifestações da infecção por vírus da dengue.

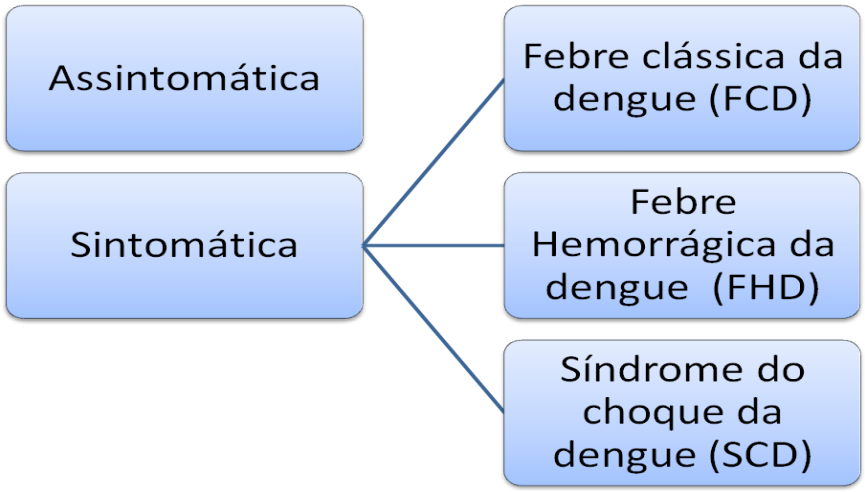

Fonte: http://www.dedetizacao -consulte.com.br/dengue-tipos-de-virus-da-dengue.asp. Acesso em: 29/01/2014. Traduzido pela autora.

O vírus DENV pertence à família *Flaviviridae* e ao gênero *Flavivirus*. A inclusão do DENV neste gênero é baseada na sua reatividade antigênica com outros *flavivírus* bem como na organização do genoma. O vírus apresenta-se como uma partícula esférica medindo 40-50 nm de diâmetro, com um envelope lipídico e RNA de fita simples, com polaridade positiva, possui um genoma de aproximadamente 11 kb que codifica três proteínas estruturais, o capsídeo, a membrana e o envelope, e sete proteínas não estruturais, NS1, NS2A, NS2B, NS3, NS4A, NS4B e NS5, conforme a figura 3 (GUZMAN et al., 2010).

Figura 4: Representação esquemática do genoma do vírus Dengue.

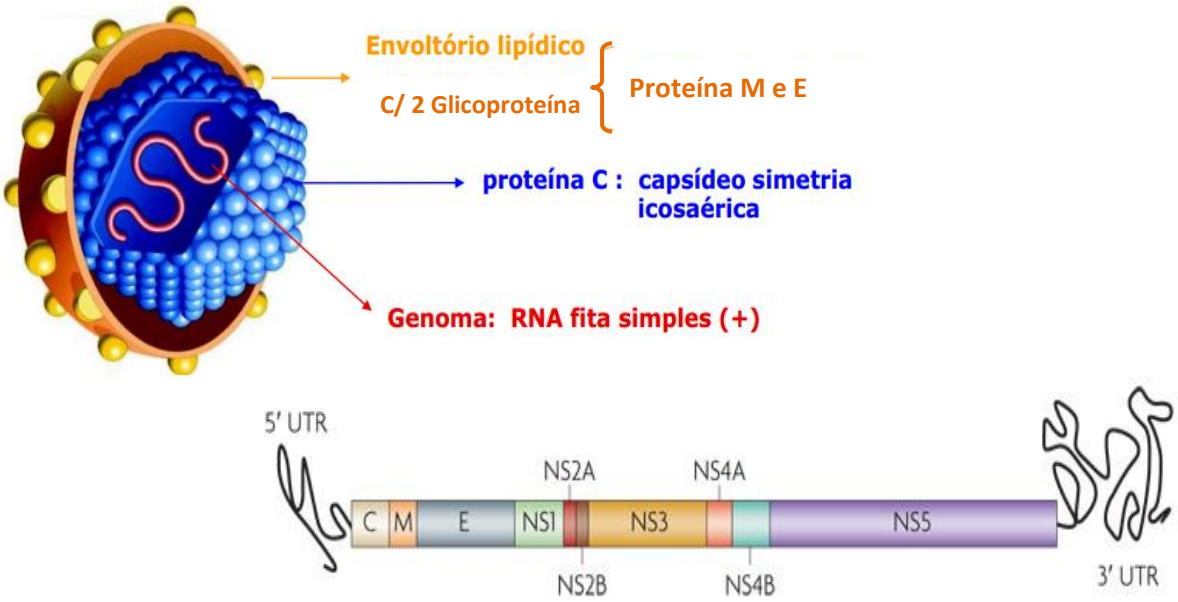

Fonte (GUZMAN et al., 2010). Traduzido pela autora.

Quando infecta uma célula saudável, o genoma viral é transcrito em uma poliproteína, que é então direcionada ao retículo endoplasmático, onde é processada por proteases provenientes do vírus e da própria célula infectada. Ao atingir a conformação ativa, as proteínas NS iniciam a replicação do genoma viral. Apesar do processo de replicação viral ser entendido de maneira geral, falta ainda informação estrutural e funcional com relação às proteínas NS, principalmente a NS1, NS2A e NS4A/B (PERERA & KUHN 2008). (RODENHUIS-ZYBERT et.al. 2010).

2.1.1 Aspecto Histórico

Os primeiros registros de uma doença semelhante à dengue estão descritos na Enciclopédia Chinesa de sintomas e remédios e datam da Dinastia China (265-420 a.C.) (NOBUCHI T, TAKAHARA S, 1979; POLONI, 2009). Este vírus também pode ter sido o causador de surtos de doença febril no século XVII na região das ilhas a oeste do oceano Pacífico e no Panamá, bem como epidemias registradas em Jacarta, Indonésia e Egito no século XVIII, época em que a doença já apresentava uma distribuição global (CAREY, 1971; MCSHERRY, 1982). Os primeiros relatos de uma grande epidemia de uma doença com sintomas semelhante à Dengue Clássica aconteceram nos três continentes (Ásia, África e norte da América) em 1779 e 1780 (AASKOV, 2003).

A II Guerra Mundial foi um evento de grande importância para a dispersão do Dengue vírus e do seu mosquito transmissor. Antes, as epidemias aconteciam em intervalos de 10 a 40 anos. A partir de 1954, a doença começou a exibir novo padrão caracterizado por hemorragia grave e/ou choque provocando óbito em 40% dos enfermos: era chamada febre hemorrágica da dengue/síndrome do choque da dengue, descrita pela primeira vez por Hammon et al., em 1960, nas Filipinas (HAMMON et al., 1960; GUBLER, D. J.;KUNO, 1997) Após a década de 70, o problema das epidemias de dengue agravou-se, particularmente nos países tropicais de todos os continentes sendo que, atualmente, a dengue apresenta um sério problema de saúde pública em áreas tropicais da Ásia, África, América Latina e Caribe. A primeira grande epidemia de FHD nas Américas foi registrada no ano de 1981 em Cuba, com um total de 344.203 casos notificados, dos quais 10.312 foram classificados como FHD. Houve 116.143 hospitalizações, 158 óbitos e custo que excederam a cifra de U$$ 103 milhões (MACIEL, I. J., SIQUEIRA JÚNIOR, J. B., & MARTELLI, 2008).

Entre os fatores que contribuíram para a emergência da FD/FHD destacou-se o rápido crescimento populacional e urbanização da America Latina e Caribe, o aumento do número de pessoas se deslocando geograficamente facilitando a disseminação da virose, e a circulação dos quatro sorotipos nas

Américas gerando um estado de hiperendemicidade que aumenta o risco de FHD e a pouca eficiência dos programas de controle do vetor (WHO, 1997).

2.1.2 Dengue no Brasil

No Brasil, a primeira epidemia documentada clínica e laboratorialmente ocorreu em 1981-1982, em Boa Vista (RR), causada pelos sorotipos 1 e 4. Em 1986, ocorreram epidemias, atingindo o Rio de Janeiro e algumas capitais da região nordeste. Desde então, a Dengue vem ocorrendo no Brasil de forma continuada, intercalando-se com a ocorrência de epidemias, geralmente associadas com a introdução de novos sorotipos em áreas anteriormente não atingidas e ou alteração do sorotipo circulante. Na epidemia de 1986, foi identificada ocorrência da circulação do sorotipo DENV-1, inicialmente no estado do Rio de Janeiro, disseminando-se, a seguir, para outros seis estados até 1990. Na década 90, foi identificada circulação de um novo sorotipo, o DENV-2, também no estado do Rio de Janeiro. A circulação do DENV-3 foi reconhecida, pela primeira vez, em 2000, no estado do Rio de Janeiro e, posteriormente, no estado de Roraima, em 2001. Em 2004, 23 dos 27 estados do país já apresentaram a circulação simultânea dos sorotipos 1, 2 e 3 do DENV (NOGUEIRA et al., 2007; BRASIL, 2010). O aumento significativo da incidência, reflexo da ampla dispersão do *Aedes aegypti* no território nacional e, sobretudo nos grandes centros urbanos das regiões Sudeste e Nordeste do Brasil, responsáveis pela maior parte dos casos notificados. As regiões Centro-Oeste e Norte foram acometidas mais tardiamente, com epidemias registradas a partir da segunda metade da década de 90 (MACIEL, I. J., SIQUEIRA JÚNIOR, J. B., & MARTELLI, 2008).

Os adultos jovens foram os mais atingidos pela doença desde a introdução do vírus no Brasil. No entanto, a partir de 2006, alguns estados apresentaram a recirculação do sorotipo DENV2 após alguns anos de predomínio do sorotipo DENV3. Esse cenário levou a um aumento no número de casos, de formas graves e de hospitalizações em crianças, principalmente no Nordeste do país. Em 2008 foram notificados 585.769 casos e novas epidemias causadas pelo sorotipo DENV2 ocorreram em diversos estados do

país, marcando o pior cenário da doença no Brasil, em relação ao total de internações e óbitos até a presente data. Essas epidemias foram caracterizadas por um padrão de migração de gravidade para as crianças, que representaram mais de 50% dos pacientes internados nos municípios de maior contingente populacional. Mesmo em municípios com menor população, mais de 25% dos pacientes internados por Dengue eram crianças, ressaltando que todo o país vem sofrendo, de maneira semelhante, essas alterações no perfil da doença. No ano de 2009, foram notificados 266.285 casos de dengue, representando um declínio de 52%, em relação ao mesmo período de 2008 (MINISTÉRIO DA SAÚDE, 2013).

O cenário da situação epidemiológica da Dengue no Brasil de 1986 a 2010 está demonstrado na figura 5, na qual se observa que após significativo aumento do número de casos em 2002, ocorre uma diminuição do número de casos até 2004, que voltam a aumentar gradativamente, chegando a mais de 1.200.000 casos notificados em 2010 (CONASS, 2011). Na mesma figura se observa na última década um crescimento progressivo no número de internações por Dengue ou Febre Hemorrágica da Dengue (chegando a mais de 80.000 internações em 2010), indicando um aumento do número de casos mais graves que demandaram internação hospitalar (MARZOCHI[1], 2011), estas estimativas exigem medidas imediatas no controle da Dengue no Brasil.

Figura 5: Casos notificados e internações por Dengue/FHD Brasil, 1986-2010.

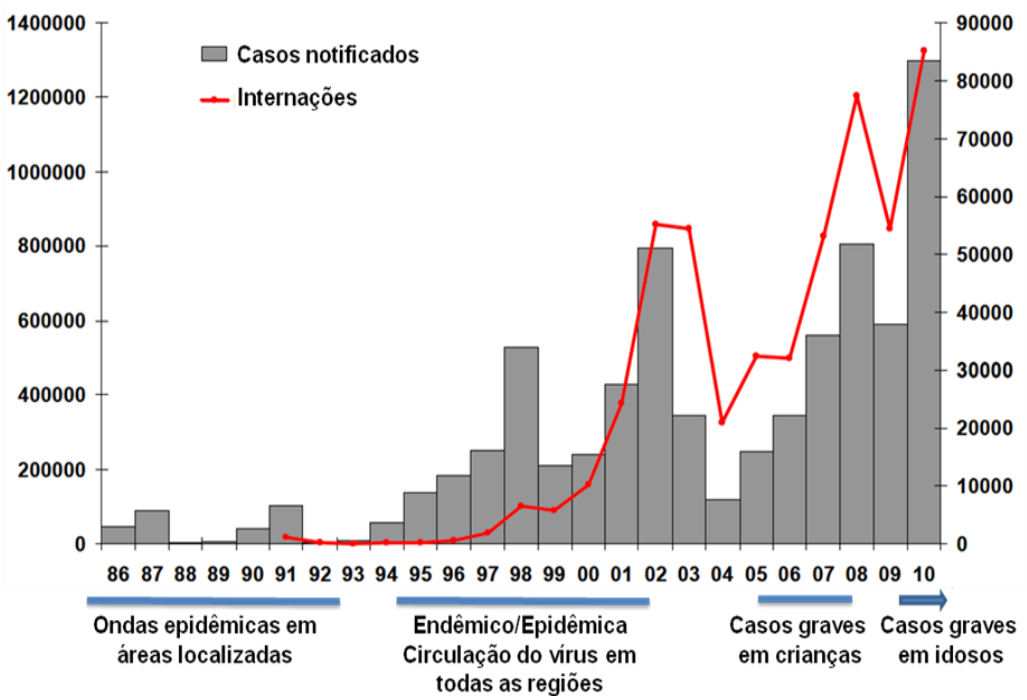

Fonte: Ministério da saúde/ Secretaria de vigilância Sanitária.

2.1.3 Diagnostico Laboratorial

Clinicamente, o diagnóstico da Dengue é difícil de ser realizado, pois os sintomas são comuns a outras infecções febris agudas como a Malária, Tifo, Leptospirose, Sarampo, Rubéola, Gripe e varias Arboviroses. Deste modo é importante considerar a confirmação laboratorial da infecção pelo DENV, e imprescindível, em muitos casos, o diagnóstico diferencial (GUBLER et al., 1981). Além dos cuidados clínicos com os pacientes o diagnóstico também contribuem na vigilância epidemiológica, formulação de vacinas, detecção precoce de epidemias, com informações úteis às autoridades sanitárias em tempo hábil para que sejam feitas a localização e a concentração da disseminação da transmissão do vírus (OLLIVEIRA et al., 2011). Diversos métodos podem ser empregados para o diagnóstico (Figura 6), que podem ser

divididos em métodos direto tais como o isolamento do vírus em cultura de células, a detecção do RNA viral pela reação em cadeia da polimerase, associada à transcrição reversa (RT-PCR), a detecção da proteína NS1 (antígeno viral) no sangue e em tecidos (óbitos) teste mais específicos, e testes indiretos que usam a detecção de anticorpos específicos no soro testes mais viáveis economicamente (GUZMAN et al., 2010). A janela ideal para o diagnóstico de uma infecção por dengue é mais ou menos a partir do início da febre até 10 dias pós-infecção, no entanto, como nem todos os pacientes são diagnosticados dentro deste período, um teste de diagnostico ideal deve ser sensível, especifico e ser viável independentemente do estágio da infecção (PEELING, ROSANNA W. et al., 2010).

Figura 6: Comparativos de métodos laboratoriais diretos e indiretos para o diagnóstico da dengue.

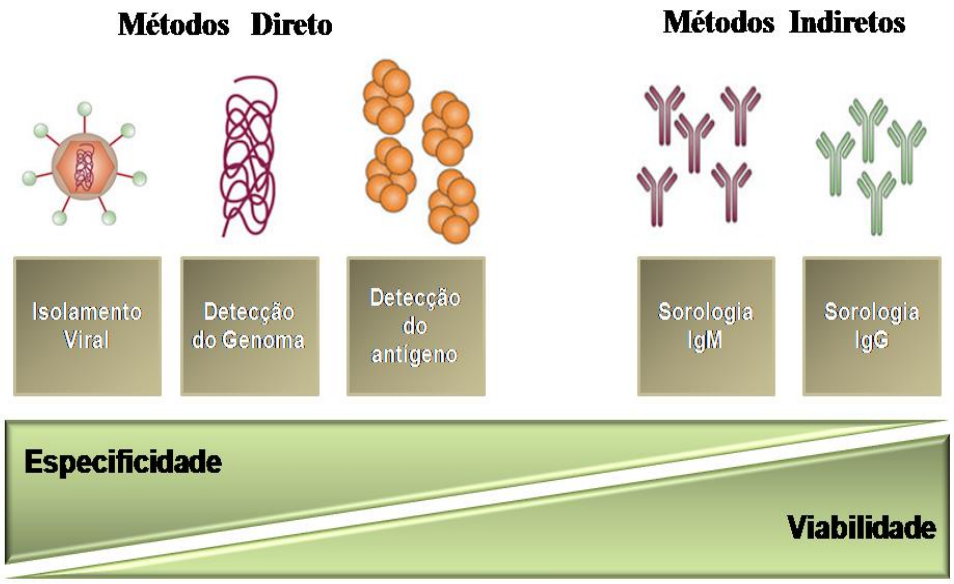

Fonte: (PEELING, ROSANNA W. et al., 2010). Traduzida pela autora.

2.1.3.1 Isolamento Viral

O isolamento viral é considerado o teste padrão-ouro para o diagnóstico e sorotipagem das infecções por DENV. O principal método utilizado para o

isolamento viral pode ser conseguido por meio da inoculação da amostra de sangue e ou soro em culturas de células, principalmente as originadas de mosquito, como o clone C6/36 de *Aedes albopicuts* (SHU; HUANG, 2004; KAO et al., 2005). Entretanto, essa técnica não é necessária para diagnóstico de rotina, mas sim para determinar o sorotipo do vírus causador da infecção, para fins de pesquisa e estudos epidemiológicos. Ressalta-se também a necessidade de pessoal e laboratório especializados cujo resultado só é obtido em uma a duas semanas (DATTA; WATTAL, 2010a). No Brasil, o isolamento viral é realizado pelos Laboratórios de Saúde Pública de Referência em Dengue, pertencente à Rede Nacional de Laboratórios do Ministério da Saúde.

2.1.3.2 Diagnóstico Molecular

O diagnóstico molecular realizado pela RT-PCR, cujo alvo é a detecção do genoma viral, tem um papel eficaz tendo em vista ser capaz de identificar de forma rápida a presença do vírus durante a fase aguda da doença e em algumas metodologias, quantificar a carga viral (YAP et al., 2011). Entretanto, a exigência de uma equipe treinada, a necessidade de vários equipamentos especiais, bem como o custo elevado associado aos métodos moleculares tem limitado sua aplicação como diagnóstico de rotina (DATTA; WATTAL, 2010a).

2.1.3.3 Diagnóstico Sorológico

O diagnóstico sorológico detecta anticorpos específicos para o vírus da Dengue e complementa o diagnóstico virológico ou, quando este não é possível, serve como meio alternativo de diagnóstico. O teste pode ser feito através de vários métodos (inibição da hemaglutinação, teste de neutralização, etc). O ensaio imunoenzimático ELISA (do inglês - *Enzyme-linked Immunossorbent Assay*) é o mais utilizado, sendo de grande utilidade devido a sua alta sensibilidade e fácil execução (PAULA, DE; FONSECA, 2004).

O ELISA tem sido usado para detectar anticorpos IgM na fase aguda e na convalescença, além dos anticorpos IgG anti-Dengue (Tabela 1). Os anticorpos IgM são melhores detectados a partir do quinto dia após o início da doença, tornando essa técnica inviável para um diagnóstico precoce, ou seja, nos primeiros dias de doença (PAULA, DE; FONSECA, 2004; HALSTEAD, 2007; LIMA et al., 2010; BRASIL, 2011).

Tabela 1: Testes de ELISA para o diagnostico da dengue

Método Elisa IgM	Baseado em detecção de anticorpo, este método costuma positivar após o sexto dia da doença;
Método Elisa IgG	Baseado em detecção de anticorpo, este método costuma positivar a partir do nono dia de doença, na infecção primária, e já estar detectável desde o primeiro dia de doença na infecção secundária;
Método Elisa IgM e IgG	Teste rápido, baseado na detecção qualitativa e diferencial de anticorpos IgM e IgG, permite diagnóstico ou descarte.

2.1.3.4 Detecção do antígeno NS1

O NS1 foi reconhecido primeiramente como antígeno de fixação de complemento solúvel em cultura de célula infectada (BRANDT et al., 1970). O antígeno de fixação foi reconhecido como uma glicoproteína viral de 46 KD (SMITH; WRIGHT, 1985) e posteriormente denominado de NS1 (RICE et al., 1985). A glicoproteína com cerca de 353 - 354 aminoácidos, que possui elevada quantidade de aminoácidos e nucleotídeos homólogos entre flavivirus,

não faz parte da partícula viral, mas é liberada das células infectadas pelo DENV. Estudos preliminares têm mostrado que a proteína NS1 está envolvida na replicação do RNA viral, e foi encontrada em amostras da fase aguda do sangue de pacientes com infecções primárias ou secundárias. Isto sugeriu um maior envolvimento desta proteína viral na patogenicidade do vírus Dengue e sua possível utilização como um marcador adequado para a referida infecção (BLOK et al., 1992; YOUNG et al., 2000). Dentre as proteínas não estruturais, é a mais conservada e apresenta elevado grau de reação cruzada entre os 4 sorotipos (ZAINAH et al., 2009a).

O NS1, encontrado no soro ou plasma durante a fase aguda da doença, tem oferecido um novo caminho para o diagnóstico precoce e rápido ainda na fase inicia da infecção (figura 7).

Figura 7: Representação esquemática dos métodos empregados no diagnóstico da Dengue conforme os dias de doença.

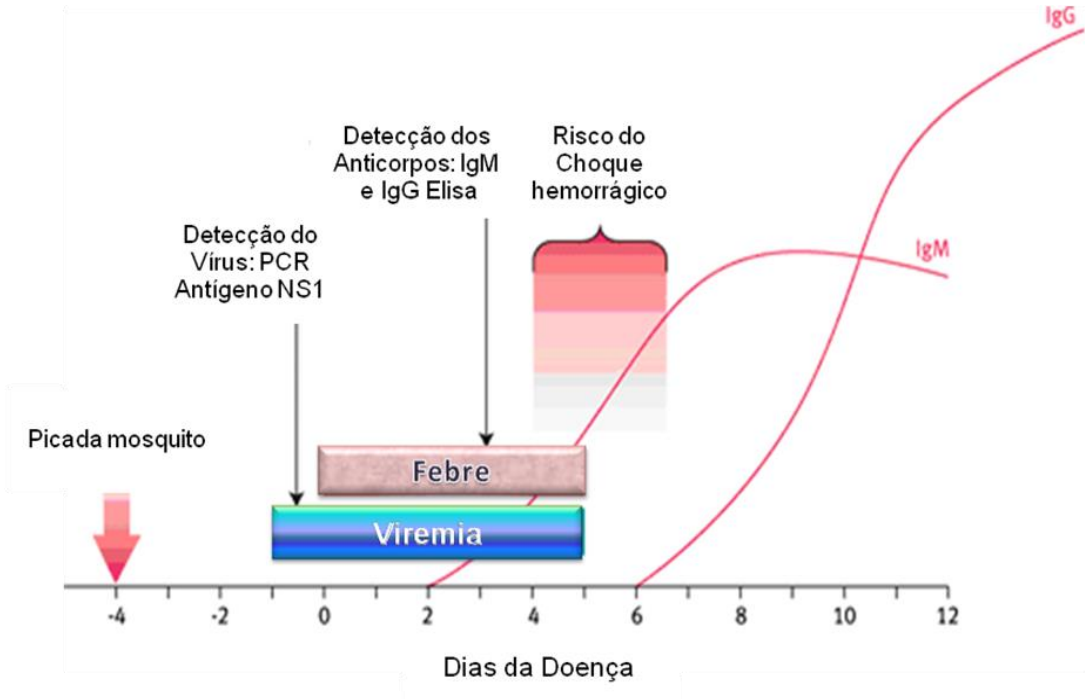

Fonte:http://www.health.qld.gov.au/cdcg/index/dengue.asp. Acesso em: 10/11/2013. Adaptado pela autora.

O diagnostico pelo NS1 é uma ferramenta de análise e é um teste qualitativo, usado na detecção da antigenemia NS1 da Dengue pela técnica

ELISA de captura. Esta auxilia no diagnóstico sorológico da doença em amostras colhidas principalmente até o terceiro dia do início dos sintomas e seu desempenho equivale ao do RT-PCR, porém, não permite a identificação do sorotipo. Atualmente, ensaios imunoenzimáticos e imunocromatográficos para a detecção da proteína viral NS1 estão disponíveis no mercado. O Ministério da Saúde disponibiliza kits para o uso em amostras de unidades-sentinela de monitoramento do vírus da Dengue (BRASIL, 2011).

Dado ao importante papel do NS1 como marcador precoce da fase aguda diversos sistemas de detecção, tais como imunocromatograficos imunossensores têm sido desenvolvidos. Silva et. al. em seu trabalho avaliou diferentes kits de detecção da proteína NS1 do vírus dengue, tendo como referência o isolamento viral (Tabela 2). De forma geral, os kits avaliados podem ser empregados no diagnóstico, sempre associados a critério clínico e epidemiológico ou outros métodos laboratoriais (SILVA, F. G., DOS SANTOS SILVA, S. J., ROCCO, I. M., DA, 2011).

Tabela 2: Sensibilidade para quatro kits testados para detecção de antígenos NS1 em relação aos dias de doença e intervalo de confiança. Adaptado (Silva et al. 2011)

Kits analisados	**Sensibilidade (0-3 dias de doença)**	**Intervalo de confiança (IC 95%)**
NS1 Ag Strip (Bio- Rad)	90,0%	79,8-95,3
Duo Test (Bioeasy) Strip	90,0%	79,8-95,3
Platelia NS1 (Bio-Rad) ELISA	93,1%	83,6-97,2
Early ELISA NS1 (Panbio)	85,7%	75,0-92,3

Atualmente, imunossensores para detecção do antígeno NS1 tem sido bastante explorado na literatura através de diferentes abordagens. Os trabalhos citados alcançaram ótimos resultados e diferem entre si, basicamente, quanto às técnicas de imobilização dos anticorpos anti-NS1 sobre a superfície eletródica, sensibilidade e possibilidade de amplificação dos sinais (Tabela 3). Tendo em vista a importância de um imunossensor que se adéqüe a todas as necessidades para um diagnóstico rápido, preciso, miniaturizado e de baixo custo para detecção da NS1, ainda é necessário a continuação das pesquisas na área

Tabela 3: Imunossensores para detecção de anticorpos anti-NS1.

Método de Detecção de imunossensor	Limite de detecção	Referência
Eletroquímico	12 ng/mL^{-1}	(DIAS et al., 2013)
Eletroquímico	0,33 ng/mL^{-1}	(CAVALCANTI et al., 2012)
Piezoelétrico	1,727/µg mL^{-1}	(WU et al., 2005)

As concentrações da NS1 no início das infecções primárias e secundárias variam entre 10 ng.mL^{-1} a 2 µg.mL^{-1} e pode chegar até cerca de 50 µg.mL^{-1} (ALCON et al., 2002b; LIBRATY et al., 2002). Como a concentração atingida no sangue pode ser considerada alta, este torna-se um alvo relativamente fácil de se detectar, ainda mais se considerado o ponto de vista clínico, onde o interesse reside no diagnóstico baseado na presença ou ausência da proteína. Embora a sensibilidade das plataformas encontradas na literatura apresente uma queda significativa nas concentrações dos anticorpos anti-NS1 nas infecções secundárias, a busca por dispositivos com um limite de

detecção menor é de grande interesse (KUMARASAMY et al., 2007; DIAS et al., 2013).

Tomando como premissa a necessidade da realização de métodos de diagnósticos mais rápidos, práticos e de custo reduzido, os biossensores se destacam, podendo ser desenvolvidos para serem usados em serviços descentralizados com ausência de ferramentas diagnósticas. Por outro lado, quando comparados aos testes imunocromatográficos para NS1 (ZAINAH et al., 2009a), eles têm a vantagem de fornecer resultados quantitativos, além de requererem amostras de reduzido volume, na ordem de poucos microlitros.

O diagnóstico precoce, graças à detecção do antígeno NS1 do DENV, permite uma melhora considerável no cuidado do paciente, possibilitando também um tratamento apropriado, precoce, evitando as complicações graves e desta forma auxiliando a dirimir a disseminação da doença (MCBRIDE, 2009).

Neste contexto, o desenvolvimento de biossensores para captura do NS1 representa uma alternativa para o diagnóstico precoce, pois permitirá a detecção do DENV (na fase aguda) evitando a evolução para FHD e SCD, resultando em maior sobrevida por parte dos enfermos. Deste modo é também possível a orientação de uma conduta médica mais rápida, sobretudo, quando desenvolvidos biossensores sob a forma de "*point-of-care-testing*" (SOPER et al., 2006).

2.2 Biossensores

Nas últimas décadas as ciências analíticas têm apresentado um avanço considerável relacionado à capacidade de obtenção de informações químicas em diversos sistemas, proporcionando um alto desenvolvimento analítico, resultando na automação, miniaturização e simplificação destes dispositivos estudados (MURPHY, 2006). Neste âmbito, os biossensores têm adquirido primordial importância devido à possibilidade de análises de processos sintéticos ou biológicos, bem como a compreensão dos mesmos (ZHANG et al., 2000). Deste modo, têm sido utilizados em diferentes áreas, e setores da indústria, como as de alimentos, farmacêuticas, clínicas e na agricultura, tendo

como base a necessidade de métodos analíticos rápidos, exatos e confiáveis na determinação das espécies de interesse. Outrossim, os biossensores propiciam análises com monitoramento contínuo e em tempo real em tempo real, substituindo técnicas analíticas destrutivas ou que venham a exigir elevadas quantidades de amostras, aumentando sua potencialidade para o uso comercial (MURPHY, 2006).

Biossensores são dispositivos capazes de providenciar informação quanti ou semi-quantitativa usando moléculas biológicas imobilizadas em um transdutor (THÉVENOT et al., 2001). Duas de suas principais características conferidas a esse tipo de sensor são seletividade e especificidade. Tais peculiaridades são atraentes viabilizando o desenvolvimento de diferentes tipos de biossensores aplicados a análises em tempo real de amostras diversas.

Os biossensores são formados fundamentalmente por uma superfície, um componente biológico receptor com um elemento conversor e o transdutor. A interação do analito com o bioreceptor produz um sinal químico captado medido pelo transdutor que o converte em um sinal elétrico mensurável. A figura 8 ilustra o princípio do funcionamento de biossensores (COLLINGS; CARUSO, 1997; WILSON; GIFFORD, 2005; VO-DINH; CULLUM, 2008).

Figura 8. Representação esquemática dos elementos constituintes de um biossensor.

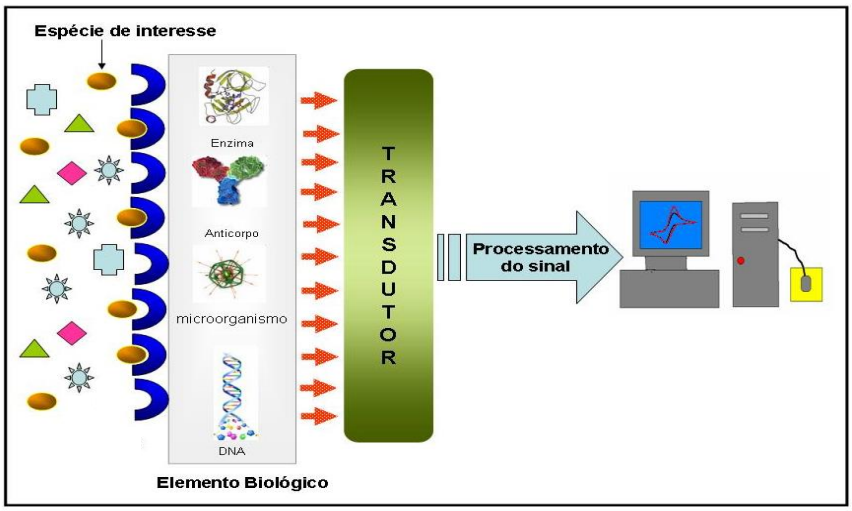

Fonte: Elaborada pela autora**.**

A molécula biológica que reconhecerá o analito de interesse é imobilizada no transdutor. O conhecimento do método adequado de imobilização é muito importante uma vez que este procedimento influi em muitas das características desejáveis para os biossensores (MARQUES; YAMANAKA, 2008). Segue na tabela 4 a representação das principais técnicas de imobilização e suas características.

Na construção dos biossensores, a biocompatibilidade da superfície eletrônica e a imobilização das moléculas constituem fatores responsáveis pelo bom desempenho e estabilidade do sistema (ZHANG et al., 2000; LOJOU; BIANCO, 2006). As moléculas mais utilizadas são as enzimas seguidas pelos anticorpos, entretanto, diferentes moléculas de origem biológica podem ser utilizadas em biossensores como células, organelas, DNA, lectinas e outras (LIU; LIN, 2007; CHINALIA et al., 2008). Existem ainda, os materiais abióticos que mimetizam moléculas biológicas como éteres de coroa e polímeros molecularmente impressos (TAN et al., 2001; FRANZOI et al., 2009).

Tabela 4: Principais metodologias de imobilização de biomoléculas.

Tipos de imobilização	Princípio	Desenho esquemático
Oclusão	Aprisionamento da molécula biológica dentro dos espaços intersticiais das ligações covalentes de um polímero insolúvel.	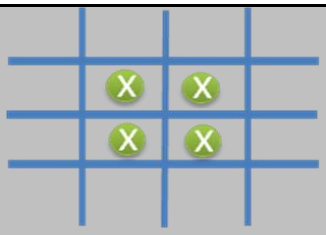
Ligação covalente	Ligação covalente dos grupos funcionais não ativos a grupos reativos ligados na superfície solida do suporte insolúvel.	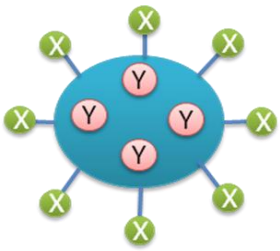
Adsorção	Interação do tipo iônica, ligações de hidrogênio ou hidrofóbicas a superfície do eletrodo.	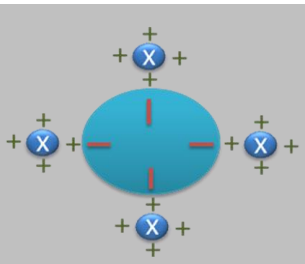
Encapsulamento	Confinamento das moléculas biológicas em pequenas esferas que permitem somente a movimentação dos substratos e produtos da interação molécula biológica substrato	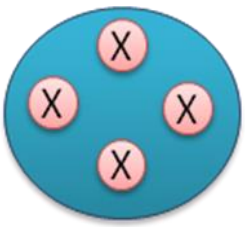

Cada tipo de interação da molécula biológica com o analito deve ser previamente estudada a fim de verificar se a mesma será passiva de detecção pelo transdutor escolhido. Um exemplo disso é o biossensor biocatalítico baseado em elementos que favorecem a ocorrência de reações químicas a partir de um ou mais substratos, havendo a formação de um ou mais produtos, sem o consumo do biocatalisador, que pode ser regenerado e reutilizado (MARAZUELA; MORENO-BONDI, 2002). Os tipos de biocatalisadores

comumente utilizados são as enzimas, células e tecidos. O biossensor por bioafinidade, de outra forma, envolve anticorpos e ou antígenos, ligação protéica ou receptor protéico, o qual forma um composto complexo com o correspondente ligante. Este complexo é estável o bastante para resultar em um sinal de transdução (RIZZONI; HARTLEY, 2000).

O Transdutor, componente que processa o sinal no biossensor transforma o sinal gerado no processo de reconhecimento analito/bioreceptor em um sinal mensurável. De acordo com o princípio de energia envolvida na transdução, os transdutores podem ser classificados em: **eletroquímicos** baseado em propriedades elétricas como corrente, potencial, condutividade, resistência elétrica, etc. (amperométricos, condutimétricos, potenciométricos e impedimétricos) (WU et al., 2007), **eletromagnéticos** são baseados na análise das variações na freqüência de oscilação de um cristal piezoelétrico (microbalança de cristal de quartzo, QCM, do inglês *Quartz Crystal Microbalance*) (PAVEY et al., 2003), **ópticos** baseado nos fenômenos de ondas evanescentes (ressonância de plásmon de superfície, SPR, do inglês *Surface Plasmon Resonance*) (TANG et al., 2006) e os **calorimétricos** (CHAUBEY; MALHOTRA, 2002). O transdutor a ser utilizado juntamente com o material biológico, deve detectar apenas um reagente ou produto específico, não respondendo a outras substâncias presentes na amostra a ser analisada.

A escolha de um determinado transdutor não depende apenas do elemento de reconhecimento selecionado, já que este determina quais variações das propriedades físico-químicas ocorreriam em função da interação, mas depende também de outros fatores como tempo de resposta, seletividade e sensibilidade (RICCARDI et al., 2002).

2.2.1 Imunossesores

Quando o reconhecimento da molécula de interesse é dado pela formação de imunocomplexos, este biossensor recebe o nome de imunossensor. (LUPPA et al., 2001). Os imunossensores resultam em respostas altamente seletivas, pois não somente a sensibilidade deve ser considerada, mas também a alta especificidade (RICCARDI et al., 2002).

Existem diversos métodos através dos quais é possível monitorar o sinal resultante das interações antígeno-anticorpo (Ab-Ag) e obtê-los na forma de dados que possam ser tratados posteriormente. Estes dispositivos podem monitorar as reações imunológicas na superfície sensora com alta sensibilidade e especificidade, sendo uma importante ferramenta para análise da dinâmica da interação antígeno-anticorpo (CHEN et al., 2009).

Os anticorpos ou imunoglobulinas são glicoproteínas produzidas pelos plasmócitos em resposta a substâncias estranhas ao organismo, os antígenos. A característica básica da reação antígeno-anticorpo é a especificidade, representada por uma estreita relação de complementaridade entre as estruturas tridimensionais das duas moléculas (Figura 9). Esta complementaridade permite a aproximação máxima entre os sítios de ligação das moléculas de antígeno, os epítopos e o anticorpo. As forças de interação moleculares no complexo "antígeno-anticorpo" não são covalentes (Van der Waals, ligação eletrostática, ponte de hidrogênio ou ligações hidrofóbicas) e, embora sejam individualmente fracas, a multiplicidade das uniões leva a uma considerável energia de coesão (TSEKENIS et al. 2008)

Figura 9: Desenho esquemático imunocomplexo.

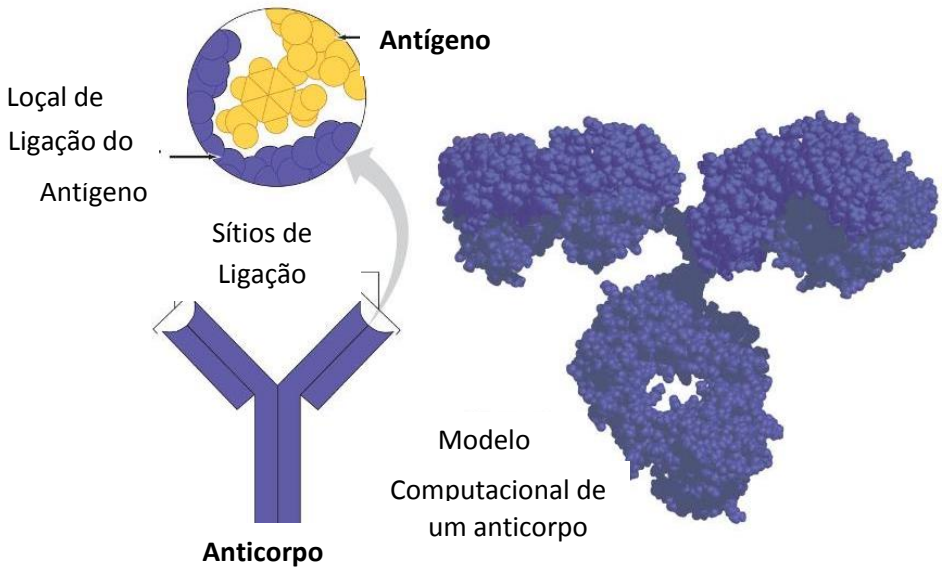

Fonte:http://drcercone.iculearn.com/bio2/wpcontent/uploads/Lectures/immune%20system/Immune_system10.html. Acesso em: 20/12/2013.Adaptado pela autora.

2.2.1.1 *Imunossensores eletroquímicos amperométricos*

Os transdutores eletroquímicos são os mais comumente utilizados em biossensores, principalmente por proporcionarem vantagens como: simplicidade, rapidez na resposta, menor custo, elevada sensibilidade, portabilidade e serem compatíveis com as tecnologias de micro fabricação (JIN et al., 2007).

Biossensores eletroquímicos têm como princípio básico a detecção de espécies eletroativas consumidas e ou geradas durante o processo de interação do elemento biológico com seu substrato específico (MEHRVAR; ABDI, 2004). Esses sensores são projetados através do acoplamento de moléculas biológicas à superfície eletródica, que respondem ao serem aplicados impulsos elétricos, tais como corrente (I) ou potencial (E) (SADIK et al., 2009).

A detecção de glicose usando a enzima glicose oxidase acoplada a um eletrodo para oxigênio de Clark foi o primeiro biossensor amperométrico, desenvolvido por Updike e Hicks Revisão Bibliográfica 21 em 1967 (HABERMÜLLER et al., 2000). Desde então, enzimas têm sido usadas em conjunto com diferentes materiais de eletrodo para produzir biossensores amperométricos. Os biossensores amperométricos são assim denominados devido ao seu mecanismo de transdução. Durante as medidas amperométricas é mantido um potencial constante entre o Eletrodo de Trabalho (ET) e o Eletrodo de Referencia (ER). A corrente gerada pela oxidação ou redução de espécies eletroativas na superfície do Eletrodo de Trabalho é medida e o sinal gerado é diretamente proporcional a concentração das espécies eletroativa (SCHUHMANN et al., 2000; LOWINSOHN et al., 2006). Essa corrente observada a partir de oxi-redução é faradáica, denominada assim por obedecer a lei de Faraday, a qual a corrente faradáica gerada é produzida pela reação redox de espécies eletroativas na superfície sensora, sendo diretamente proporcional à concentração do analito (CHAUBEY; MALHOTRA, 2002). Este processo obedece à lei de Faraday, a qual determina que a quantidade de

reagentes formados ou consumidos na interface do eletrodo é proporcional à corrente (LOWINSOHN et al., 2006).

Os biossensores amperométricos se classificam em três gerações, podendo ser de primeira, segunda e terceira geração, de acordo com o processo envolvido na transferência de cargas, reconhecimento do analito, geração e processamento do sinal (i) pela eletroatividade do substrato ou produto enzimático - biossensores de primeira geração; (ii) pelo auxílio de mediadores, livres em solução ou imobilizados juntamente com a enzima - biossensores de segunda geração - e, finalmente, (iii) pela transferência eletrônica direta entre a superfície do eletrodo e o centro ativo da enzima - biossensores de terceira geração (FREIRE; PESSOA, 2003).

No caso de imunossensores eletroquímicos, o monitoramento da corrente elétrica pode ser feito através do uso de marcadores da reação, tendo em vista que a reação é de afinidade entre o anticorpo e o antígeno. Sendo assim, o anticorpo ou o antígeno pode ser marcado, por exemplo, com fluoróforos, partículas magnéticas e enzimas. A biomolécula marcada com enzima é conhecida como conjugado. Por conseguinte, a medida da corrente elétrica será correlacionada em função do produto da reação enzimática após a adição do substrato na célula eletroquímica. Portanto, a revelação da interação antígeno-anticorpo segue o mesmo principio dos biossensores catalíticos, porém a determinação do analito é baseada na reação de afinidade e não na reação catalítica (THÉVENOT et al., 2001; RICCARDI et al., 2002).

Além dos biossensores amperométricos que utilizam marcadores (*label*) para a detecção do analito como foi visto anteriormente, é possível realizar o monitoramento do analito sem o uso de marcadores (*label free*) (Figura 10). Na literatura é crescente o numero de trabalhos sem o uso de marcadores (WU et al., 2007; LEE et al., 2007). Essa configuração de biossensor oferece algumas vantagens em relação aos sistemas que utilizam marcadores: detecção em tempo real, menor custo da análise, redução nas etapas de manipulação e redução nos resultados falso-positivos (DANIELS; POURMAND, 2007; NIRSCHL et al., 2011). Nesse biossensores a detecção é baseada nas mudanças das propriedades elétricas da superfície, por exemplo: aumento na constante elétrica e resistência, na presença da molécula-alvo.

Figura 10: Desenho esquemático de imunossensores amperométricos que utilizam marcadores (*label*) e sem o uso de marcadores (*label free*).

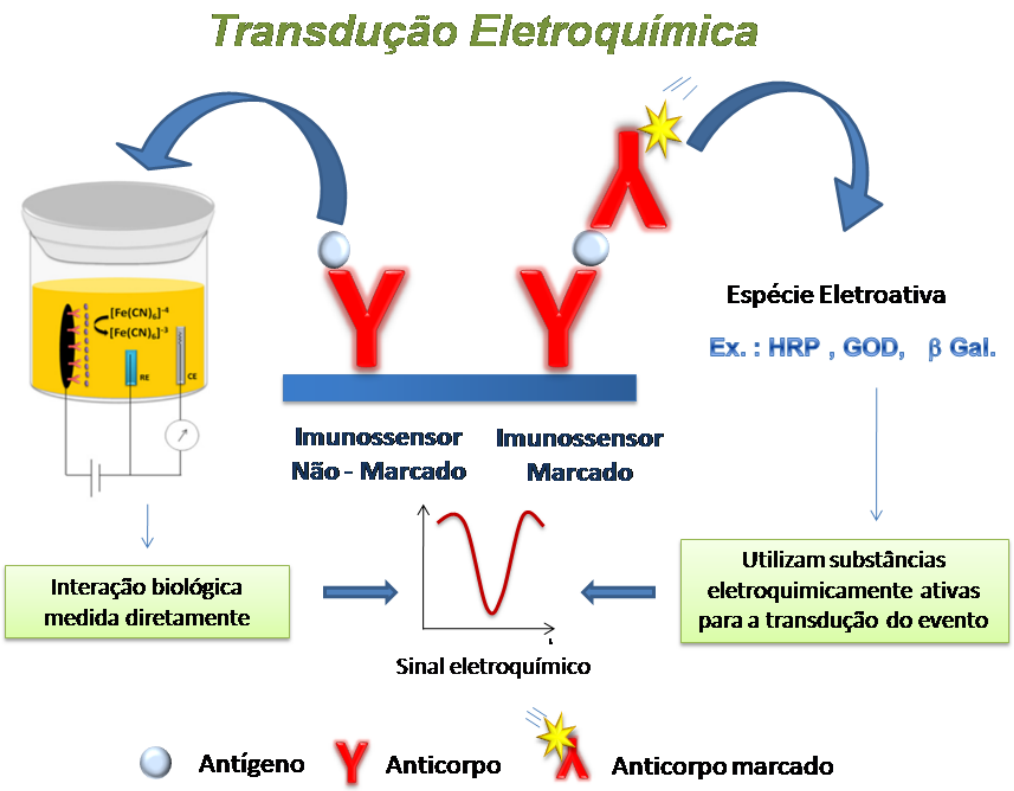

Fonte: Elaborada pela autora.

2.2.2 Técnicas eletroanalíticas

A eletroquímica surgiu como uma ferramenta para diversos tipos de analises e posteriormente associada a uso dos biossensores. As técnicas eletroanalíticas possibilitam estabelecer relação entre a concentração do analito e as propriedades elétricas como: corrente, potência, condutividade, resistência e cargas elétricas. A técnica se refere a fenômenos químicos associados à transferência de elétrons, que podem ocorrer homogeneamente em solução, ou heterogeneamente na superfície do eletrodo (LOWINSOHN et al., 2006).

As técnicas eletroanalíticas apresentam vantagens frente às técnicas tradicionais. A principal delas é a possibilidade, na maioria das vezes, de

análises direta da amostra sem a necessidade de etapas de separação ou pré-tratamento (POWER; MORRIN, 2013). Além disso, pode favorecer opções viáveis para mediar fproblemas na construção de novos métodos para o diagnóstico clínico (JUSTINO et al., 2010). Uma das vantagens da eletroquímica em relação à química convencional é a não utilização de grandes quantidades de reagentes nas análises eletroquímicas, além do fácil controle de variáveis que combinadas de formas diversas levam a técnicas eletroquímicas particulares, tais como: voltametria cíclica, voltametria de onda quadrada, voltametria de pulso diferencial, dentre estas, a voltametria cíclica teve destaque neste trabalho.

2.2.2.1 Voltametria Cíclica

A Voltametria cíclica compreende um grupo de métodos eletroanalíticos nos quais as informações sobre a concentração do analito são derivadas a partir das medidas de corrente em função do potencial aplicado sob condições de completa polarização do eletrodo de trabalho, através do uso de microeletrodos (KIMMEL et al., 2012). Consiste numa técnica de varredura reversa do potencial, onde o potencial aplicado ao eletrodo é variado numa velocidade conhecida, e ao atingir o potencial final desejado, a varredura é revertida ao valor inicial, na mesma velocidade (LINDINO et al., 2006). Obtém-se, como resposta a essa perturbação, por exemplo, um par de picos, catódico (Ipc) e anódico (Ipa) (Figura 11).

Para a realização da técnica, é necessário um potenciostato com gerador de programa de potencial, conectado a um computador para registrar os gráficos de corrente em função do potencial, de uma célula convencional de três eletrodos e uma solução contendo o analito e eletrólito suporte. Obtém-se, como resposta a essa perturbação, por exemplo, um par de picos, catódico e anódico. Para conseguir isso, aplica-se uma voltagem chamada onda triangular à célula eletrolítica (Figura 11).

Figura 11: Representação gráfica da técnica de voltametria cíclica: (a) variação linear do potencial *vs* tempo e (b) voltamograma cíclico onde observa-se, potencial do pico anódico e catódico (Epa e Epc) e corrente de pico anodico e catódico (Ipa e Ipc), para uma reação reversível.

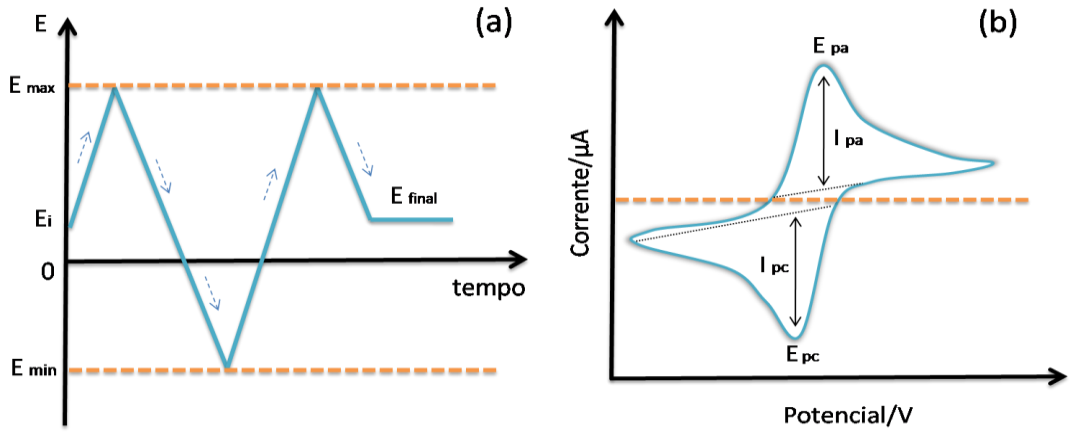

Fonte: BARD & FAULKNER (2006) e BRETT & BREET (1993).

Considerando os parâmetros eletroquímicos mais importantes, ou seja, os potenciais de picos catódicos e anódicos (Epc e Epa), as correntes de picos catódico e anódico (Ipc e Ipa) e os potenciais de meia onda ($E_{1/2}$) ou pico de meia altura (Ep2).É possível também analisar o processo eletródico ocorrido, a dependência do potencial e da corrente com a variação da velocidade de varredura, com a concentração da substância eletroativa a partir da adição de eletrófilos ou prótons, com análise baseada em testes de diagnósticos. Isso permite obter informações importantes de reversibilidade e irreversibilidade e do processo de transferência de elétrons, da presença de reações químicas acopladas, adsorção e fenômenos catalíticos, além de se poder caracterizar o fenômeno que controla a corrente de pico (REIS et al., 2009). Geralmente a própria feição da onda é que é indicativa de processo reversível; presença de um par de picos (catódico e anódico) de mesma altura, com potenciais de picos separados por uma distância de 59/n mv (caso as espécies oxidadas e reduzidas sejam estáveis). Já o espectro eletroquímico de um sistema

irreversível evidencia a completa ausência de pico reverso, apesar de esse não ser o único critério de análise (GRIESHABER et al., 2008).

2.2.3 *Tecnologia de eletrodos impressos*

O desenvolvimento de eletrodos impressos de carbono (EIs) ou *screen printing* tem atendido a demanda do mercado oferecendo um completo sistema de eletrodos projetados com grande simplicidade, economia, alta reprodutibilidade e facilidade de fabricação (BERGAMINI; ZANONI, 2005). Por estas razões, o uso dessa tecnologia na produção serial de eletrodos para a determinação eletroquímica de uma ampla faixa de substâncias está em pleno crescimento. (NASCIMENTO, VALBERES B.; ANGNES, 1998).

Este tipo de configuração de eletrodos é baseado na deposição de finos filmes sobre substratos inertes, sendo bastante adequada para produção em massa de dispositivos portáteis. Os EIs (figura 12) são produzidos a partir da impressão de diferentes tintas e vários tipos de substratos inertes, a maioria de PVC policarbonato poliéster ou cerâmica (WANG et al., 2008).

Figura 12: Desenho esquemático da fabricação de eletrodo impresso de trabalho.

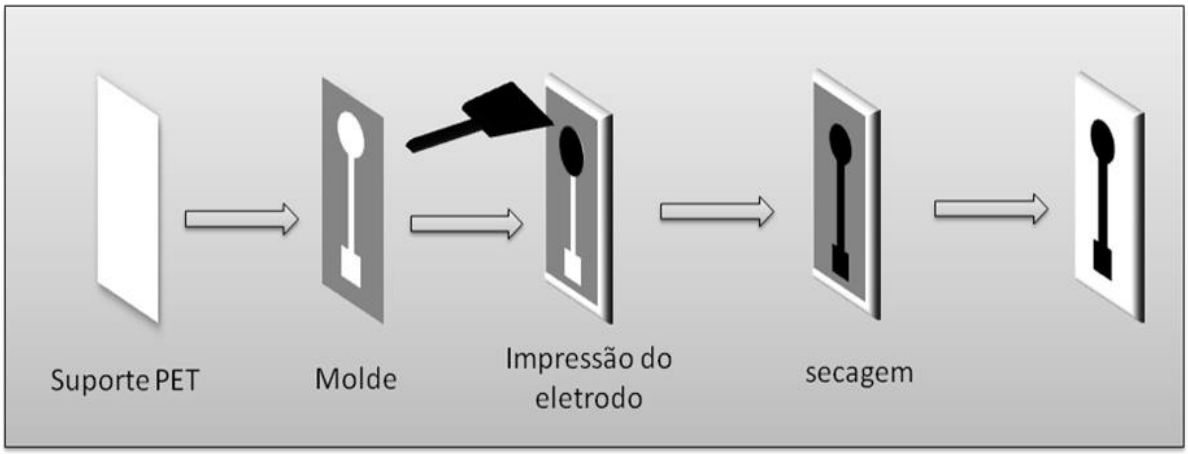

Fonte: Elaborado pela autora.

Um dos principais aspectos dos EIs, que os tornam extremamente atrativos quando se busca o desenvolvimento de sensores comerciais, é a possibilidade de total automação na fabricação de um sistema completo contendo os eletrodos de trabalho, auxiliar e referência, todos impressos no mesmo suporte (figura 13).

Figura 13: Desenho esquemático de eletrodo impresso com sistema tri-eletródico.

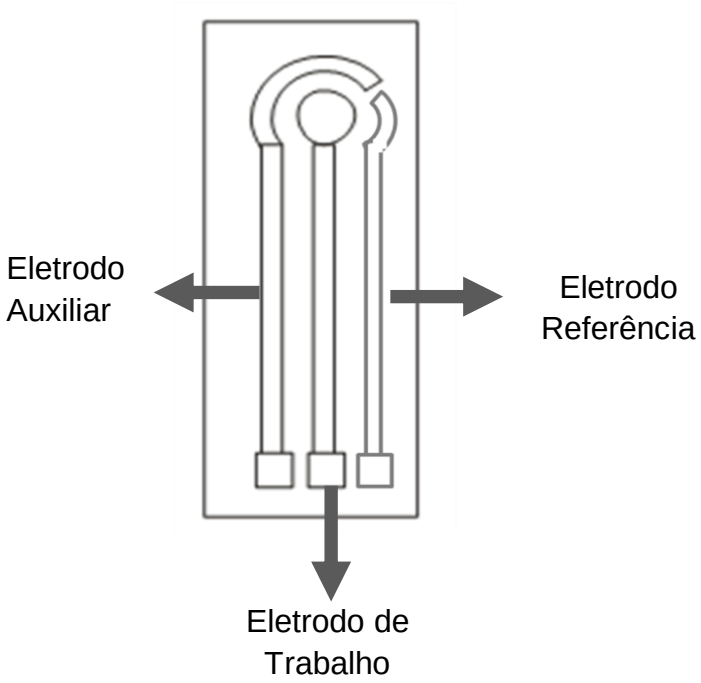

Fonte: Elaborado pela autora.

Tintas de carbono ou metálicas (platina, ouro e prata) têm sido comumente utilizadas para impressão de sensores. Em particular, as tintas de carbono tem se destacado como filme condutor mais utilizado na fabricação de EIs, devido às suas características atrativas, tais como ampla janela de potencial, boa condutividade elétrica, estabilidade, baixa corrente residual e baixo custo (USLU; OZKAN, 2007; ZHANG et al., 2011). O material impresso pode ser alterado pela adição de diferentes substâncias, tais como metais, enzimas, polímeros, agentes complexantes, dentre outros. Assim, a

seletividade e a sensibilidade requeridas para cada análise é determinada pela composição da pasta utilizada para impressão dos eletrodos (RENEDO et al., 2007).

A modificação dos EIs com diferentes mediadores químicos tem sido uma alternativa comum nos sistemas de detecção, obtendo dispositivos cada vez mais seletivos (AVRAMESCU et al., 2002). O uso desses compostos no desenvolvimento de EIs possui muitas vantagens, dentre elas estão: aumento da reprodutibilidade; medidas menos dependentes da concentração de O_2, determinação do potencial de trabalho do eletrodo pelo potencial de oxidação do mediador e diminuição da interferência de espécies indesejadas (CHAUBEY; MALHOTRA, 2002). Em geral, o mediador é misturado diretamente à pasta a ser utilizada na fabricação dos eletrodos. O seu papel é estabelecer uma espécie de contato elétrico entre o sítio ativo da enzima e a superfície sensora, através do seguinte mecanismo: o mediador sofre um processo de redução no sítio ativo da enzima, reconduzindo-a a seu estado fundamental, em seguida o mediador sofre um processo de oxidação na superfície do eletrodo, sendo também reconduzido ao seu estado fundamental, completando um ciclo que restaura a enzima e o mediador (MELLO; KUBOTA, 2002).

2.3 A nanotecnologia no desenvolvimento de biossensores eletroquímicos

Com o exponencial desenvolvimento nos últimos anos da ciência em nanoescala, alguns termos surgiram para instituir essa área do conhecimento: o termo *nanociência* vem sendo utilizado para descrever a preparação e o estudo do comportamento de materiais em escala nanométrica, enquanto que o termo *nanotecnologia* se refere ao desenvolvimento e aproveitamento desses materiais com propriedades diferenciadas ou potencializadas (ISLAM; MIYAZAKI, 2009).

A nanotecnologia tem assumido um papel importante no desenvolvimento de biossensores (VASHIST et al., 2012). A utilização de

materiais na escala nanométrica (em termos gerais, uma partícula é considerada nanométrica quando apresenta um tamanho inferior az 100 nm) em biossensores tem permitido aumentar a quantidade de proteínas imobilizadas na superfície do transdutor, promover a reação eletroquímica e aumentar o sinal do bioreconhecimento. A sensibilidade será o maior atributo que o uso de nanomateriais oferece na construção de um biossensor (ZHANG et al., 2009).

2.3.1 Nanotubos de carbono

Durante vários séculos, o diamante e o grafite eram os únicos materiais conhecidos formados somente por carbono. Em 1985, os cientistas descobriram que os átomos de carbono também podiam se organizar no espaço como bolas, os fulerenos (TERRONES, 2004). As pesquisas científicas envolvendo estruturas baseadas em carbono puro cresceram significativamente após a descoberta dos fulerenos, o que ocasionou um maior interesse no estudo dessas estruturas, levando à descoberta de uma série de novas formas, como os nanotubos de carbono (NTCs), os quais foram obtidos por Lijima em 1991 como subproduto na síntese de fulerenos (SOUZA, 2007) 2007). Desde então numerosas pesquisas têm sido feitas para elucidar o uso deste nanomaterial em distintos dispositivos.

Os NTCs possuem uma das mais simples composições químicas e configurações atômicas, mostrando uma diversidade de riqueza entre os nanomateriais (RIVAS et al., 2007). Desde a sua descoberta, os NTCs foram objeto de inúmeras investigações devido a sua estrutura original conter propriedades eletrônicas e mecânicas que os tornam um material muito atrativo para uma gama de aplicações (SGOBBA; GULDI, 2009).

A estrutura química dos nanotubos de carbono é formada por uma folha de grafeno enrolada (que consiste em um arranjo bidimensional de átomos de carbono com hibridização sp2, ligados em hexágonos (Figura 14), cujo empilhamento resulta na estrutura do grafite), em dimensões nanométricas, formando uma cavidade interna oca (AWASTHI et al., 2005; RIVAS et al., 2007).

Figura 14: Estrutura química básica dos nanotubos de carbono.

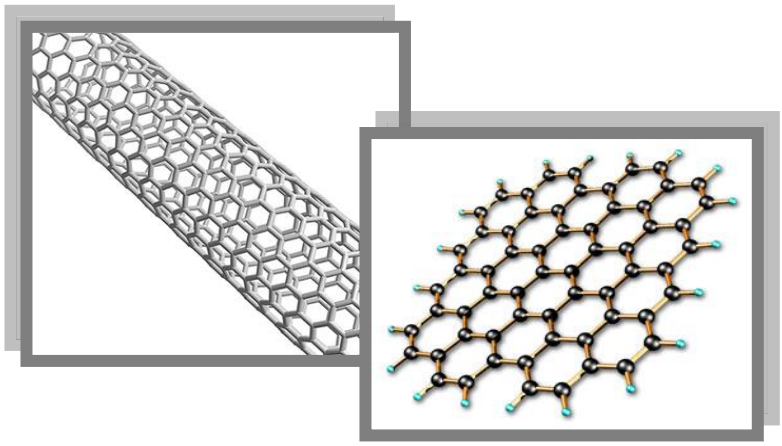

Fonte: www.fp6-nano.com/2007/wp-content/uploads/Buckytubes2.jpg. Acesso em 16/012/2013.

Estruturalmente, os NTCs podem ser divididos em duas classes: os Nanotubos de Carbono de Única Parede (NTCsUP) e Nanotubos de Carbono de Múltiplas Parede (NTCsMP), representados na Figura 15.

Figura 15: Ilustração dos Nanotubos de Carbono de Única Parede (NTCsUP) (a) e os de Carbono de Múltiplas Parede (NTCsMP) (b).

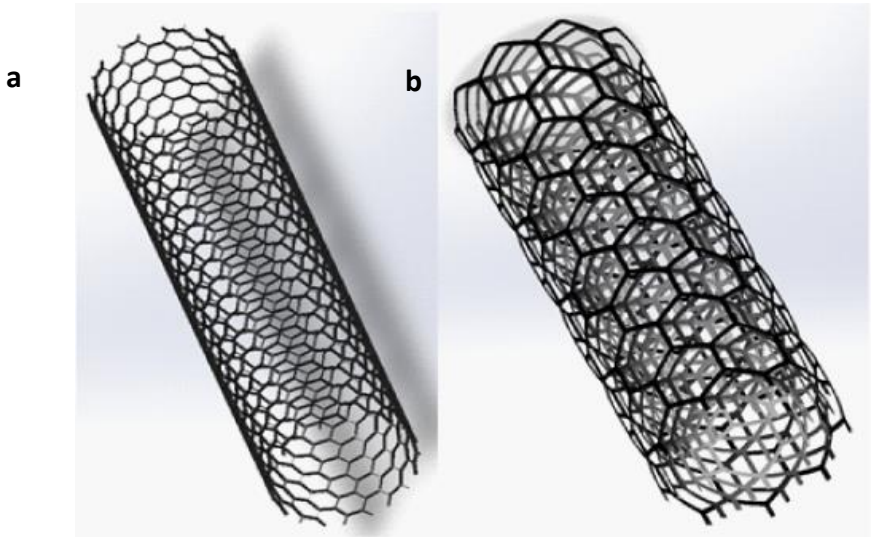

Fonte: http://www.omicsonline.org/2157-7439/2157-7439-3-e121.php. Acesso em: 20/12/2013.

Nanotubos de carbono de única parede são formados por um único cilindro de grafeno e podem ser obtidos isoladamente ou em bandos contendo dezenas de nanotubos (GROBERT, 2007). A maneira pela qual a folha de grafeno é enrolada determina a estrutura dos nanotubos e suas propriedades. Um nanotubo pode ser construído a partir de uma folha de grafeno enrolada de tal forma que coincidam dois sítios cristalograficamente equivalentes de sua rede hexagonal (VASHIST, 2012).

Os nanotubos de carbono de múltiplas paredes são constituídos de dois ou mais cilindros concêntricos de grafeno espaçados uns dos outros por 0,34 nm, de maneira análoga à separação existente entre os planos (002) do grafite (BELIN; EPRON, 2005). A interação existente entre estes tubos é do tipo Van der Waals. Vários estudos demonstram que o uso de eletrodos modificados com NTCsMP contribui favoravelmente para detecções analíticas por resultar em dispositivos de sensibilidade elevada, além de sua estabilidade e baixo custo (HEGDE et al., 2009).

Os NTCs têm encontrado várias aplicações, dentre elas: ponteiras para microscopia de varredura por sonda, como transistores de efeito de campo, retificadores eletrônicos, eletrodos para supercapacitores e para sensores (RIVAS et al., 2007; HEGDE et al., 2009). A primeira aplicação dos NTCs para biossensores foi proposta em 1996 por (BRITTO et al., 1996)BRITTO et al. (1996). Desde então, NTCs vêm sendo usados para preparação de diversos biossensores, aumentando a eficiência das interações eletrodo-proteína, resultando em correntes faradaicas muito mais altas.

Os NTCs têm elevada razão área superfície/volume, alta condutividade elétrica, boa estabilidade química e resistência mecânica. Além disso, conferem aos eletrodos modificados maior área eletroativa, promovem reações de transferência de elétrons e baixos sobrepotenciais, melhoram a reversibilidade de alguns processos, permitem melhor imobilização de enzimas, antígeno, anticorpo, ácidos nucléicos(OU et al., 2007; REZAEI; DAMIRI, 2008).

Diversas vantagens da aplicação dos NTCs ainda não foram completamente exploradas por causa da dificuldade em se obter NTCs dispersos; embora os NTCs sejam solubilizados por meio da funcionalização de suas paredes. Através da modificação dos NTCs é possível torná-los

seletivos. Isto pode ser alcançado pela correta funcionalização conjugando grupos reativos, tais como grupos carboxílicos ou aminas, assim os NTCs são imobilizados facilmente e ficam mais estáveis na superfície do eletrodo. Tal fato é muito interessante para o desenvolvimento de biossensores em que as ligações de materiais biológicos são desejadas (FENG et al., 2003; YUN et al., 2007).

2.3.2 Nanopartículas Metálicas

Os nanomateriais tais com as nanopartículas metálicas são de extrema importância no campo da Nanotecnologia devido às suas propriedades físicas e químicas, com vantagem na interação com biomoléculas que faz prever inúmeras aplicações a nível biotecnológico (SCHMID, 2011).

Inúmeros são os empregos das nanopartículas metálicas. Estas podem ser usadas para a modificação da superfície de eletrodos, ou para modificar moléculas biológicas como enzimas, anticorpos ou oligonucleotídeos (MURPHY, 2006). Uma das funções mais importantes das nanopartículas é a alta atividade associada com enzimas para muitas reações, especialmente as nanopartículas de metais nobres (EL-ANSARY, 2010). Tal propriedade possibilita que estas sejam utilizadas em biossensores eletroquímico pela capacidade de promover uma rápida transferência de elétrons entre o eletrodo e a proteína (MURPHY, 2006; KAUSHIK et al., 2008).

2.4 Polímeros condutores em sensores

Os Polímeros Intrinsecamente Condutores (PIC) constituem uma classe de materiais poliméricos que tem recebido especial interesse da comunidade científica nos últimos 30 anos devido ao seu enorme potencial de aplicações nas mais diversas áreas do conhecimento, todavia, o uso dos polímeros conjugados em sensores é uma das aplicações que mais cresceu nos últimos anos(MÜLLER et al., 2011). Esse crescimento está relacionado com a possibilidade do uso de suas propriedades elétricas, eletroquímicas e óticas para converter informações físicas e químicas, tal como concentração,

atividade e pressão parcial num sinal analiticamente mensurável (MEDEIROS et al., 2012) .

Os sensores usando polímeros podem ser ferramentas de baixo custo na qualificação ou quantificação de um grande número de substâncias químicas e biológicas, indústrias farmacêuticas, ao diagnóstico clínico e detecção de armas químicas e biológicas (D. KHODAGHOLY, G.G. MALLIARAS, 2012).

Polímeros têm atraído muito interesse como matrizes para imobilização de biomoléculas, pois podem servir como intermediários nos processos de interação entre o receptor e o analito e na transdução do sinal com o objetivo de melhorar o tempo de resposta, a sensibilidade e o limite de detecção de biossensores para diversas aplicações que vão desde o diagnóstico de doenças até determinação de contaminantes em água (OLIVEIRA et al., 2013).

2.4.1 Hidrocloreto de Polialilamina (PAH)

Filmes poliméricos têm sido empregados em eletrodos quimicamente modificados e usados no desenvolvimento de sensores para proteger a superfície dos eletrodos de impurezas, bloquear interferentes, imobilizar biocomponentes, incorporar mediadores e fornecer biocompatibilidade (SILVA; CARAPUÇA, 2006). Devido à grande variedade das características dos polímeros, suas propriedades podem ser exploradas conforme o interesse. Dessa forma, o polímero eletroativo (eletrocatálise), o quimicamente ativo (propriedades ligantes ou de troca-iônica para pré-concentração) e o inerte (apenas exclusão de interferentes) são frequentemente utilizados para aplicações em dispositivos eletrônicos inovadores (ZHAO et al., 2006).

Dentre os polímeros, o hidrocloreto de polialilamina (PAH) tem recebido grande atenção por sua estabilidade química em condições ambientais e facilidade de polimerização (HO et al., 2002). O PAH é um polieletrólito fraco com uma natureza básica (pKa = 9,67; massa do monômero equivalente = 93,55) com partes hidrofílicas (grupos amina) e hidrofóbicas (estrutura hidrocarbônica), cujas características como densidade de carga e conformação, em solução, podem ser alteradas com pH e força iônica (ARIGA

et al., 1997; COOPER; STONE, 1998). A estrutura química do PAH está representada na Figura 16**.**

Figura 16: Estrutura do policátion PAH.

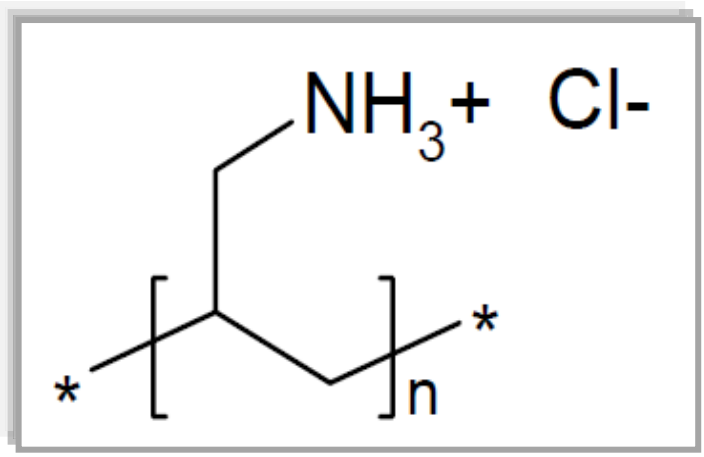

Fonte: chemistrytackexchange.com/ what-is-the-specific-structure-of-polyallylamine-hydrochloride. Acesso em 20/12/2013.

O filme PAH tem sido frequentemente usado na preparação de multicamadas, produzindo novos materiais multifuncionais para diversos fins, que vão desde sensores analíticos a membranas de nanofiltração ou materiais de liberação controlada (SILVA; CARAPUÇA, 2006). Na química de superfícies, RUBNER et al. (1998) mostraram que a polaridade de uma superfície pode ser alterada com a presença de uma única bicamada de polieletrólito adsorvido (YOO et al., 1998; BARROS, 2006).

Neste contexto, o PAH mostra-se como uma ótima matriz para a imobilização dos NTCs carboxilados (COO^-) que irá interagir eletrostaticamente com os grupos NH_3^+ do PAH, favorecendo ao eletrodo uma superfície nanoestruturada para a fabricação de imunossensores (BARRETO, M. L., & TEIXEIRA, 2008).

2.4.2 Tiofeno

O tiofeno é um hidrocarboneto constituído por 4 átomos de Hidrogênio (H) e um de Enxofre (S) ligados a 4 átomos de *Carbono* (C), formando um pentágono regular podendo ser considerado, por isso, uma molécula cíclica (Figura 17). Compostos análogos ao tiofeno são os furanos e o pirrol os quais são respectivamente, o Oxigênio (O) e o Nitrogênio (N) no lugar do enxofre. Devido à sua estrutura anelar e ao fato de possuir no anel um elemento diferente do carbono (sendo os mais comuns o oxigênio, enxofre ou nitrogênio), o tiofeno é um composto heterocíclico (MCQUADE et al., 2000).

Tendo em conta a sua configuração eletrônica, ele faz parte dos hidrocarbonetos aromáticos visto que os elétrons que pertencem à segunda ligação são capazes de se mover por todo o anel. Por esta razão a fórmula estrutural do tiofeno pode, e é geralmente representada por um círculo no interior do pentágono. O politiofeno (PT) possui boa mobilidade de cargas, capacidade doadora de elétrons, alta estabilidade química, térmica e elétrica (NOWACKI, 2011).

Figura 17: Estrutura do policátion Tiofeno

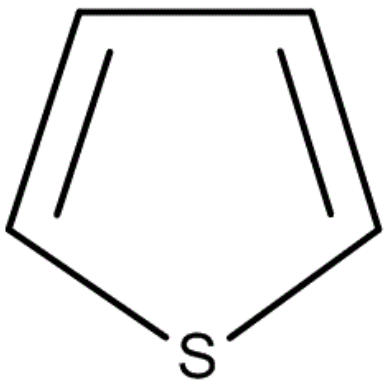

Fonte: http://commons.wikimedia.org /wiki/ File:Thiophene_structure.png. Acesso em 20/12/2013.

As propriedades eletrônicas dos politiofenos e dos oligômeros de tiofeno estão associadas à grande conjugação e deslocalização de elétrons π ao longo da cadeira, responsável pelo comportamento ótico não linear e pela condutividade eletrônica. É a densidade e a distribuição que determinam que as moléculas de tiofeno comportem-se como condutores para a captura de eletricidade.(SANTOS, 2008).

3 OBJETIVOS

3.1 Objetivo geral

Avaliar a contribuição de nanomateriais em imunossensores voltados para a detecção de NS1, um marcador da fase aguda da dengue viral.

3.2 Objetivos específicos

1 Modificar quimicamente as superfícies dos eletrodos de carbono vítreo com base na deposição dos NTCs-COOH e incorporação do filme polimérico;

2 Caracterizar a superfície modificada com NTCs-COOH e PAH por microscopia eletrônica de varredura (MEV) e microscopia de força atômica (AFM);

3 Otimizar parâmetros experimentais empregados na detecção dos anticorpos NS1 dos immunosensores;

4 Viabilizar a realização do imunoensaio completo do tipo “sanduíche”, usando como princípio a captura do antígeno NS1 do DENV e a sua detecção através de um sistema enzimático da reação com a peroxidase;

5 Elaborar eletrodos impressos associados com monômero Tiofeno para constituírem plataformas descartáveis para detecção da NS1;

6 Caracterizar as respostas dos imunossensores, através da técnica da voltametria cíclica;

7 Estabelecer a curva de calibração dos imunossensores para a detecção da NS1 obtidos de amostras comerciais em tampão;

8 Caracterizar o sistema dos imunossensores propostos quanto a sua sensibilidade, especificidade e reprodutibilidade das suas respostas em amostras sanguíneas; CEP/UPE 193/09.

4 Referência

AASKOV, M. J. G. Dengue. **Infectious Diseases**, v. 4, n. September, p. 66–71, 2003.

AHAMMAD, A. J. S.; LEE, J.; RAHMAN, A. Electrochemical Sensors Based on Carbon Nanotubes. **Sensors**, v. 9, p. 2289–2319, 2009.

ALCON, S.; TALARMIN, A.; DEBRUYNE, M.; et al. Enzyme-Linked Immunosorbent Assay Specific to Dengue Virus Type 1 Nonstructural Protein NS1 Reveals Circulation of the Antigen in the Blood during the Acute Phase of Disease in Patients Experiencing Primary or Secondary Infections Enzyme-Linked Immunosorb. **Journal of clinical microbiology**, v. 40, n. 2, p. 376–381, 2002a.

ALCON, S.; TALARMIN, A.; DEBRUYNE, M.; et al. Enzyme-Linked Immunosorbent Assay Specific to Dengue Virus Type 1 Nonstructural Protein NS1 Reveals Circulation of the Antigen in the Blood during the Acute Phase of Disease in Patients Experiencing Primary or Secondary Infections Enzyme-Linked Immunosorb. **JOURNAL OF CLINICAL MICROBIOLOGY,**, v. 40, n. 2, p. 1–7, 2002b.

ALONSO-LOMILLO, M. A.; DOMÍNGUEZ-RENEDO, O.; FERREIRA-GONÇALVES, L.; ARCOS-MARTÍNEZ, M. J. Sensitive enzyme-biosensor based on screen-printed electrodes for Ochratoxin A. **Biosensors & bioelectronics**, v. 25, n. 6, p. 1333–7, 2010. Disponível em: <http://www.ncbi.nlm.nih.gov/pubmed/19914816>. Acesso em: 19/10/2013.

ARIGA, K.; LVOV, Y.; KUNITAKE, T. Assembling Alternate Dye−Polyion Molecular Films by Electrostatic Layer-by-Layer Adsorption. **Journal of the American Chemical Society**, v. 119, n. 9, p. 2224–2231, 1997.

AVRAMEAS, S. Coupling of enzymes to proteins with glutaraldehyde. **Immunochemistry**, v. 6, n. 1, p. 43–52, 1969.

AVRAMESCU, A.; ANDREESCU, S.; NOGUER, T.; et al. Biosensors designed for environmental and food quality control based on screen-printed graphite electrodes with different configurations. **Analytical and bioanalytical chemistry**, v. 374, n. 1, p. 25–32, 2002.

AWASTHI, K.; SRIVASTAVA, A.; SRIVASTAVA, O. N. Synthesis of Carbon Nanotubes. **Journal of Nanoscience and Nanotechnology**, v. 5, n. 10, p. 1616–1636, 2005.

BABACAN, S.; PIVARNIK, P.; LETCHER, S.; RAND, A G. Evaluation of antibody immobilization methods for piezoelectric biosensor application.

Biosensors & bioelectronics, v. 15, n. 11-12, p. 615–21, 2000. Disponível em: <http://www.ncbi.nlm.nih.gov/pubmed/11213222>. .

BARD, A. J.; FAULKNER, L. R. **Electrochemical methods: principles and applications. Electrochemical Methods: Principles and Applications**. 2001.

BARRETO, M. L., & TEIXEIRA, M. G. Dengue no Brasil: situação epidemiológica e contribuições para uma agenda de pesquisa. **Estudos Avançados**, v. 22, n. 64, p. 53–72, 2008.

BARROS, D. S. DE. **Estudo Espectroscópico e Morfológico de Filmes Automontados de Azocompostos**, 2006. Universidade Estadual de Campinas.

BEATTY, M. E.; BEUTELS, P.; MELTZER, M. I.; et al. Health economics of dengue: a systematic literature review and expert panel's assessment. **The American journal of tropical medicine and hygiene**, v. 84, n. 3, p. 473–88, 2011.

BELIN, T.; EPRON, F. Characterization methods of carbon nanotubes: a review. **Materials Science and Engineering: B**, v. 119, n. 2, p. 105–118, 2005.

BERGAMINI, M. F.; ZANONI, F. C. M. D. O. M. V. B. Análise voltamétrica do corante têxtil do tipo antraquinona empregando eletrodos de carbono impresso . **Análise**, v. 30, n. 2, p. 53–59, 2005.

BESSOFF, K.; DELOREY, M.; SUN, W.; HUNSPERGER, E. Comparison of two commercially available dengue virus (DENV) NS1 capture enzyme-linked immunosorbent assays using a single clinical sample for diagnosis of acute DENV infection. **Clinical and vaccine immunology : CVI**, v. 15, n. 10, p. 1513–8, 2008. Disponível em: <http://www.pubmedcentral.nih.gov/articlerender.fcgi?artid=2565928&tool=pmcentrez&rendertype=abstract>. Acesso em: 19/10/2013.

BLACKSELL, S. D.; JARMAN, R. G.; BAILEY, M. S.; et al. Evaluation of six commercial point-of-care tests for diagnosis of acute dengue infections: the need for combining NS1 antigen and IgM/IgG antibody detection to achieve acceptable levels of accuracy. **Clinical and vaccine immunology : CVI**, v. 18, n. 12, p. 2095–101, 2011. Disponível em: <http://www.pubmedcentral.nih.gov/articlerender.fcgi?artid=3232692&tool=pmcentrez&rendertype=abstract>. Acesso em: 19/10/2013.

BLACKSELL, S. D.; JARMAN, R. G.; GIBBONS, R. V; et al. Comparison of seven commercial antigen and antibody enzyme-linked immunosorbent assays for detection of acute dengue infection. **Clinical and vaccine immunology : CVI**, v. 19, n. 5, p. 804–10, 2012. Disponível em: <http://www.pubmedcentral.nih.gov/articlerender.fcgi?artid=3346317&tool=pmcentrez&rendertype=abstract>. Acesso em: 19/10/2013.

BLACKSELL, S. D.; MAMMEN, M. P.; THONGPASEUTH, S.; et al. Evaluation of the Panbio dengue virus nonstructural 1 antigen detection and immunoglobulin M antibody enzyme-linked immunosorbent assays for the diagnosis of acute dengue infections in Laos. **Diagnostic microbiology and infectious disease**, v. 60, n. 1, p. 43–9, 2008.

BLOK, J.; MCWILLIAM, S. M.; BUTLER, H. C.; et al. Comparison of a dengue-2 virus and its candidate vaccine derivative: Sequence relationships with the flaviviruses and other viruses. **Virology**, v. 187, n. 2, p. 573–590, 1992.

BRANDT, W. E.; CHIEWSLIP, D.; HARRIS, D. L.; RUSSELL, P. K. Partial purification and characterization of a dengue virus soluble complement-fixing antigen. **Journal of immunology (Baltimore, Md. : 1950)**, v. 105, n. 6, p. 1565–8, 1970.

BRASIL, M. DA SAÚDE-. Análise da situação das doenças transmissíveis no Brasil no período de 2000 a 2010. , p. 1–92, 2010.

BRASIL, M. DA SAÚDE-. **Dengue diagnóstico e manejo clínico criança**. 2011.

BRITTO, P. J.; SANTHANAM, K. S. V.; AJAYAN, P. M. Carbon nanotube electrode for oxidation of dopamine. **Bioelectrochemistry and Bioenergetics**, v. 41, n. 1, p. 121–125, 1996.

CAREY, D. E. Chikungunya and dengue: A Case of Mistaken Identity? **Journal of the History of Medicine and Allied Sciences**, v. XXVI, n. 3, p. 243–262, 1971.

CAVALCANTI, I. T.; GUEDES, M. I. F.; SOTOMAYOR, M. D. P. T.; YAMANAKA, H.; DUTRA, R. F. A label-free immunosensor based on recordable compact disk chip for early diagnostic of the dengue virus infection. **Biochemical Engineering Journal**, v. 67, p. 225–230, 2012. Elsevier B.V.

CHATERJI, S.; ALLEN, J. C.; CHOW, A.; LEO, Y.; OOI, E. Evaluation of the NS1 rapid test and the WHO dengue classification schemes for use as bedside diagnosis of acute dengue fever in adults. **The American journal of tropical medicine and hygiene**, v. 84, n. 2, p. 224–8, 2011.

CHAUBEY, A.; MALHOTRA, B. D. Mediated biosensors. **Biosensors & bioelectronics**, v. 17, n. 6-7, p. 441–56, 2002.

CHINALIA, F. A.; PATON, G. I.; KILLHAM, K. S. Physiological and toxicological characterization of an engineered whole-cell biosensor. **Bioresource technology**, v. 99, n. 4, p. 714–21, 2008.

COLLINGS, A. F.; CARUSO, F. Biosensors: recent advances. **Reports on Progress in Physics**, v. 60, n. 11, p. 1397–1445, 1997.

CONASS. Situação atual, desafios e estratégias para enfrentamento. ,2011. Disponível em: <http://www.conass.org.br/notas tecnicas/nt_05_2011_dengue.pdf>. .

COOPER, T. M.; STONE, M. O. Investigation of Self-Assembly upon Formation of an Electrostatic Complex of Congo Red and a Helical Peptide. **Langmuir**, v. 14, n. 23, p. 6662–6668, 1998.

D. KHODAGHOLY, G.G. MALLIARAS, R. M. O. **Polymer Scien A Comprehensive Reference, Volume 8**. Elsevier ed. 2012.

DAI, Y.; SHIU, K. Glucose Biosensor Based on Multi-Walled Carbon Nanotube Modified Glassy Carbon Electrode. **Electroanalysis**, v. 16, n. 20, p. 1697–1703, 2004.

DANIELS, J. S.; POURMAND, N. Label-Free Impedance Biosensors: Opportunities and Challenges. **Electroanalysis**, v. 19, n. 12, p. 1239–1257, 2007.

DATTA, S.; WATTAL, C. Dengue NS1 antigen detection: a useful tool in early diagnosis of dengue virus infection. **Indian journal of medical microbiology**, v. 28, n. 2, p. 107–10, 2010a.

DATTA, S.; WATTAL, C. Dengue NS1 antigen detection: a useful tool in early diagnosis of dengue virus infection. **Indian journal of medical microbiology**, v. 28, n. 2, p. 107–10, 2010b.

DATTA, S.; WATTAL, C. Dengue NS1 antigen detection: a useful tool in early diagnosis of dengue virus infection. **Indian journal of medical microbiology**, v. 28, n. 2, p. 107–10, 2010c.

DEEN, J. L.; HARRIS, E.; WILLS, B.; et al. The WHO dengue classification and case definitions: time for a reassessment. **Lancet**, v. 368, n. 9530, p. 170–3, 2006.

DIAS, A. C. M. S.; GOMES-FILHO, S. L. R.; SILVA, M. M. S.; DUTRA, R. F. A sensor tip based on carbon nanotube-ink printed electrode for the dengue virus NS1 protein. **Biosensors & bioelectronics**, v. 44, p. 216–21, 2013. Disponível em: <http://www.ncbi.nlm.nih.gov/pubmed/23428736>. Acesso em: 19/10/2013.

EL-ANSARY, A. Nanoparticles as biochemical sensors. **Nanotechnology, Science and Applications**, p. 65, 2010.

ENDY, T. P. Epidemiology of Inapparent and Symptomatic Acute Dengue Virus Infection: A Prospective Study of Primary School Children in Kamphaeng Phet, Thailand. **American Journal of Epidemiology**, v. 156, n. 1, p. 40–51, 2002. Disponível em: <http://aje.oupjournals.org/cgi/doi/10.1093/aje/kwf005>. Acesso em: 1/11/2013.

FANJUL-BOLADO, P.; LAMAS-ARDISANA, P. J.; HERNÁNDEZ-SANTOS, D.; COSTA-GARCÍA, A. Electrochemical study and flow injection analysis of paracetamol in pharmaceutical formulations based on screen-printed electrodes and carbon nanotubes. **Analytica chimica acta**, v. 638, n. 2, p. 133–8, 2009.

FELIX, A. C.; ROMANO, C. M.; CENTRONE, C. D. C.; et al. Low sensitivity of NS1 protein tests evidenced during a dengue type 2 virus outbreak in Santos, Brazil, in 2010. **Clinical and vaccine immunology : CVI**, v. 19, n. 12, p. 1972–6, 2012.

FENG, L.; LI, H.; LI, F.; SHI, Z.; GU, Z. Functionalization of carbon nanotubes with amphiphilic molecules and their Langmuir–Blodgett films. **Carbon**, v. 41, n. 12, p. 2385–2391, 2003.

FERREIRA, H. E. A.; DANIEL, D.; BERTOTTI, M.; RICHTER, E. M. A Novel Disposable Electrochemical Microcell: Construction and Characterization. **J. Braz. Chem. Soc.**, v. 19, n. 8, p. 1538–1545, 2008.

FRANZOI, A. C.; PERALTA, R. A; NEVES, A.; VIEIRA, I. C. Biomimetic sensor based on MnIIIMnII complex as manganese peroxidase mimetic for determination of rutin. **Talanta**, v. 78, n. 1, p. 221–6, 2009.

FREIRE, R. S.; PESSOA, C. A. EMPREGO DE MONOCAMADAS AUTO-ORGANIZADAS NO DESENVOLVIMENTO DE SENSORES ELETROQUÍMICOS. **Quim. Nova**, v. 26, n. 3, p. 381–389, 2003.

FRY, S. R.; MEYER, M.; SEMPLE, M. G.; et al. The diagnostic sensitivity of dengue rapid test assays is significantly enhanced by using a combined antigen and antibody testing approach. **PLoS neglected tropical diseases**, v. 5, n. 6, p. e1199, 2011.

GAVALAS, V. G.; LAW, S. A.; CHRISTOPHER BALL, J.; ANDREWS, R.; BACHAS, L. G. Carbon nanotube aqueous sol-gel composites: enzyme-friendly platforms for the development of stable biosensors. **Analytical biochemistry**, v. 329, n. 2, p. 247–52, 2004.

GOMES-FILHO, S. L. R.; DIAS, A. C. M. S.; SILVA, M. M. S.; SILVA, B. V. M.; DUTRA, R. F. A carbon nanotube-based electrochemical immunosensor for cardiac troponin T. **Microchemical Journal**, v. 109, p. 10–15, 2013. Elsevier B.V.

GRIESHABER, D.; MACKENZIE, R.; VÖRÖS, J.; REIMHULT, E. Electrochemical Biosensors - Sensor Principles and Architectures. **Sensors**, v. 8, n. 3, p. 1400–1458, 2008.

GROBERT, N. Carbon nanotubes – becoming clean. **Materials Today**, v. 10, n. 1-2, p. 28–35, 2007.

GUBLER, D. J.; SUHARYONO, W.; LUBIS, I.; ERAM, S.; GUNARSO, S. Epidemic dengue 3 in central Java, associated with low viremia in man. **The American journal of tropical medicine and hygiene**, v. 30, n. 5, p. 1094–9, 1981.

GUBLER, D. J.;KUNO, G. Dengue and dengue hemorrhagic fever. **Seminars in Pediatric Infectious Diseases.**, v. 8, n. 1, p. 3–9, 1997.

GURUGAMA, P.; GARG, P.; PERERA, J.; WIJEWICKRAMA, A.; SENEVIRATNE, S. L. Dengue viral infections. **Indian journal of dermatology**, v. 55, n. 1, p. 68–78, 2010.

GUZMAN, M. G.; HALSTEAD, S. B.; ARTSOB, H.; et al. Dengue: a continuing global threat. **Nature reviews. Microbiology**, v. 8, n. 12 Suppl, p. S7–16, 2010. Nature Publishing Group.

HABERMÜLLER, K.; MOSBACH, M.; SCHUHMANN, W. Electron-transfer mechanisms in amperometric biosensors. **Fresenius' journal of analytical chemistry**, v. 366, n. 6-7, p. 560–8, 2000.

HALSTEAD, S. B. Dengue. **Lancet**, v. 370, n. 9599, p. 1644–52, 2007.

HAMMON, W. M.; RUNDNICK, A.; SATHER, G. E. Viruses Associated with Epidemic Hemorrhagic Fevers of the Philippines and Thailand. **Science**, v. 131, n. 3407, p. 1102–1103, 1960.

HANG, V. T.; NGUYET, N. M.; TRUNG, D. T.; et al. Diagnostic accuracy of NS1 ELISA and lateral flow rapid tests for dengue sensitivity, specificity and relationship to viraemia and antibody responses. **PLoS neglected tropical diseases**, v. 3, n. 1, p. e360, 2009. Disponível em: <http://www.pubmedcentral.nih.gov/articlerender.fcgi?artid=2614471&tool=pmcentrez&rendertype=abstract>. Acesso em: 9/10/2013.

HART, J. P.; WRING, S. A. Recent developments in the design and application of screen-printed electrochemical sensors for biomedical, environmental and industrial analyses. **TrAC Trends in Analytical Chemistry**, v. 16, n. 2, p. 89–103, 1997.

HAYAT, A.; BARTHELMEBS, L.; SASSOLAS, A.; MARTY, J.-L. An electrochemical immunosensor based on covalent immobilization of okadaic acid onto screen printed carbon electrode via diazotization-coupling reaction. **Talanta**, v. 85, n. 1, p. 513–8, 2011. Elsevier B.V. Disponível em: <http://www.ncbi.nlm.nih.gov/pubmed/21645734>. Acesso em: 19/10/2013.

HE, J.-B.; JIN, G.-P.; CHEN, Q.-Z.; WANG, Y. A quercetin-modified biosensor for amperometric determination of uric acid in the presence of ascorbic acid. **Analytica chimica acta**, v. 585, n. 2, p. 337–43, 2007.

HEGDE, R. N.; HOSAMANI, R. R.; NANDIBEWOOR, S. T. Voltammetric oxidation and determination of cinnarizine at glassy carbon electrode modified with multi-walled carbon nanotubes. **Colloids and surfaces. B, Biointerfaces**, v. 72, n. 2, p. 259–65, 2009.

HU, Y.; ZHAO, Z.; WAN, Q. Facile preparation of carbon nanotube-conducting polymer network for sensitive electrochemical immunoassay of Hepatitis B surface antigen in serum. **Bioelectrochemistry (Amsterdam, Netherlands)**, v. 81, n. 2, p. 59–64, 2011. Elsevier B.V.

HUA, M.; CHEN, H.; TSAI, R.; et al. Preparation of Polybenzimidazole-Carboxylated Multiwalled Carbon Nanotube Composite for Intrinsic Sensing of Hydrogen Peroxide. **The Journal of Physical Chemistry C**, v. 115, n. 31, p. 15182–15190, 2011.

HUANG, J.; TSAI, Y. Direct electrochemistry and biosensing of hydrogen peroxide of horseradish peroxidase immobilized at multiwalled carbon nanotube/alumina-coated silica nanocomposite modified glassy carbon electrode. **Sensors and Actuators B: Chemical**, v. 140, n. 1, p. 267–272, 2009.

HUY, T. Q.; HANH, N. T. H.; THUY, N. T.; et al. A novel biosensor based on serum antibody immobilization for rapid detection of viral antigens. **Talanta**, v. 86, p. 271–7, 2011. Elsevier B.V. Disponível em: <http://www.ncbi.nlm.nih.gov/pubmed/22063541>. Acesso em: 19/10/2013.

ISLAM, N.; MIYAZAKI, K. Nanotechnology innovation system: Understanding hidden dynamics of nanoscience fusion trajectories. **Technological Forecasting and Social Change**, v. 76, n. 1, p. 128–140, 2009. Elsevier Inc.

JIN, Y.; YAO, X.; LIU, Q.; LI, J. Hairpin DNA probe based electrochemical biosensor using methylene blue as hybridization indicator. **Biosensors & bioelectronics**, v. 22, n. 6, p. 1126–30, 2007.

JUSOH, N.; ABDUL-AZIZ, A.; SUPRIYANTO, E. Improvement of Glucose Biosensor Performances Using Poly (hydroxyethyl methacrylate) Outer Membrane. **INTERNATIONAL JOURNAL OF BIOLOGY AND BIOMEDICAL ENGINEERING Improvement**, v. 6, n. 1, p. 77 – 86, 2012.

JUSTINO, C. I. L.; ROCHA-SANTOS, T. A.; DUARTE, A. C. Review of analytical figures of merit of sensors and biosensors in clinical applications. **TrAC Trends in Analytical Chemistry**, v. 29, n. 10, p. 1172–1183, 2010. Elsevier Ltd.

KANG, X.; MAI, Z.; ZOU, X.; CAI, P.; MO, J. A novel glucose biosensor based on immobilization of glucose oxidase in chitosan on a glassy carbon electrode modified with gold-platinum alloy nanoparticles/multiwall carbon nanotubes. **Analytical biochemistry**, v. 369, n. 1, p. 71–9, 2007.

KAO, C.-L.; KING, C.-C.; CHAO, D.-Y.; WU, H.-L.; CHANG, G.-J. J. Laboratory diagnosis of dengue virus infection: current and future perspectives in clinical diagnosis and public health. **Journal of microbiology, immunology, and infection = Wei mian yu gan ran za zhi**, v. 38, n. 1, p. 5–16, 2005.

KAUSAITE-MINKSTIMIENE, A.; RAMANAVICIENE, A.; KIRLYTE, J.; RAMANAVICIUS, A. Comparative study of random and oriented antibody immobilization techniques on the binding capacity of immunosensor. **Analytical chemistry**, v. 82, n. 15, p. 6401–8, 2010.

KAUSHIK, A.; KHAN, R.; SOLANKI, P. R.; et al. Iron oxide nanoparticles-chitosan composite based glucose biosensor. **Biosensors & bioelectronics**, v. 24, n. 4, p. 676–83, 2008.

KIM, J.; PREMKUMAR, T.; LEE, K.; GECKELER, K. E. A Facile Approach to Single-Wall Carbon Nanotube/Poly(allylamine) Nanocomposites. **Macromolecular Rapid Communications**, v. 28, n. 3, p. 276–280, 2007.

KIMMEL, D. W.; LEBLANC, G.; MESCHIEVITZ, M. E.; CLI, D. E. Electrochemical Sensors and Biosensors. **Analytical Chemistry**, v. 84, p. 685–707, 2012.

KONCKI, R.; MASCINI, M. Screen-printed ruthenium dioxide electrodes for pH measurements. **Analytica Chimica Acta**, v. 351, n. 1-3, p. 143–149, 1997. Disponível em: <http://linkinghub.elsevier.com/retrieve/pii/S000326709700367X>. .

KONG, B.; YOO, H.; JUNG, H. Electrical conductivity of graphene films with a poly(allylamine hydrochloride) supporting layer. **Langmuir : the ACS journal of surfaces and colloids**, v. 25, n. 18, p. 11008–13, 2009.

KORAKA, P.; ZELLER, H.; NIEDRIG, M.; OSTERHAUS, A. D. M. .; GROEN, J. Reactivity of serum samples from patients with a flavivirus infection measured by immunofluorescence assay and ELISA. **Microbes and Infection**, v. 4, n. 12, p. 1209–1215, 2002.

KUMAR, S.; VICENTE-BECKETT, V. Glassy carbon electrodes modified with multiwalled carbon nanotubes for the determination of ascorbic acid by square-wave voltammetry. **Beilstein journal of nanotechnology**, v. 3, p. 388–96, 2012.

KUMARASAMY, V.; WAHAB, A H. A.; CHUA, S. K.; et al. Evaluation of a commercial dengue NS1 antigen-capture ELISA for laboratory diagnosis of acute dengue virus infection. **Journal of virological methods**, v. 140, n. 1-2, p. 75–9, 2007.

LAVIRON, E. General expression of the linear potential sweep voltammogram in the case of diffusionless electrochemical systems. **Journal of**

Electroanalytical Chemistry and Interfacial Electrochemistry, v. 101, n. 1, p. 19–28, 1979.

LEE, J.; KIM, M.; HONG, C. K.; SHIM, S. E. Measurement of the dispersion stability of pristine and surface-modified multiwalled carbon nanotubes in various nonpolar and polar solvents. **Measurement Science and Technology**, v. 18, n. 12, p. 3707–3712, 2007.

LI, N.; YUAN, R.; CHAI, Y.; CHEN, S.; AN, H. Sensitive immunoassay of human chorionic gonadotrophin based on multi-walled carbon nanotube-chitosan matrix. **Bioprocess and biosystems engineering**, v. 31, n. 6, p. 551–8, 2008.

LIBRATY, D. H.; YOUNG, P. R.; PICKERING, D.; et al. High circulating levels of the dengue virus nonstructural protein NS1 early in dengue illness correlate with the development of dengue hemorrhagic fever. **The Journal of infectious diseases**, v. 186, n. 8, p. 1165–8, 2002.

LIMA, M. D. R. Q.; NOGUEIRA, R. M. R.; SCHATZMAYR, H. G.; SANTOS, F. B. DOS. Comparison of three commercially available dengue NS1 antigen capture assays for acute diagnosis of dengue in Brazil. **PLoS neglected tropical diseases**, v. 4, n. 7, p. e738, 2010.

LIN, J.; HE, C.; ZHANG, L.; ZHANG, S. Sensitive amperometric immunosensor for a -fetoprotein based on carbon nanotube / gold nanoparticle doped chitosan film. **Analytical Biochemistry**, v. 384, n. 1, p. 130–135, 2009. Elsevier Inc.

LINDINO, C. A.; PELAQUIM, L. DE L.; PREVIATTO, M. D. DETERMINAÇÃO DE IODATO EM SAL CULINÁRIO COM TÉCNICA AMPEROMÉTRICA. **ARTIGOS & ENSAIOS**, v. 06, n. 11, p. 51–59, 2006.

LIU, G.; LIN, Y. Nanomaterial labels in electrochemical immunosensors and immunoassays. **Talanta**, v. 74, n. 3, p. 308–17, 2007.

LOJOU, É.; BIANCO, P. Application of the electrochemical concepts and techniques to amperometric biosensor devices. **Journal of Electroceramics**, v. 16, n. 1, p. 79–91, 2006.

LOWINSOHN, D.; QUÍMICA, I. DE; SÃO, U. DE; SP, S. P. SENSORES ELETROQUÍMICOS: CONSIDERAÇÕES SOBRE MECANISMOS DE FUNCIONAMENTO E APLICAÇÕES NO MONITORAMENTO DE ESPÉCIES QUÍMICAS EM AMBIENTES MICROSCÓPICOS. **Quim. Nova**, v. 29, n. 6, p. 1318–1325, 2006.

LUPPA, P. B.; SOKOLL, L. J.; CHAN, D. W. Immunosensors--principles and applications to clinical chemistry. **Clinica chimica acta; international journal of clinical chemistry**, v. 314, n. 1-2, p. 1–26, 2001.

LYNAM, C.; GILMARTIN, N.; MINETT, A. I.; KENNEDY, R. O.; WALLACE, G. Carbon nanotube-based transducers for immunoassays. **Carbon**, v. 47, n. 10, p. 2337–2343, 2009. Elsevier Ltd.

MACHADO, J. M.; OLIVEIRA, T. A. DE; ZÓBOLI, A. P. Desenvolvimento de teste imunocromatográfico para detecção de proteínas não estruturais da Dengue . **BBR-Biochemistry and Biotechnology Reports**, v. 2, n. 2, p. 73–75, 2013.

MACIEL, I. J., SIQUEIRA JÚNIOR, J. B., & MARTELLI, C. M. T. EPIDEMIOLOGIA E DESAFIOS NO CONTROLE DO DENGUE. **Revista de Patologia Tropical**, v. 37, n. 2, p. 111–130, 2008.

MAIRUHU, A T. A; WAGENAAR, J.; BRANDJES, D. P. M.; GORP, E. C. M. VAN. Dengue: an arthropod-borne disease of global importance. **European journal of clinical microbiology & infectious diseases : official publication of the European Society of Clinical Microbiology**, v. 23, n. 6, p. 425–33, 2004.

MAIRUHU, A. T. A.; BRANDJES, D. P. M.; GORP, E. C. M. VAN. Treating viral hemorrhagic fever. **IDrugs : the investigational drugs journal**, v. 6, n. 11, p. 1061–6, 2003.

MARAZUELA, D.; MORENO-BONDI, M. C. Fiber-optic biosensors--an overview. **Analytical and bioanalytical chemistry**, v. 372, n. 5-6, p. 664–82, 2002.

MARQUES, P. R. B. DE O.; YAMANAKA, H. Biossensores Baseados no processo de iniBição enzimática. **Quim. Nova**, v. 31, n. 7, p. 1791–1799, 2008.

MARTINA, B. E. E.; KORAKA, P.; OSTERHAUS, A. D. M. E. Dengue virus pathogenesis: an integrated view. **Clinical microbiology reviews**, v. 22, n. 4, p. 564–81, 2009.

MARZOCHI[1], K. B. F. DENGUE SITUAÇÃO ATUAL, DESAFIOS E ESTRATÉGIAS PARA ENFRENTAMENTO. **Revista da Sociedade Brasileira de Medicina Tropical**, v. 37, n. 5, p. 413–415, 2011.

MCBRIDE, W. J. H. Evaluation of dengue NS1 test kits for the diagnosis of dengue fever. **Diagnostic microbiology and infectious disease**, v. 64, n. 1, p. 31–6, 2009. Elsevier Inc.

MCQUADE, D. T.; PULLEN, A E.; SWAGER, T. M. Conjugated polymer-based chemical sensors. **Chemical reviews**, v. 100, n. 7, p. 2537–74, 2000.

MCSHERRY, J. A. Some medical aspects of the Darien scheme: was it dengue? **Scottish medical journal**, v. 27, n. 2, p. 183–4, 1982. Disponível em: <http://www.ncbi.nlm.nih.gov/pubmed/7046045>. Acesso em: 17/10/2013.

MEDEIROS, E. S.; OLIVEIRA, J. E.; PATERNO, L. G.; MATTOSO, L. H. C. Uso de Polímeros Condutores em Sensores . **Revista Eletrônica de Materiais e Processos**, v. 7, n. 2, p. 62–77, 2012.

MEHRVAR, M.; ABDI, M. Recent Developments, Characteristics, and Potential Applications of Electrochemical Biosensors. **Analytical Sciences**, v. 20, n. 8, p. 1113–1126, 2004.

MELLO, L. D.; KUBOTA, L. T. Review of the use of biosensors as analytical tools in the food and drink industries. **Food Chemistry**, v. 77, n. 2, p. 237–256, 2002.

METTERS, J. P.; KADARA, R. O.; BANKS, C. E. New directions in screen printed electroanalytical sensors: an overview of recent developments. **The Analyst**, v. 136, n. 6, p. 1067–76, 2011. Disponível em: <http://www.ncbi.nlm.nih.gov/pubmed/21283890>. Acesso em: 27/10/2013.

MINISTÉRIO DA SAÚDE. Diretrizes Nacionais para a Prevenção e Controle de Epidemias de Dengue. ,2013. Disponível em: <http://portal.saude.gov.br/portal/arquivos/pdf/diretrizes_nacionais_dengue.pdf> . .

MOI, M. L.; OMATSU, T.; TAJIMA, S.; et al. Detection of dengue virus nonstructural protein 1 (NS1) by using ELISA as a useful laboratory diagnostic method for dengue virus infection of international travelers. **Journal of travel medicine**, v. 20, n. 3, p. 185–93, 2013. Disponível em: <http://www.ncbi.nlm.nih.gov/pubmed/23577865>. Acesso em: 19/10/2013.

MOREIRA, F. T. C.; DUTRA, R. A. F.; NORONHA, J. P. C.; CUNHA, A. L.; SALES, M. G. F. Biosensors and Bioelectronics Artificial antibodies for troponin T by its imprinting on the surface of multiwalled carbon nanotubes : Its use as sensory surfaces. **Biosensors and Bioelectronics**, v. 28, n. 1, p. 243–250, 2011. Elsevier B.V.

MÜLLER, F.; FERREIRA, C. A.; AMADO, F. D. R.; RODRIGUES, M. A. S. Desenvolvimento de membranas e filmes auto-suportados a partir de polianilina: síntese, caracterização e aplicação. **Polímeros**, v. 21, n. 4, p. 259–264, 2011.

MURPHY, L. Biosensors and bioelectrochemistry. **Current opinion in chemical biology**, v. 10, n. 2, p. 177–84, 2006.

NASCIMENTO, VALBERES B.; ANGNES, L. ELETRODOS FABRICADOS POR “SILK-SCREEN.”**Quim. Nova**, v. 21, n. 5, p. 614–629, 1998.

NIRSCHL, M.; REUTER, F.; VÖRÖS, J. Review of Transducer Principles for Label-Free Biomolecular Interaction Analysis. **Biosensors**, v. 1, n. 4, p. 70–92, 2011.

NOBUCHI T, TAKAHARA S, H. H. Studies on the survival rate of ray parenchyna cells with ageing process in coniferous secondary xylem. **Bull. Kyoto Univ.**, p. 239–46, 1979.

NOGUEIRA, R. M. R.; ARAÚJO, J. M. G. DE; SCHATZMAYR, H. G. Dengue viruses in Brazil, 1986-2006. **Revista panamericana de salud pública = Pan American journal of public health**, v. 22, n. 5, p. 358–63, 2007.

NOWACKI, B. F. **Síntese, Caracterização e Propriedades Fotofísicas de Copolímeros Contendo Unidades Fluoreno, Fenileno e Tiofeno**, 2011. Universidade Federal do Paraná.

O'REILLY, J. M.; MOSHER, R. A. FUNCTIONAL GROUPS IN CARBON BLACK BY FTIR SPECTROSCOPY. **Carbon**, v. 21, n. 1, p. 47–51, 1981.

OLIVEIRA, J. E.; PATERNO, L. G.; MATTOSO, L. H. C.; MEDEIROS, E. S. Uso de Polímeros Condutores em Sensores. Parte 3: Biossensores. **Revista Eletrônica de Materiais e Processos**, v. 1, n. 1, p. 1–11, 2013.

OLIVEIRA, M. D. L.; CORREIA, M. T. S.; DINIZ, F. B. A novel approach to classify serum glycoproteins from patients infected by dengue using electrochemical impedance spectroscopy analysis. **Synthetic Metals**, v. 159, n. 21-22, p. 2162–2164, 2009.

OLIVEIRA, M. D. L.; NOGUEIRA, M. L.; CORREIA, M. T. S.; COELHO, L. C. B. B.; ANDRADE, C. A. S. Sensors and Actuators B : Chemical Detection of dengue virus serotypes on the surface of gold electrode based on Cratylia mollis lectin affinity. **Sensors & Actuators: B. Chemical**, v. 155, n. 2, p. 789–795, 2011. Elsevier B.V.

OLLIVEIRA, A. S. DE; DUTRA, N. R.; SANTOS, E. C. DOS; et al. Dengue endêmico: o desafio das estratégias de vigilância. **Revista da Sociedade Brasileira de Medicina Tropical**, v. 37, n. 5, p. 413–415, 2011.

OU, C.; YUAN, R.; CHAI, Y.; et al. A novel amperometric immunosensor based on layer-by-layer assembly of gold nanoparticles-multi-walled carbon nanotubes-thionine multilayer films on polyelectrolyte surface. **Analytica chimica acta**, v. 603, n. 2, p. 205–13, 2007.

PARK, H. J.; KIM, J.; CHANG, J. Y.; THEATO, P. Preparation of transparent conductive multilayered films using active pentafluorophenyl ester modified multiwalled carbon nanotubes. **Langmuir : the ACS journal of surfaces and colloids**, v. 24, n. 18, p. 10467–73, 2008.

PARK, J.; WOOK, S.; MAO, J.; SEOB, I.; YUN, Y. Recovery of Pd (II) from hydrochloric solution using polyallylamine hydrochloride-modified Escherichia coli biomass. **Journal of Hazardous Materials**, v. 181, n. 1-3, p. 794–800, 2010. Elsevier B.V.

PAULA, S. O. DE; FONSECA, B. A. L. DA. Dengue: a review of the laboratory tests a clinician must know to achieve a correct diagnosis. **The Brazilian journal of infectious diseases : an official publication of the Brazilian Society of Infectious Diseases**, v. 8, n. 6, p. 390–8, 2004.

PAVEY, K. D.; HUNTER, A. C.; PAUL, F. Real-time evaluation of macromolecular surface modified quartz crystal resonant sensors under cryogenic stress for biological applications. **Biosensors and Bioelectronics**, v. 18, n. 11, p. 1349–1354, 2003.

PEELING, ROSANNA W; ARTSOB, H.; PELEGRINO, J. L.; et al. Evaluation of diagnostic tests : dengue. **Nature Publishing Group**, , n. 12, p. S30–S37, 2010. Nature Publishing Group.

PEELING, ROSANNA W.; ARTSOB, H.; PELEGRINO, J. L.; et al. Evaluation of diagnostic tests: dengue. **Nature Reviews Microbiology**, v. 8, n. 12, p. S30–S37, 2010. Nature Publishing Group.

PEI, Z.; ANDERSON, H.; MYRSKOG, A.; et al. Optimizing immobilization on two-dimensional carboxyl surface : pH dependence of antibody orientation and antigen binding capacity. **Analytical Biochemistry**, v. 398, n. 2, p. 161–168, 2010. Elsevier Inc. Disponível em: <http://dx.doi.org/10.1016/j.ab.2009.11.038>. .

POLONI, T. R. R. S. **Detecção e tipificação do vírus da dengue por RT-PCR em tempo real Detecção e tipificação do vírus da dengue por RT-PCR em tempo real**, 2009. Universidade de São Paulo.

POWER, A. C.; MORRIN, A. Electroanalytical Sensor Technology. ,2013.

PUERTAS, S.; GRACIA VILLA, M. DE; MENDOZA, E.; et al. Improving immunosensor performance through oriented immobilization of antibodies on carbon nanotube composite surfaces. **Biosensors & bioelectronics**, v. 43, p. 274–80, 2013.

REIS, N. S.; SERRANO, S. H. P.; MENEGHATTI, R.; GIL, E. D. S. Métodos Eletroquímicos usados para Avaliação da Atividade Antioxidante de Produtos Naturais. **Latin American Journal of Pharmacy**, v. 28, n. 6, p. 949–953, 2009.

RENEDO, O. D.; ALONSO-LOMILLO, M. A; MARTÍNEZ, M. J. A. Recent developments in the field of screen-printed electrodes and their related applications. **Talanta**, v. 73, n. 2, p. 202–19, 2007.

REZAEI, B.; DAMIRI, S. Voltammetric behavior of multi-walled carbon nanotubes modified electrode-hexacyanoferrate(II) electrocatalyst system as a sensor for determination of captopril. **Sensors and Actuators B: Chemical**, v. 134, n. 1, p. 324–331, 2008.

RICCARDI, C. DOS S.; COSTA, P. I. DA; YAMANAKA, H. IMUNOSSENSOR AMPEROMÉTRICO Quim. **Quim. Nova**, v. 25, n. 2, p. 316–320, 2002.

RICCI, F.; ADORNETTO, G.; PALLESCHI, G. A review of experimental aspects of electrochemical immunosensors. **Electrochimica Acta**, v. 84, p. 74–83, 2012. Elsevier Ltd.

RICE, C.; LENCHES, E.; SHIN, S.; SHEETS, R.; STRAUSS, J. Nucleotide sequence of yellow fever virus: implications for flavivirus gene expression and evolution. **Science**, v. 229, n. 4715, p. 726–733, 1985.

RIVAS, G. A; RUBIANES, M. D.; RODRÍGUEZ, M. C.; et al. Carbon nanotubes for electrochemical biosensing. **Talanta**, v. 74, n. 3, p. 291–307, 2007.

RIZZONI, G.; HARTLEY, T. T. **Principles and Applications of Electrical Engineering**. 2000.

RUTHS, J.; ESSLER, F.; DECHER, G.; RIEGLER, H. Polyelectrolytes I: Polyanion/Polycation Multilayers at the Air/Monolayer/Water Interface as Elements for Quantitative Polymer Adsorption Studies and Preparation of Hetero-superlattices on Solid Surfaces †. **Langmuir**, v. 16, n. 23, p. 8871–8878, 2000.

SADIK, O. A.; ALUOCH, A. O.; ZHOU, A. Status of biomolecular recognition using electrochemical techniques. **Biosensors & bioelectronics**, v. 24, n. 9, p. 2749–65, 2009.

SAM, S.-S.; OMAR, S. F. S.; TEOH, B.-T.; ABD-JAMIL, J.; ABUBAKAR, S. Review of Dengue hemorrhagic fever fatal cases seen among adults: a retrospective study. **PLoS neglected tropical diseases**, v. 7, n. 5, p. e2194, 2013.

SANTOS, M. A. DOS. **Estudo Atomístico da Formação de Interfaces-Orgânico: Tiofenos sobre Oxido de Titânio**, 2008. Unoversidade de São Paulo.

SCHMID, G. **Nanoparticles - From Theory to Application**. 2011.

SCHUHMANN, W.; ZIMMERMANN, H.; HABERMÜLLER, K.; LAURINAVICIUS, V. Electron-transfer pathways between redox enzymes and electrode surfaces: reagentless biosensors based on thiol-monolayer-bound and polypyrrole-entrapped enzymes. **Faraday discussions**, , n. 116, p. 245–55; discussion 257–68, 2000.

SEABRA, G.; MENDONÇA, I. **Educação ambiental : Responsabilidade para a conservação da sociobiodiversidade**. 2011.

SGOBBA, V.; GULDI, D. M. Carbon nanotubes--electronic/electrochemical properties and application for nanoelectronics and photonics. **Chemical Society reviews**, v. 38, n. 1, p. 165–84, 2009.

SHU, P.; HUANG, J. Current advances in dengue diagnosis. **Clinical and diagnostic laboratory immunology**, v. 11, n. 4, p. 642–50, 2004.

SILVA, B. V. M.; CAVALCANTI, I. T.; SILVA, M. M. S.; DUTRA, R. F. Talanta A carbon nanotube screen-printed electrode for label-free detection of the human cardiac troponin T. **Talanta**, v. 117, p. 431–437, 2013. Elsevier. Disponível em: <http://dx.doi.org/10.1016/j.talanta.2013.08.059>. .

SILVA, C. P.; CARAPUÇA, H. M. Glassy carbon electrodes coated with poly(allylamine hydrochloride), PAH: Characterization studies and application to ion-exchange voltammetry of trace lead(II) at combined PAH/mercury film electrodes. **Electrochimica Acta**, v. 52, n. 3, p. 1182–1190, 2006.

SILVA, F. G., DOS SANTOS SILVA, S. J., ROCCO, I. M., & R. DA. Avaliação de kits comerciais para detecção de antígenos NS1-dengue – São Paulo. , v. 8, n. 91, p. 14–26, 2011.

SIMMONS, C. P.; FARRAR, J. J.; NGUYEN, VAN V. C.; WILLS, B. Dengue. **The New England journal of medicine**, v. 366, n. 15, p. 1423–32, 2012.

SINGH, M. P.; MAJUMDAR, M.; SINGH, G.; et al. NS1 antigen as an early diagnostic marker in dengue: report from India. **Diagnostic microbiology and infectious disease**, v. 68, n. 1, p. 50–4, 2010. Elsevier Inc.

SMITH, G. W.; WRIGHT, P. J. Synthesis of Proteins and Glycoproteins in Dengue Type 2 Virus-infected Vero and Aedes albopictus Cells. **Journal of General Virology**, v. 66, n. 3, p. 559–571, 1985.

SOMERSET, V.; LEANER, J.; MASON, R.; IWUOHA, E.; MORRIN, A. Development and application of a poly(2,2′-dithiodianiline) (PDTDA)-coated screen-printed carbon electrode in inorganic mercury determination. **Electrochimica Acta**, v. 55, n. 14, p. 4240–4246, 2010. Elsevier Ltd. Disponível em: <http://linkinghub.elsevier.com/retrieve/pii/S0013468609001066>. Acesso em: 19/10/2013.

SOPER, S. A.; BROWN, K.; ELLINGTON, A.; et al. Point-of-care biosensor systems for cancer diagnostics/prognostics. **Biosensors & bioelectronics**, v. 21, n. 10, p. 1932–42, 2006.

SOUZA, A. G. DE. FUNCIONALIZAÇÃO DE NANOTUBOS DE CARBONO. **Quim. Nova**, v. 30, n. 7, p. 1695–1703, 2007.

SPECIAL PROGRAMME FOR RESEARCH, TRAINING IN TROPICAL DISEASES, W. H. O.-W. **Dengue: guidelines for diagnosis, treatment, prevention and control**. World Heal ed. 2009.

STANTON, B. W.; HARRIS, J. J.; MILLER, M. D.; BRUENING, M. L. Ultrathin, Multilayered Polyelectrolyte Films as Nanofiltration Membranes. **Langmuir**, v. 19, n. 17, p. 7038–7042, 2003.

STRADIOTTO, N. R.; YAMANAKA, H.; ZANONI, M. V. B. Electrochemical Sensors : A Powerful Tool in Analytical Chemistry. **J. Braz. Chem. Soc.**, v. 14, n. 2, p. 159–173, 2003.

SUAYA, J. A; SHEPARD, D. S.; SIQUEIRA, J. B.; et al. Cost of dengue cases in eight countries in the Americas and Asia: a prospective study. **The American journal of tropical medicine and hygiene**, v. 80, n. 5, p. 846–55, 2009.

SUAYA, J. A.; SHEPARD, D. S.; BEATTY, M. E. Dengue : Burden Of Disease And Costs Of Illness. **TDR. Report of the Scientific Working Group Meeting on Dengue.**, , n. October 2006, p. 35–49, 2007.

TAN, Y.; YIN, J.; LIANG, C.; et al. A study of a new TSM bio-mimetic sensor using a molecularly imprinted polymer coating and its application for the determination of nicotine in human serum and urine. **Bioelectrochemistry (Amsterdam, Netherlands)**, v. 53, n. 2, p. 141–8, 2001.

TANG, J.-L.; CHENG, S.-F.; HSU, W.-T.; CHIANG, T.-Y.; CHAU, L.-K. Fiber-optic biochemical sensing with a colloidal gold-modified long period fiber grating. **Sensors and Actuators B: Chemical**, v. 119, n. 1, p. 105–109, 2006.

TERRONES, M. Carbon nanotubes: synthesis and properties, electronic devices and other emerging applications. **International Materials Reviews**, v. 49, n. 6, p. 325–377, 2004.

THÉVENOT, D. R.; TOTH, K.; DURST, R. A.; WILSON, G. S. Electrochemical biosensors: recommended definitions and classification1International Union of Pure and Applied Chemistry: Physical Chemistry Division, Commission I.7 (Biophysical Chemistry); Analytical Chemistry Division, Commission V.5 (Electroanalytical. **Biosensors and Bioelectronics**, v. 16, n. 1-2, p. 121–131, 2001.

TONTULAWAT, P.; PONGSIRI, P.; THONGMEE, C.; et al. Evaluation of rapid immunochromatographic NS1 test, anti-dengue IgM test, semi-nested PCR and IgM ELISA for detection of dengue virus. **The Southeast Asian journal of tropical medicine and public health**, v. 42, n. 3, p. 570–8, 2011.

TRAN, Q. H.; HANH NGUYEN, T. H.; MAI, A. T.; et al. Development of electrochemical immunosensors based on different serum antibody immobilization methods for detection of Japanese encephalitis virus. **Advances**

in Natural Sciences: Nanoscience and Nanotechnology, v. 3, n. 1, p. 015012, 2012.

USLU, B.; OZKAN, S. Electroanalytical Application of Carbon Based Electrodes to the Pharmaceuticals. **Analytical Letters**, v. 40, n. 5, p. 817–853, 2007.

VASCONCELOS, E. A.; PERES, N. G.; PEREIRA, C. O.; et al. Potential of a simplified measurement scheme and device structure for a low cost label-free point-of-care capacitive biosensor. **Biosensors & bioelectronics**, v. 25, n. 4, p. 870–6, 2009.

VASHIST, S. K. Carbon Nanotubes-Based Electrochemical Sensors and Drug Delivery Systems: Prospects and Challengesc. **Journal of Nanomedicine & Nanotechnology**, v. 03, n. 08, p. 1–2, 2012. Disponível em: <http://www.omicsonline.org/2157-7439/2157-7439-3-e121.digital/2157-7439-3-e121.html>. Acesso em: 1/12/2013.

VASHIST, S. K.; VENKATESH, A. G.; MITSAKAKIS, K.; et al. Nanotechnology-Based Biosensors and Diagnostics: Technology Push versus Industrial/Healthcare Requirements. **BioNanoScience**, v. 2, n. 3, p. 115–126, 2012.

VO-DINH, T.; CULLUM, B. Biosensors and biochips: advances in biological and medical diagnostics. **Fresenius' journal of analytical chemistry**, v. 366, n. 6-7, p. 540–51, 2008.

WANG, Y.; XU, H.; ZHANG, J.; LI, G. Electrochemical Sensors for Clinic Analysis. **Sensors**, v. 8, n. 4, p. 2043–2081, 2008.

WHO, W. H. O.-. Dengue hemorrhagic fever: diagnosis, treatment and control. World Health Organization, Geneva,Switzerland. , p. 1–11, 1997.

WHO, W. H. O.-. Global Strategy for Dengue Prevention and Control 2012–2020. **World Health Organiszation, Geneva, Switzerland**, 2012.

WILSON, G. S.; GIFFORD, R. Biosensors for real-time in vivo measurements. **Biosensors & bioelectronics**, v. 20, n. 12, p. 2388–403, 2005.

WU, L.; YAN, F.; JU, H. An amperometric immunosensor for separation-free immunoassay of CA125 based on its covalent immobilization coupled with thionine on carbon nanofiber. **Journal of immunological methods**, v. 322, n. 1-2, p. 12–9, 2007.

WU, T.; SU, C.; CHEN, L.; et al. Piezoelectric immunochip for the detection of dengue fever in viremia phase. **Biosensors & bioelectronics**, v. 21, n. 5, p. 689–95, 2005.

WU, Z.; LI, C.; WEI, Z.; YING, P.; XIN, Q. FT-IR Spectroscopic Studies of Thiophene Adsorption and Reactions on Mo 2 N/γ-Al 2 O 3 Catalysts. **The Journal of Physical Chemistry B**, v. 106, n. 5, p. 979–987, 2002.

YAP, G.; SIL, B. K.; NG, L. Use of saliva for early dengue diagnosis. **PLoS neglected tropical diseases**, v. 5, n. 5, p. e1046, 2011.

YOO, D.; SHIRATORI, S. S.; RUBNER, M. F. Controlling Bilayer Composition and Surface Wettability of Sequentially Adsorbed Multilayers of Weak Polyelectrolytes. **Macromolecules**, v. 31, n. 13, p. 4309–4318, 1998.

YOUNG, P. R.; HILDITCH, P. A.; BLETCHLY, C.; HALLORAN, W. An antigen capture enzyme-linked immunosorbent assay reveals high levels of the dengue virus protein NS1 in the sera of infected patients. **Journal of clinical microbiology**, v. 38, n. 3, p. 1053–7, 2000.

YUN, Y.; BANGE, A.; HEINEMAN, W. R.; et al. A nanotube array immunosensor for direct electrochemical detection of antigen–antibody binding. **Sensors and Actuators B: Chemical**, v. 123, n. 1, p. 177–182, 2007.

ZAINAH, S.; WAHAB, A. H. A.; MARIAM, M.; et al. Performance of a commercial rapid dengue NS1 antigen immunochromatography test with reference to dengue NS1 antigen-capture ELISA. **Journal of virological methods**, v. 155, n. 2, p. 157–60, 2009a.

ZAINAH, S.; WAHAB, A. H. A.; MARIAM, M.; et al. Performance of a commercial rapid dengue NS1 antigen immunochromatography test with reference to dengue NS1 antigen-capture ELISA. **Journal of virological methods**, v. 155, n. 2, p. 157–60, 2009b.

ZHANG, G.-J.; ZHANG, L.; HUANG, M. J.; et al. Silicon nanowire biosensor for highly sensitive and rapid detection of Dengue virus. **Sensors and Actuators B: Chemical**, v. 146, n. 1, p. 138–144, 2010. Elsevier B.V. Disponível em: <http://linkinghub.elsevier.com/retrieve/pii/S0925400510001255>. Acesso em: 19/10/2013.

ZHANG, S.; WRIGHT, G.; YANG, Y. Materials and techniques for electrochemical biosensor design and construction. **Biosensors & bioelectronics**, v. 15, n. 5-6, p. 273–82, 2000.

ZHANG, X.; CUI, Y.; LV, Z.; et al. Carbon nanotubes , Conductive Carbon Black and Graphite Powder Based Paste Electrodes. **Int. J. Electrochem**, v. 6, p. 6063–6073, 2011.

ZHANG, X.; GUO, Q.; CUI, D. Recent advances in nanotechnology applied to biosensors. **Sensors (Basel, Switzerland)**, v. 9, n. 2, p. 1033–53, 2009.

ZHAO, W.; XU, J.-J.; CHEN, H.-Y. Electrochemical Biosensors Based on Layer-by-Layer Assemblies. **Electroanalysis**, v. 18, n. 18, p. 1737–1748, 2006.

ZHU, X.; YURI, I.; GAN, X.; SUZUKI, I.; LI, G. Electrochemical study of the effect of nano-zinc oxide on microperoxidase and its application to more sensitive hydrogen peroxide biosensor preparation. **Biosensors & bioelectronics**, v. 22, n. 8, p. 1600–4, 2007.

5 *MANUSCRITOS 1*

Research Article

Received: 29 September 2013 Revised: 15 December 2013 Accepted article published: 6 January 2014 Published online in Wiley Online Library:

(wileyonlinelibrary.com) DOI 10.1002/jctb.4305

Electrochemical detection of dengue virus NS1 protein with a poly(allylamine)/carbon nanotube layered immunoelectrode

Mízia M. S. Silva,[a] Ana C. M. S. Dias,[a] Bárbara V. M. Silva,[a] Sérgio L. R. Gomes-Filho,[a] Lauro T. Kubota,[b,c] Marília O. F. Goulart[c,d] and Rosa F. Dutra[a*]

Abstract

BACKGROUND: A sensitive nanostructured immunoelectrode based on poly(allylamine) (PAH) sandwich is developed for non-structural 1 (NS1) of dengue virus. NS1 is a secretory protein abundant in the acute phase of disease associated to hemorrhagic fever. Anti-NS1 antibodies are immobilized on the electrode surface by a thin layer of PAH assembled on carboxylated carbon nanotubes (CNTs). PAH is cationic polymer acting as bi-functional agent to tightly attach CNTs to the electrode surface and anti-NS1 antibodies through their Fc terminal, avoiding random immobilization. Electrochemical responses of immunoassay are generated at a controlled potential by a reaction between H_2O_2 and peroxidase enzyme conjugated to anti-NS1 antibodies.

RESULTS: The immunosensor developed exhibited a linear range to NS1 varying between 0.1 μg mL^{-1} and 2.5 μg mL^{-1}, with clinical range for early diagnostic of acute dengue and a limit of detection of 0.035 μg mL^{-1} that is much lower than the concentration observed from the first day after the onset of fever up to the 9th day. Serum samples are also tested showing good accuracy and specificity.

CONCLUSIONS: An immunosensor for NS1 protein of dengue virus was developed. This versatile and reproducible PAH-sandwich platform can be applied to other immunoassays to give reliable and highly sensitive responses.

Keywords: poly(allylamine) film; carbon nanotubes; NS1; dengue virus; immunosensor

INTRODUCTION

Dengue fever is a disease causing successive epidemics in many tropical and subtropical regions of the world.[1] It is estimated that 50–100 million dengue cases occur annually, ranging from mild fever to life-threatening dengue hemorrhagic fever (DHF) and dengue shock syndrome (DSS).[2] DHF is associated with thrombocytopenia, coagulopathy, acute inflammation, frequent hepatomegaly, and, most importantly, plasma leakage, with which the risk of fatal hypovolemic shock (DSS) is associated.[3,4] Rapid and easy diagnosis of dengue can assist patient trials and care management. Recently, the non-structural 1 (NS1) protein of dengue virus has been proposed as a predictive marker of DHF.[5,6] Enzyme-linked immunosorbent assays (ELISA) for NS1 antigen in serum samples have demonstrated that NS1 is present in high concentrations during the early clinical phase of the disease[7] and can be detected from the first day of onset of the disease.[5] Moreover, the NS1 protein is prevalent in all four serotypes of dengue virus.[8] Recently, point-of-care rapid diagnostic tests (RDTs) have been proposed by offering a fast route to a presumptive dengue diagnosis.[9,10] However, the RDTs have limitations regarding their sensitivity since they offer only qualitative responses; so far they cannot differentiate stages of disease that are correlated with changes in serum levels of the NS1. Alternatively, biosensors can offer quantitative responses through a transducer that converts biochemical reactions to an electrical measurable signal; besides, they turn out to be a point-of-care assay.[11] Some biosensors based on electrochemical transduction have been proposed for the detection of NS1,[12,13] and have used the Cratylia mollis lectin as bioreceptor. However, due to the reaction with glycoproteins or carbohydrates, these biosensors present low specificity.

The development of a highly efficient antibodies immobilization method is essential to obtain biosensors with high sensitivity and specificity.[14] In particular, in immunosensors (i.e. biosensors for immunoassays), the way the antibodies are immobilized

* *Correspondence to: Rosa Fireman Dutra, Biomedical Engineering Laboratory, Federal University of Pernambuco, Av. Prof. Moraes Rego, 1235 - Cidade Universitária, 50670-901, Recife, PE, Brazil. E-mail: rfiremandutra@yahoo.com.br / rosa.dutra@ufpe.br*

a *Biomedical Engineering Laboratory, Federal University of Pernambuco, Av. Prof. Moraes Rego, 1235 - Cidade Universitária, 50670-901, Recife, PE, Brazil*

b *Chemical Institute, State University of Campinas, Rua Carlos Gomes, 241 - Cidade Universitária, 13083-970, Campinas, SP, Brazil*

c *National Institute of Science and Technology in Bioanalysis, Brazil*

d *Institute of Chemical and Biotechnology, Federal University of Alagoas, Av.Tabuleiro do Martins, 57072-970, Maceió, AL, Brazil*

leaving their active sites prone to react with epitopes and also a controlled and optimal amount of charge demanded are important criteria for good performance.[15] Herein, a strategy of non-random immobilization for anti-NS1 antibodies is presented. The orientation of anti-NS1 by the Fc terminal is carried out through the PAH, due to its ability to form amide bonds.[16,17] Its linear structure favors the building of thin films in the sub-nanometer range, which implies non-reducing electron transfer charge at electrochemical sensors.[18,19]

In recent years, possible applications for carbon nanotubes (CNTs) have excited scientists and engineers due to their excellent structural, electrical and mechanical properties.[19,20] For electrochemical biosensors, CNTs enhance the electrochemical reactivity of important electroactive species with faster ion-to-electron transfer.[21,22] Moreover, they increase the electroactive area permitting an increase of immobilized biomolecules on electrode surfaces.[23] Thus, it is possible to improve the amperometric responses through CNTs on the electrode surface, without any reinforcement of chemical mediators or other compounds which may interfere with the analysis.[24] When CNTs are simply deposited on the carbon electrode surface it is difficult to obtain reproducible and stable matrices due to leaching of CNTs because of their weak interactions with the electrode surface.[25,26] In attempting to circumvent these difficulties, an amine polymer film is assembled on the carbon nanotubes surface in order to ensure the CNTs are retained. In this assembly, PAH behaves as a bi-functional linker towards carboxylated carbon nanotubes on one side, and as anti-NS1 antibodies through their Fc portions, on the other side. In this immunoassay, it is possible to measure the NS1 present in serum samples at concentrations in the clinical range for dengue virus diagnosis with good reproducibility and sensitivity.

EXPERIMENTAL

Materials and reagents

Anti-dengue virus NS1 glycoprotein mouse monoclonal antibody (Anti-NS1) and dengue virus NS1 glycoprotein were purchased from Abcam (USA). COOH-functionalized multi-walled carbon nanotubes (COOH-MWCNT) with an average diameter of ~10 nm, average length 1–2 μm and 95% purity were obtained from DropSens (Spain) and the PAH polymer from Sigma-Aldrich (USA). Dimethylformamide (DMF), hydrogen peroxide (H_2O_2) (30% w/v) and ethanol (99.3% v/v) were obtained from F. Maia (Brazil). All the solutions used in the experiments were prepared in ultrapure water (>18 MΩ cm), obtained from a Milli-Q water purification system from Millipore (USA).

Anti-NS1 antibody was labelled with horseradish peroxidase (HRP) from Sigma (USA) according to Avrameas' method.[27] For the coupling of HRP to anti-NS1, 12 mg of peroxidase were dissolved in 1 mL of 0.1 mol L^{-1} phosphate buffer (pH 6.8) containing 5 mg of anti-NS1 antibody. While the solution was gently stirred, 0.05 mL of a 1% aqueous solution of glutaraldehyde was added. The reaction mixture was left for 2 h at room temperature and then dialyzed against two changes of 5 L of PBS at 4°C overnight. The precipitate was removed by centrifugation for 30 min at +4°C and 20 000 rpm. This stock solution of peroxidase labeled-antibody was kept at +4°C until use.

A pool of serum samples consisted of five serum samples from voluntary donors kindly provided by the Oswaldo Cruz Hospital of the Pernambuco University, Brazil, according to the ethics committee's recommendations. All voluntary donors were found negative for dengue virus. The serum samples were collected from venous blood and immediately centrifuged for 120 s at 3000g and stored at −20°C. The positive control was prepared by spiking NS1 antigens in concentrations similar to those detected in viremic dengue patients.[28]

Synthesis of the anti-NS1 nanostructured electrode surface

Prior to modifications, the glassy carbon electrode (GCE) was cleaned on a polishing cloth with 1.0, 0.3, 0.05 μm alumina powder, respectively, followed by sonication in water and 95% ethanol for 10 s to remove residual alumina particles. After cleaning, 10 μL of a COOH-MWCNT solution previously dispersed in DMF was pipetted onto the electrode surface and dried for 30 min at 40°C. The COOH-MWCNT solution consisted of 1 mg of COOH-MWCNT suspended in 1 mL of DMF and sonicated in an ultrasonic bath (40 kHz) for 2 h.[14] After this coating step, forming COOH-MWCNT/GCE, an aliquot (5 μL) of the 2% (v/v) PAH aqueous solution was dropped and left to react for 1 h at room temperature (~25°C) to promote strong bonds with COOH-MWCNT.

To immobilize the Anti-NS1 on the nanostructured electrode, an aliquot (5 μL) of the anti-NS1 solution (10 μg mL^{-1}) was dropped onto the electrode surface and incubated for 1 h at room temperature. Non-specific bindings were blocked by incubating the electrode surface in a solution of 50 mmol L^{-1} glycine, prepared in PB (pH 6.5, 10 mmol L^{-1}) for 40 min.

The stepwise modification of the electrode surface was accomplished by cyclic voltammetry (CV) at a potential ranging from −0.2 to 0.8 V, at 100 mV s^{-1} scan rate, in the presence of 5 mmol L^{-1} $K_3Fe(CN)_6/K_4Fe(CN)_6$ solution prepared in 0.1 mol L^{-1} KCl.

Analytical responses to the NS1

The analytical responses of the immunosensor were obtained by incubating the anti-NS1 nanostructured electrode surface with 10 μL of NS1 antigen samples for 30 min. For analytical responses, 10 μL of anti-NS1-HRP (10 μg mL^{-1}) were pippeted onto the NS1 coated electrode. Afterwards, amperometric responses were generated by reaction between H_2O_2 (0.75 mmol L^{-1}) and peroxidase conjugated to anti-NS1 in PB (pH 6.5, 10 mmol L^{-1}), at −0.2 V potential vs. Ag/AgCl

Anti-NS1 nanostructured electrode surface characterization and electrochemical measurement

Analyses using Fourier transform infrared (FTIR) spectra of the samples were recorded using a Bruker IFS 66 model FT-IR spectrometer at 4000 to 400 cm^{-1} by employing a standard KBr pellet technique.

Scanning electron microscopy (SEM) images were obtained in a JSM 5900 (JEOL Instruments, Japan) at an acceleration voltage of 20 kV and a working distance of 0.5 μm.

Cyclic voltammetry and amperometric experiments were carried out on an Ivium Compact Stat potentiostat/galvanostat (Ivium Technologies, Netherlands) coupled to a microcomputer and controlled by Ivium Soft software. A conventional three-electrode system using a glassy carbon electrode (GCE) with an area of 0.7 mm^2 as the working electrode, an Ag/AgCl electrode as reference and a platinum electrode as an auxiliary electrode.

RESULTS AND DISCUSSION

COOH-MWCNT film on the electrode surface

One of the most important requirements in developing regular and homogeneous COOH-MWCNT electrode surfaces, includes a uniform and reproducible dispersion.[25] Comparing five different

dispersing agents (DMF, ethanol, 5% nafion in ethanol, 1% SDS and water) after sonication, DMF dispersion resulted in a black and homogenous solution. Taking account that the stability of the dispersion is also very important for preparing the modified electrodes with high reproducibility, the stability was then checked by observing the mixture 24 h after sonication. In this case, DMF dispersion was also most satisfactory, preventing coalescence and aggregation. Except for DMF, all other dispersing agents yielded COOH-MWCTNs either glued to the walls of vials or having large aggregates. This fact can also be attributed to the anionic nature of DMF, which provokes a more repulsive electrostatic force against negatively charged carboxylated nanotubes.

Different methods to form a COOH-MWCNT film have been employed; among them drop coating is one of simplest and was chosen in this work. The morphology of CNT film mainly depends on the temperature used for solvent drying, solvent type and droplet size. Herein, solvent drying was fixed at 40°C due to limitations of the glass carbon electrode used. Then, the droplet size was investigated in order to yield a COOH-MWCNT coating with a desired thickness. Modification of the electrode surface was accomplished by CVs using $K_3Fe(CN)_6/K_4Fe(CN)_6$ as redox probe. A gradual increase of the redox peaks with increase of the COOH-MWCNT droplet size was observed (Fig. 1). However, analysis of the cathodic and anodic current peaks ratio (Ipc/Ipa) evidenced a decrease of the electrochemical reversibility applying a droplet size greater than 10 µL, which may represent a non-homogeneous CNT film (Fig. 1 inset). This non-homogeneity can be attributed to the capillary forces induced by drying droplets that ball up the CNTs or bundle and separate CNTs within the droplet creating noncongruent layers. Thus, 10 µL droplet size was adopted in all remaining experiments.

After preparation of the COOH-MWCNT/GCE film, the electroactive area of the modified electrode was calculated according to the Randles–Sevcik Equation.[29]

$$I_p = (2.69 \times 10^5)\ A\ D^{1/2} n^{3/2} v^{1/2} C$$

where, I_p is the peak current value, A represents the electroactive area of the electrode (cm^2), D is the diffusion coefficient of the probe molecule in solution ($cm^2\ s^{-1}$), n is the number of electrons involved in the redox reaction, v is the potential scan rate ($V\ s^{-1}$) and C is the concentration of the probe molecule in solution. Under these conditions, an increase of 87.7% in the electroactive area was achieved in relation to the bare electrode, indicating a good COOH-MWCNT coating.

PAH film on the nanostructured electrode

The effect of film thickness on electrochemical response was evaluated changing the concentration of PAH solution (0.5, 1.0, 1.5, 2.0, 2.5, 3.0 and 3.5% v/v). The COOH-MWCNT/GCE modified with 2% PAH showed the best performance, reaching 29% increase of the anodic current and 23% of the cathodic one, when compared with COOH-MWCNT/GCE. Although the insulating nature of PAH can result in a decrease of redox peaks, herein, an increase of the redox peaks of the negatively charged hexacyanoferrate was possible due to the electrostatic attraction experienced with the positively charged polymer.[30] Thus, a concentration of 2.0% PAH was chosen for further experiments.

Scan rate studies were performed on the PAH/COOH-MWCNT/GCE varying from 10 mV s^{-1} to 120 mV s^{-1} (Fig. 2). The voltammograms presented highly symmetric redox peaks. The currents of cathodic and anodic peaks increased linearly with increase of the square root of the scan rate, indicating a diffusion controlled electron transfer (Fig. 2 inset).

The stability of the PAH film on the electrode was checked by performing 15 consecutive voltammetric cycles in the potential range from −0.2 V to 0.8 V in 5 mmol L^{-1} $K_3Fe(CN)_6/K_4Fe(CN)_6$ solution. The coefficients of variation were 0.04% and 0.09% for anodic and cathodic peaks, respectively, indicating good stability of PAH film. The results show a strong synergism between COOH-MWCNT and PAH. Presumably, interactions formed between carboxylated carbon nanotubes and PAH allowed a stable immobilization matrix.

To characterize the interaction of COOH-MWCNT with PAH and the consequent formation of the nanostructured film, analyses using FTIR were performed. Figure 3(A), curve (a) shows the CNTs FTIR spectrum with typical bands of the carboxylic groups at 3436 cm^{-1} corresponding to molecular stretching of O–H groups. Other peak was observed at 1633 cm^{-1}, corresponding to molecular stretching of C=O.[14,22,23] PAH spectra (curve (b)) show a remarkable band around 3400 cm^{-1}, which is associated with

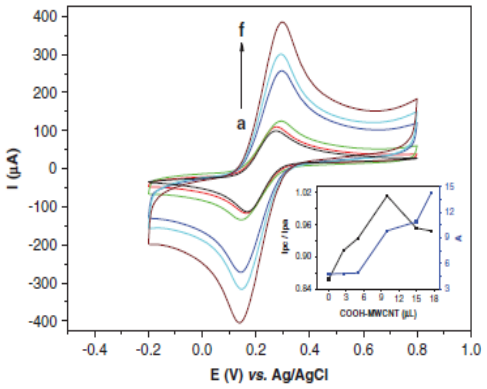

Figure 1. Cyclic voltammograms of the electrode modified with different COOH-MWCNT droplet size: (a) bare GCE; (b) 2.5 µL; (c) 5 µL; (d) 10 µL; (e) 15 µL; and (f) 17.5 µL, in the presence of 5 mmol L^{-1} $K_3Fe(CN)_6/K_4Fe(CN)_6$, at a scan rate of 100 mV s^{-1}. Inset: I_{pc}/I_{pa} (solid line) and area (dashed line) depending on the COOH-MWCNT droplet size.

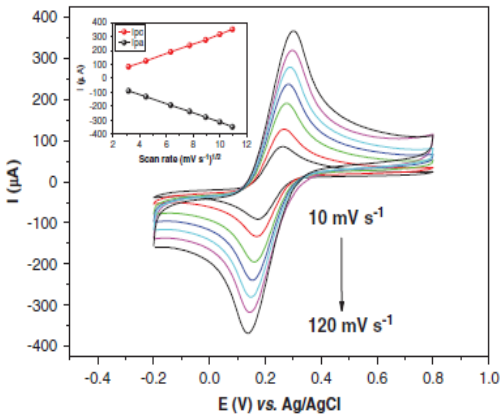

Figure 2. Voltammetric profile of the PAH/COOH-MWCNT/GCE in 5 mmol L^{-1} $K_3Fe(CN)_6/K_4Fe(CN)_6$ under different scan rates (10, 20, 40, 60, 80, 100 and 120 mV s^{-1}). Inset: Current at the anodic and cathodic peaks *vs.* square root of the scan rate.

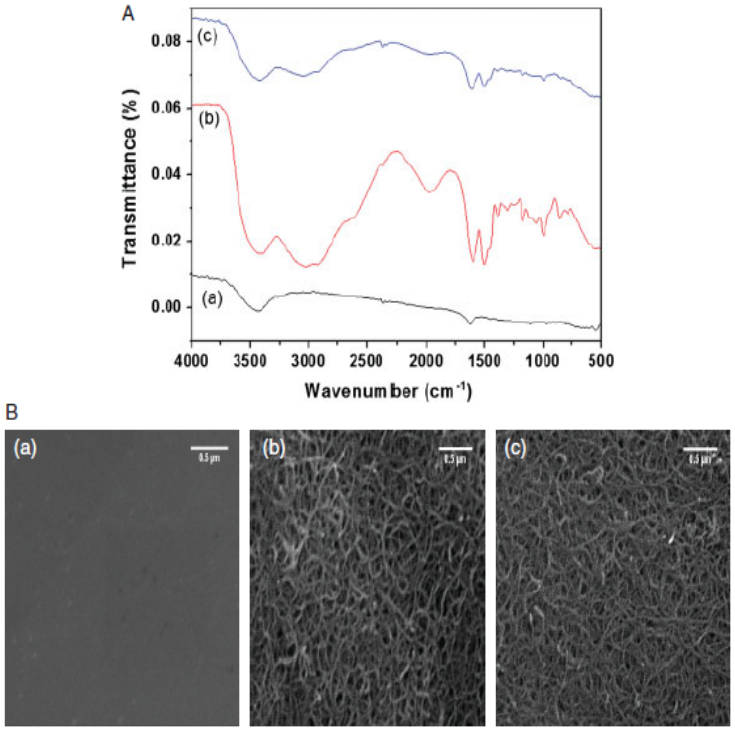

Figure 3. (A) FTIR spectra in transmission mode (a) COOH-MWCNT, (b) PAH, (c) PAH/COOH-MWCNT and c(B) SEM images of (a) bare GCE, (b) GCE modified with COOH-MWCNT and (c) GCE modified with COOH-MWCNT and PAH.

primary amine groups of the polymer. Further, bands observed at 1608 cm^{-1} and 1466 cm^{-1} that are associated with N–H asymmetric bending and C–H stretch.[24] The curve (c) shows the spectrum of COOH-MWCNT after deposition of the PAH film, displaying bands between 825 cm^{-1} and 1380 cm^{-1} which confirm the PAH–COOH-MWCNT linkage.[25,26]

The stepwise modification of the GCE surface with COOH-MWCNT and PAH film under optimal conditions was accomplished by SEM (Fig. 3(B)). Micrographs (a) and (b) show the bare GCE and the COOH-MWCNT modified electrode, respectively. It is observed that COOH-MWCNTs are deposited on the GCE forming an irregular surface composed of entangled cross-linked fibrils. COOH-MWCNT-modified electrode surface after the PAH film deposition is shown in micrograph (c). The image shows the COOH-MCWCNTs also distributed as spaghetti-like structures, however, brightness and contrast of the image were diminished, attributed to the reduction of backscattered electrons and secondary effects that are perturbed by the low-conductivity of polymer film.[31,32]

Immobilization of anti-NS1 on the PAH/COOH-MWCNT/GCE

A schematic illustration of the anti-NS1/PAH/COOH-MWCNT/GCE electrode assembling and principle of the immunoassay by H_2O_2–peroxidase reaction is shown in Fig. 4(A). PAH film is assembled between the carbon nanotubes and biomolecules. Due to its linear structure, the PAH permits bonds on both sides, one side with COOH-MWCNT and the other with the anti-NS1, thus, acting as a bi-functional linker.

In order to electrochemically characterize the anti-NS1 immobilization, cyclic voltammetric (CV) profiles of the electrode surface were carried out using the $K_3Fe(CN)_6/K_4Fe(CN)_6$ as redox probe (Fig. 4(B)). The electrochemical proprieties of the COOH-MWCNT and PAH resulted in an increase of the catalytic activity, confirmed by increase of the anodic and cathodic peaks compared with the bare GCE and PAH/COOH-MWCNT/GCE.[33] After anti-NS1 immobilization, a decrease in redox peak currents was observed. This same behaviour also occurred after blocking the non-specific bindings with incubation of the electrode in 50 mmol L^{-1} glycine solution.[34]

Optimization of experimental conditions

To investigate the optimum pH for enzyme activity of the anti-NS1-HRP conjugate, a study of the pH influence on the catalytic current was carried out. It was observed that the peak current gradually increased when changing the solution pH from 5.5 to 6.5, and then decreased when the pH value was higher than 6.5.

The effect of the incubation time of NS1 antigen on the amperometric response of the sensor was also investigated. This allowed one to analyse the time in which interactions between the NS1 antigen and previously immobilized anti-NS1 antibody are considered maximum, i.e. with the maximum number of occupied binding sites. It was observed that the amperometric signal gradually increased with incubation time, achieving a plateau at 60 min.

In order to obtain the maximum response, the work potential of electrode vs. Ag/AgCl for amperometric measurements was determined from catalytic response of the peroxidase. The presence of the enzyme conjugate (anti-NS1-HRP) was established by CVs in PB (pH 6.5, 0.1 mol L^{-1}) at a scan rate of 100 mV s^{-1}. Detection of the enzyme was based on the current produced by

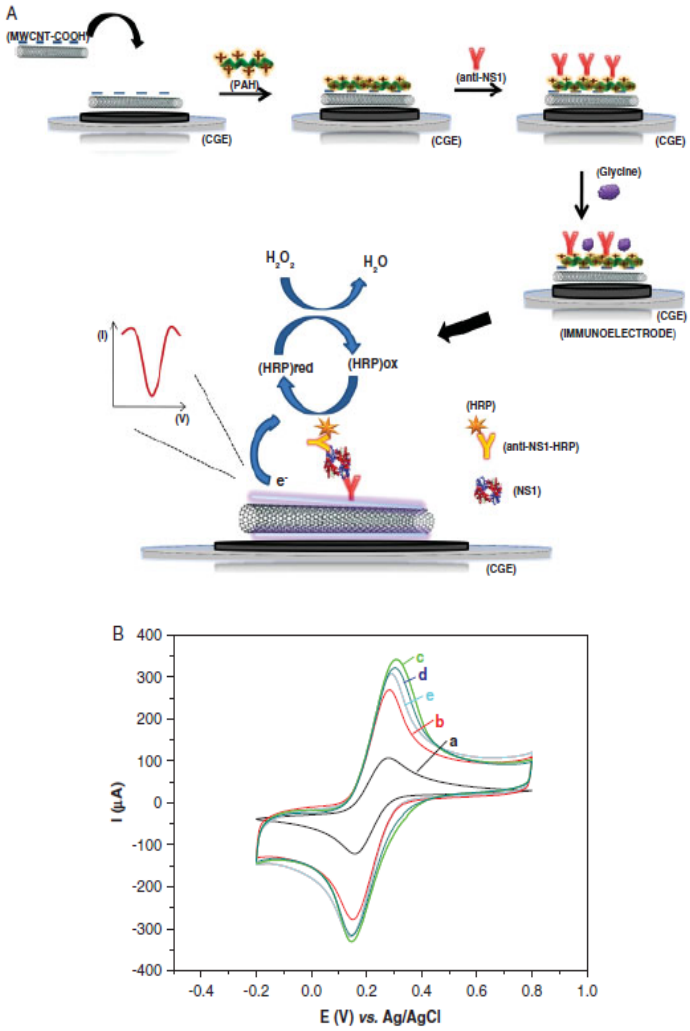

Figure 4. (A) Principle of the amperometric immunosensor showing the stepwise construction of immunoelectrode and principle of immunoassay. (B) Cyclic voltammograms at (a) bare GCE, (b) COOH-MWCNT/GCE, (c) PAH/COOH-MWCNT/GCE, (d) anti-NS1/PAH/COOH-MWCNT/GCE, (e) glycine/anti-NS1/PAH/COOH-MWCNT/GCE. The scans were performed in 5 mmol L^{-1} $K_3Fe(CN)_6/K_4Fe(CN)_6$, at 100 mV s^{-1} scan rate.

the displacement of ions from the redox process undergone by the iron atom present in its structure, which may undergo oxidation and reduction under certain conditions.[35] Comparing the CVs of NS1/anti-NS1/PAH/COOH-MWCNT/GCE in the presence of the anti-NS1-HRP, a slight alteration was observed in cathodic peak due to the process of iron charge transfer from the active centre of enzyme.[36] This slight alteration is observed even in the absence of its enzymatic substrate (H_2O_2) showing that HRP conjugated to anti-NS1 is present and has an electrocatalytic response. When 0.75 mmol L^{-1} H_2O_2 was used, a significant increase in the cathodic peak ($\Delta i = +20\%$) with a slight shift in potential $E_{pc} \approx -0.2$ V and a decrease of the anodic peak were observed, indicating an electrocatalytic reduction process of the enzyme with the substrate. Also observed was a smaller cathodic peak at potential of −0.1 V attributed to load transfer from the iron active centre of the HRP enzyme and the surface. The optimal condition was established at $E_{pc} \approx -0.2$ V.

Analytical response of the immunosensor

The calibration curve was performed in different NS1 concentrations. The amperometric responses were obtained from the cathodic peaks after the H_2O_2 reaction was subtracted from that of a blank (without H_2O_2). The reductions in the peak currents were proportional to the NS1 concentrations in a linear range from 0.1 to 2.5 μg mL^{-1} (Fig. 5(A)). The data adjusted by a linear regression equation showed a correlation coefficient of 0.997 ($P \ll 0.01$, n = 8) and a low relative error (≪1%). Based on the RSD of the blank sample and the slope of the calibration curve, the LOD can be calculated as: LOD = 3(RSD/slope). This immunosensor showed a LOD of 0.035 μg mL^{-1}. Alcon *et al.*[28] reported that the NS1 antigen is found circulating from the first day after the onset of fever up to the 9th day. In primary infection, NS1 levels ranged from 0.04 to 2 μg mL^{-1} in acute-phase serum samples (up to 7 days) and in secondary infection, NS1 levels ranged from 0.01 to 2 μg mL^{-1}.

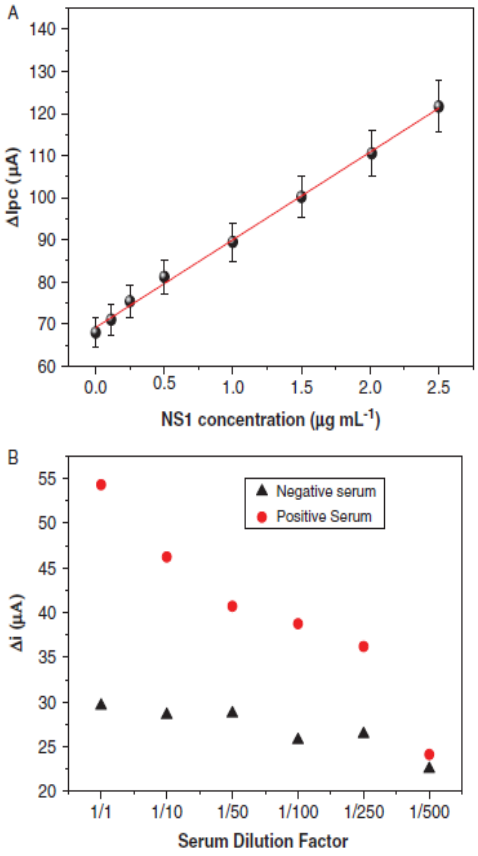

Figure 5. (A) Calibration curve of the immunosensor for NS1 antigen. (B) Response to the NS1 in negative and NS1 spiked serum samples at different PBS dilutions.

The matrix effect on the analytical anti-NS1/PAH/COOH-MWCNT/GCE responses was evaluated as shown in Fig. 5(B). A negative dengue serum was 1:1; 1:10; 1:50; 1:100; 1:250 and 1:500-fold diluted and compared with a spiked NS1 serum (with 5 μg mL^{-1} NS1). All the dilutions were carried out using PBS (10 mmol L^{-1}, pH 7.4). The dilution curve obtained from negative serum (curve I) was maintained practically constant demonstrating a non-matrix effect. The limit of detection to distinguish the serum was established at 1:250, which corresponds to approximately 0.02 μg mL^{-1} NS1. Therefore, this proposed immunosensor is suitable for NS1 detection in levels for diagnostic of dengue virus and has good selectivity.

CONCLUSIONS

An electrochemical immunosensor based on the synergic effect between PAH and carboxylated carbon nanotubes was developed for NS1 protein detection. The strategy of PAH film assembled on COOH-MWCNT ensured a stable nanostructured surface, and simultaneously promoted Fc-oriented immobilization of the anti-NS1. This uniform and homogeneous platform for antibodies immobilization could be capable of detecting NS1 protein at levels in the clinical range for an early acute dengue diagnosis.

ACKNOWLEDGEMENTS

The authors thank the National Council for Scientific and Technological Development - CNPq for supporting this work and Physics Department of Federal University of Pernambuco for performing the SEM images.

REFERENCES

1 Peeling RW, Artsob H, Pelegrino JL, Buchy P, Cardosa MJ, Devi S *et al.*, Evaluation of diagnostic tests: dengue. Nature Publishing Group, S30–S37 (2010).
2 Gurugama P, Garg P, Perera J, Wijewickrama A and Seneviratne SL, Dengue viral infections. *Indian J Dermatol* **55**:68–78 (2010).
3 Martina BEE, Koraka P and Osterhaus ADME, Dengue virus pathogenesis: an integrated view. *Clin Microbiol Rev* **22**:564–581 (2009).
4 Mairuhu ATA, Brandjes DPM and van Gorp ECM, Treating viral hemorrhagic fever. *IDrugs* **6**:1061–1066 (2003).
5 Singh MP, Majumdar M, Singh G, Goyal K, Preet K, Sarwal A *et al.*, NS1 antigen as an early diagnostic marker in dengue: report from India. *Diagn Microbiol Infect Dis* **68**:50–54 (2010).
6 Zainah S, Wahab AHA, Mariam M, Fauziah MK, Khairul AH, Roslina I *et al.*, Performance of a commercial rapid dengue NS1 antigen immunochromatography test with reference to dengue NS1 antigen-capture ELISA. *J Virol Methods* **155**:157–160 (2009).
7 Datta S and Wattal C, Dengue NS1 antigen detection: a useful tool in early diagnosis of dengue virus infection. *Indian J Med Microbiol* **28**:107–110 (2010).
8 Kumarasamy V, Wahab a HA, Chua SK, Hassan Z, Chem YK, Mohamad M *et al.*, Evaluation of a commercial dengue NS1 antigen-capture ELISA for laboratory diagnosis of acute dengue virus infection. *J Virol Methods* **140**:75–79 (2007).
9 Tontulawat P, Pongsiri P, Thongmee C, Theamboonlers A, Kamolvarin N and Poovorawan Y, Evaluation of rapid immunochromatographic NS1 test, anti-dengue IgM test, semi-nested PCR and IgM ELISA for detection of dengue virus. *Southeast Asian J Trop Med Public Health* **42**:570–578 (2011).
10 Chaterji S, Allen JC, Chow A, Leo Y and Ooi E, Evaluation of the NS1 rapid test and the WHO dengue classification schemes for use as bedside diagnosis of acute dengue fever in adults. *Am J Trop Med Hyg* **84**:224–228 (2011).
11 Vasconcelos EA, Peres NG, Pereira CO, da Silva VL, da Silva EF and Dutra RF, Potential of a simplified measurement scheme and device structure for a low cost label-free point-of-care capacitive biosensor. *Biosens Bioelectron* **25**:870–876 (2009).
12 Oliveira MDL, Correia MTS and Diniz FB, A novel approach to classify serum glycoproteins from patients infected by dengue using electrochemical impedance spectroscopy analysis. *Synth Met* **159**:2162–2164 (2009).
13 Oliveira MDL, Nogueira ML, Correia MTS, Coelho LCBB and Andrade CAS, Sensors and actuators B□: chemical detection of dengue virus serotypes on the surface of gold electrode based on Cratylia mollis lectin affinity. *Sensors Actuators B Chem* **155**:789–795 (2011).
14 Puertas S, de Gracia Villa M, Mendoza E, Jiménez-Jorquera C, de la Fuente JM, Fernández-Sánchez C *et al.*, Improving immunosensor performance through oriented immobilization of antibodies on carbon nanotube composite surfaces. *Biosens Bioelectron.* **43**:274–280 (2013).
15 Kausaite-Minkstimiene A, Ramanaviciene A, Kirlyte J and Ramanavicius A, Comparative study of random and oriented antibody immobilization techniques on the binding capacity of immunosensor. *Anal Chem* **82**:6401–6408 (2010).
16 Ruths J, Essler F, Decher G and Riegler H, Polyelectrolytes I: polyanion/polycation multilayers at the air/monolayer/water interface as elements for quantitative polymer adsorption studies and preparation of hetero-superlattices on solid surfaces. *Langmuir* **16**:8871–8878 (2000).
17 Stanton BW, Harris JJ, Miller MD and Bruening ML, Ultrathin, multilayered polyelectrolyte films as nanofiltration membranes. *Langmuir* **19**:7038–7042 (2003).
18 Kong B, Yoo H and Jung H, Electrical conductivity of graphene films with a poly(allylamine hydrochloride) supporting layer. *Langmuir* **25**:11008–11013 (2009).

19 Moreira FTC, Dutra RAF, Noronha JPC, Cunha AL and Sales MGF, Biosensors and bioelectronics artificial antibodies for troponin T by its imprinting on the surface of multiwalled carbon nanotubes□: its use as sensory surfaces. *Biosens Bioelectron* **28**:243–250 (2011).
20 Ahammad AJS, Lee J and Rahman A, Electrochemical sensors based on carbon nanotubes. *Sensors* **9**:2289–2319 (2009).
21 Lin J, He C, Zhang L and Zhang S, Sensitive amperometric immunosensor for a -fetoprotein based on carbon nanotube/gold nanoparticle doped chitosan film. *Anal Biochem* **384**:130–135 (2009).
22 Li N, Yuan R, Chai Y, Chen S and An H, Sensitive immunoassay of human chorionic gonadotrophin based on multi-walled carbon nanotube-chitosan matrix. *Bioprocess Biosyst Eng* **31**:551–558 (2008).
23 Dai Y and Shiu K, Glucose biosensor based on multi-walled carbon nanotube modified glassy carbon electrode. *Electroanalysis* **16**:1697–1703 (2004).
24 Kumar S, Vicente-Beckett V. Glassy carbon electrodes modified with multiwalled carbon nanotubes for the determination of ascorbic acid by square-wave voltammetry. *Beilstein J Nanotechnol* **Jan**:3988-396 (2012).
25 Gavalas VG, Law SA, Christopher Ball J, Andrews R and Bachas LG, Carbon nanotube aqueous sol-gel composites: enzyme-friendly platforms for the development of stable biosensors. *Anal Biochem* **329**:247–52 (2004).
26 Jusoh N, Abdul-aziz A and Supriyanto E, Improvement of glucose biosensor performances using poly (hydroxyethyl methacrylate) outer membrane. *Int J Biol Biomed Eng Improv* **6**:77–86 (2012).
27 Avrameas S, Coupling of enzymes to proetins with glutaraldehyde. *Immunochemistry* **6**:43–52 (1969).
28 Alcon S, Talarmin A, Debruyne M, Falconar A, Deubel V and Flamand M, Enzyme-linked immunosorbent assay specific to dengue virus type 1 nonstructural protein ns1 reveals circulation of the antigen in the blood during the acute phase of disease in patients experiencing primary or secondary infections. Enzyme-linked Immunosorb. *J Clin Microbiol* **40**:1–7 (2002).
29 Bard AJ and Faulkner LR, *Electrochemical Methods: Fundamentals and Applications*, 2nd Edn. Wiley, New York (2001).
30 Park HJ, Kim J, Chang JY and Theato P, Preparation of transparent conductive multilayered films using active pentafluorophenyl ester modified multiwalled carbon nanotubes. *Langmuir* **24**:10467–10473 (2008).
31 Hua M, Chen H, Tsai R, Tseng S, Hu S, Chiang C *et al.*, Preparation of polybenzimidazole-carboxylated multiwalled carbon nanotube composite for intrinsic sensing of hydrogen peroxide. *J Phys Chem C* **115**:15182–15190 (2011).
32 Park J, Wook S, Mao J, Seob I and Yun Y, Recovery of Pd(II) from hydrochloric solution using polyallylamine hydrochloride-modified *Escherichia coli* biomass. *J Hazard Mater* **181**:794–800 (2010).
33 Hu Y, Zhao Z and Wan Q, Facile preparation of carbon nanotube-conducting polymer network for sensitive electrochemical immunoassay of Hepatitis B surface antigen in serum. *Bioelectrochemistry* **81**:59–64 (2011).
34 Kim J, Premkumar T, Lee K and Geckeler KE, A facile approach to single-wall carbon nanotube/poly(allylamine) nanocomposites. *Macromol Rapid Commun* **28**:276–280 (2007).
35 Lynam C, Gilmartin N, Minett AI, Kennedy RO and Wallace G, Carbon nanotube-based transducers for immunoassays. *Carbon* **47**:2337–2343 (2009).
36 Huang J and Tsai Y, Direct electrochemistry and biosensing of hydrogen peroxide of horseradish peroxidase immobilized at multiwalled carbon nanotube/alumina-coated silica nanocomposite modified glassy carbon electrode. *Sensors Actuators B Chem* **140**:267–272 (2009).

6. Manuscrito 2

Talanta 128 (2014) 505–510

Contents lists available at ScienceDirect

Talanta

journal homepage: www.elsevier.com/locate/talanta

A thiophene-modified screen printed electrode for detection of dengue virus NS1 protein

M.M.S. Silva [a], A.C.M.S. Dias [a], M.T. Cordeiro [b], E. Marques Jr [b,c], M.O.F. Goulart [d], R.F. Dutra [a,*]

[a] Biomedical Engineering Laboratory, Federal University of Pernambuco, Av. Prof. Moraes Rego, 1235, Cidade Universitária, 50670-901 Recife, Brazil
[b] Aggeu Magalhães Research Center, FIOCRUZ-PE, Recife, Brazil
[c] Center for Vaccine Research, University of Pittsburgh, Pittsburgh, PA, USA
[d] Institute of Chemical and Biotechnology, Federal University of Alagoas, Maceió, Brazil

ARTICLE INFO

Article history:
Received 15 February 2014
Received in revised form
7 June 2014
Accepted 8 June 2014
Available online 14 June 2014

Keywords:
Screen printed electrode
Thiophene
Dengue virus
Immunosensor

ABSTRACT

A thiophene-modified screen printed electrode (SPE) for detection of the Dengue virus non-structural protein 1 (NS1), an important marker for acute phase diagnosis, is described. A sulfur-containing heterocyclic compound, the thiophene was incorporated to a carbon ink to prepare reproducible screen printed electrodes. After cured, the thiophene SPE was coated by gold nanoparticles conjugated to Protein A to form a nanostrutured surface. The Anti-NS1 antibodies immobilized via their Fc portions via Protein A, leaving their antigen specific sites free circumventing the problem of a random antibodies immobilization. Amperometric responses to the NS1 protein of dengue virus were obtained by cyclic voltammetries performed in presence of ferrocyanide/ferricyanide as redox probe. The calibration curve of immunosensor showed a linear response from 0.04 $\mu g\ mL^{-1}$ to 0.6 $\mu g\ mL^{-1}$ of NS1 with a good linear correlation (r=0.991, $p<0.05$). The detection limit (0.015 $\mu g\ mL^{-1}$ NS1) was lower than conventional analytical methods. In this work, thiophene monomers incorporated in the carbon ink enhanced the electroanalytical properties of the SPEs, increasing their reproducibility and sensitivity. This point-of-care testing represents a great potential for use in epidemic situations, facilitating the early diagnosis in acute phase of dengue virus.

1. Introduction

Dengue is a significant public health threat, with estimates of 50 to 100 million cases per year and around 3 billion people at risk of infection, mainly in tropical and subtropical regions [1]. Infection can result in a broad spectrum of disease syndromes ranging from an asymptomatic or mild infection, classical dengue fever (DF), to the potentially fatal dengue haemorrhagic fever (DHF) and dengue shock syndrome [2]. So far, there is no effective anti-viral therapeutic on the market and supportive therapy such as fluid replacement is the only treatment for severe forms of the disease. An early and accurate laboratory diagnosis of dengue could assist clinical management [3]. An ideal blood test for diagnostic should be affordable and easy to use with high performance and sensitivity to distinguish the acute-phase of dengue [4]. Additionally, it should not be costly and not require several steps, being adaptable at laboratory or at a point-of-care diagnostic without compromising its accuracy [5].

The most important development in dengue diagnostics in recent years is the advent of the specific detection of dengue virus NS1 antigen [6]. Enzyme-linked immunosorbent assays (ELISA) for detecting the NS1 were developed and demonstrated excellent sensitivity and specificity in detection of dengue infections [6–8]. NS1 glycoprotein is circulating mostly from days 1–6 after the onset of clinical symptoms, with the peak NS1 antigen detection occurring between days 3 and 5, in both primary and secondary infections, and hence is an excellent diagnostic target for acute dengue diagnosis [4,8]. Although the classical techniques are very powerful for monitoring, they are time consuming and are not adaptable for in situ and real time detection, beyond require skilled personnel [9,10]. Alternatively, rapid diagnostic test (RDT) for NS1 detection based on immunochromatography was proposed [11]. However, even if RDTs can provide opportunities for point-of-care, they have limitations regarding detectability, once their results are limited to a qualitative analyses (yes/no), becoming difficult the diagnostic of the acute-phase of dengue that is correlated with NS1 levels. Contrary, biosensors can supplier quantitative responses through a transducer that converts biochemical reactions in a measurable electric signal [12].

Electrochemical biosensors employing screen printed electrodes have emerged as adequate tools for point-of-care testings. They have

* Corresponding author. Tel.: +55 81 21268200.
E-mail address: rosa.dutra@ufpe.br (R.F. Dutra).

http://dx.doi.org/10.1016/j.talanta.2014.06.009
0039-9140/

innumerous advantages, such as ease of mass production and versatility [13]. Screen printed electrodes (SPEs) can combine good electrochemical proprieties and portability with simple and inexpensive fabrication techniques, thus being a good strategy to accomplish safety, disposable and quantitative immunonsensors [14]. In the fabrication of SPEs are used inks containing different chemical compounds, polymers or functional linking that can printed onto diverse type of plastic or ceramic substrates. The incorporation of compounds in the inks used for printing on the electrodes is a determinant factor for their selectivity and sensitivity required for each analysis [15].

Thiophene monomer derivatives have been pointed as attractive compounds to prepare electrochemical sensor, because they increase the conductivity, reduce the redox potential and improve the thermal and electrochemical stability [16]. Herein, thiophene monomers were incorporated into the carbon ink to form a homogenous and conductive composite, supplying a suitable signal amplification strategy to improve the electrochemical characteristics of the SPE increasing the sensitivity due to higher current densities and charge transfer across the interface electrode–electrolyte. Furthermore, sensitivity of immunosensors can be improved by increasing the amount of antibody immobilized on the electrode surface. Variety of nanostructures materials, with similar dimensions to biomolecules (antibodies, enzymes, DNA) owning different sizes, shapes and exceptional properties; such as metal nanoparticles (NP), quantum dots, carbon nanotubes and nanowires have employed for improvement of electrochemical biosensors. Nevertheless, NP which has capability for in situ synthesis onto the various composite films for antibody immobilization can improve the electrochemical signal and adsorption capacity of antibodies, and consequently enhance detection sensitivity. Therefore, the use of NPs represents a promising integration of electrochemical methods with new nanomaterials and electroactive complexes for electrochemical immunosensing [17].

It is well-known that way as antibodies are immobilized on the electrode surface affects the performance of an immunosensor. Fab portions of antibodies should be free for recognizing and binding to the epitopes of antigens. The Protein A extracted from Staphylococcus aureus has high affinity to the Fc portion of immunoglobulins from a variety of species, being widely used to promote an oriented antibody immobilization [18]. When the Protein A was used in a chromatographic assay, it was capable of binding antigen at over 80% of their theoretical capacity, because of the increased strength of the couple between the antibody Fc portion and protein A [19]. Stable and oriented immobilization of antibodies combined with the electrochemical advantages of thiophene as chemical modifying compound allowed a accurate detection of NS1. No labels were necessary when the antigen–antibody interactions were registered. The method described herein involves one-step preparation process and represents an advance in the production of SPEs for point-of-care testing.

2. Experimental

2.1. Materials and reagents

2.1.1. Chemical reagents and materials

Electrodag PF-407 C carbon ink with a density of 1.13 kg cm^{-3} was acquired from Acheson Henkel Corporation (Port Huron, MI, USA). Thiophene, protein A–conjugated gold nanoparticles (PtnA–AuNP) with approximately 20 nm (P6855), potassium ferricyanide ($K_3[Fe(CN)_6]$), potassium ferrocyanide ($K_4[Fe(CN)_6]$) and glycine, were acquired from Sigma-Aldrich (St. Louis, MO, USA). Phosphate buffer saline (PBS) (10 mmol L^{-1}, pH 7.4) used in all experiments was prepared by dissolving 0.2 g KCl, 8.0 g NaCl, 0.24 g KH_2PO_4 and 1.44 g Na_2HPO_4, in 1000 mL of deionized Milli-Q water from Millipore units (Bedford, MA, USA). All chemicals were of analytical grade.

2.1.2. Biological reagents

Mouse monoclonal antibodies against the NS1 glycoprotein of dengue virus (ab 138696) used to electrodes preparation and the dengue virus NS1 recombinant full-length protein (ab 64456) were purchased from Abcam (Cambridge, MA, USA). NS1 native protein was obtained from DENV-3 (strain 101.905/BR-PE/03) culture supernatant collected on the 5th day after inoculation in C6/36 cell monolayers, maintained in Leibovitz L-15 medium (GIBCO, Invitrogen, Grand Island, NY) containing 2% fetal calf serum. DENV-3 was detected and identified by RT-PCR [20]. In house ELISA, using anti-NS1 monoclonal antibodies, confirmed the presence of NS1 native protein in virus culture supernatant. As control was used supernatant from C6/36 cell culture (without virus) collected in the same conditions. Both supernatants were cleared by centrifugation for 10 min at 1.500 rpm (400 g).

2.2. Preparation of the thiophene-SPE

The electrodes were manufactured by squeezing a mixture containing carbon ink and thiophene onto a polyethylene terephtalate support to form a think conductive film. Four different concentrations of thiophene in relation to carbon ink were tested: 0.5% (w/V); 1% (w/V); 2.5% (w/V) and 10% (w/V). Prior printing, a plastic mold was used onto the PET rectangular surface (0.4 × 1.0 cm) to ensure electrodes with equal areas. After manufacturing, the electrodes were cured at 60 °C for 20 min. The manufactured thiophene-SPE consisted of with a circular area (Ø=4 mm) joined to a rectangular area (1 mm × 15 mm) used to electrical contact. After ready, the area of the electrode was delimited using a tape for galvanoplasty.

Prior to use, the thiophene-SPEs were pretreated by cyclic voltammetry (CV), scanning 30 cycles with a potential ranging from −2.0 V to 2.0 V, at a scan rate of 0.1 V s^{-1} and step potential of 2.44 mV, using 0.1 mol L^{-1} of KCl solution as the supporting electrolyte [21].

2.3. Apparatus

All the electrochemical experiments were performed in an Ivium Compact Stat potentiostat/galvanostat from Ivium Technologies (Eindhoven, The Netherlands) interfaced with a microcomputer and controlled by Ivium Soft software. A three-electrode system was used, which consisted of a thiophene-SPE as the working electrode (4 mm diameter), an Ag/AgCl electrode as the reference electrode and a helical platinum wire as the counter electrode. The electrodes were set up in a glassy electrochemical cell with 5 mL volume.

Experiments for characterizing the assembling of the thiophene-SPE were performed by CV in presence of 5 mmol L^{-1} of K3Fe(CN)6/K4Fe(CN)6 prepared in 0.1 mol L^{-1} of KCl solution, with a potential ranging from −0.6 V to 1.0 V, at 50 mV s^{-1} scan rate. Antigen–antibody interactions at the interface of the thiophene-SPE were also monitored by differential pulse voltammetry (DPV). DPV measurements were recorded from 0 V to 0.8 V, with pulse amplitude of 0.025 V, width of 0.05 s, and step potential of 0.05 V. The current signals were registered at a fixed potential (0.25 V) and the analytical response to NS1 was obtained taking into account the difference between the peak current (ΔI) of the thiophene-SPE with NS1 and the blank.

Fourier transform infrared (FTIR) spectra of samples were recorded by using a Bruker IFS 66 model FTIR spectrometer in

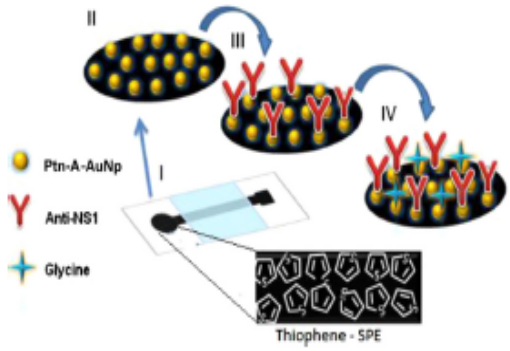

Fig. 1. Schematic illustration of the stepwise preparation of the NS1 immunosensor (I) bare thiophene-SPE; (II) AuNP–Ptn-A/thiophene-SPE; (III) anti-NS1/AuNP–Ptn-A/thiophene-SPE; and (IV) glycine/anti-NS1/AuNP–Ptn-A/thiophene-SPE.

the region of 4000 cm^{-1} to 400 cm^{-1}, by using the standard KBr pellet technique.

2.4. Immobilization of the anti-NS1

Anti-NS1 antibodies were immobilized via protein A–conjugated gold nanoparticle (AuNP–Ptn A), forming a nanostructured film on the electrode surface. 10 μL AuNP–Ptn A solution was pipetted onto the electrode surface of the thiophene-SPEs and left at 4 °C (overnight). Subsequently, 10 μL of anti-NS1 (10 μg mL^{-1}) prepared in 10 mmol L^{-1} of PBS was incubated on the electrode surface for 1 h. Non-specific bindings were blocked by incubating the electrode surface with 50 mmol L^{-1} of glycine solution for 40 min. For preservation of the anti-NS1, the immobilized thiophene-SPE was stored in a moist chamber in a refrigerator (approximately + 4 °C). A schematic design of the thiophene-SPE is shown in Fig. 1.

2.5. Immunosensor response to NS1

Initially, the analytical responses of the immunosensor were evaluated by incubating the coated anti-NS1 thiophene-SPEs with NS1 samples in different concentrations. Then, 10 μL of NS1 solutions were pippeted on the electrode surface and left to react for 30 min in a moist chamber at room temperature (24 °C). Afterwards, the electrode was washed four times in PBS and water. The immunosensor response was also evaluated in real samples against the NS1 native protein by incubating the anti-NS1 thiophene-SPEs with culture supernatant collected on the 5th day after inoculation in C6/36 cell monolayers. The supernatant solution containing NS1 native antigen was 1:128, 1:64, 1:32, 1:16, 1:8, 1:4 and 1:1 serial diluted in PBS and 10 μL of supernatant was also pippeted on the electrode surface at the same conditions described. A culture supernatant of C6/36 cells monolayers without NS1 infected serum inoculation was used as control.

3. Results and discussion

3.1. Characterization of thiophene-SPE

Chemically modified screen-printed carbon electrodes may be produced by incorporating specific reagents into the screen-printing inks, thus increasing the selectivity and detectability of measurements [22]. Among the available electroanalytical techniques, the CV technique has been widely used to understand the electroactivity and the electrochemical properties of conducter films or organic salts because it can better describe the

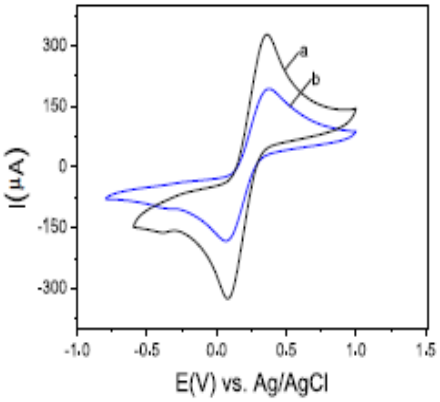

Fig. 2. (a) Cyclic voltammogram profiles of the carbon ink-printed electrode, with thiophene; and (b) without thiophene. The scans were performed in 5 mmol L^{-1} $K_3Fe(CN)_6/K_4Fe(CN)_6$, at a scanning rate of 50 mV s^{-1}.

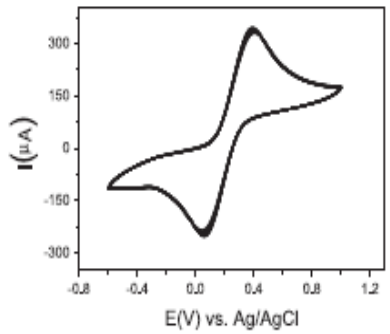

Fig. 3. Cyclic voltammograms of the thiophene-SPE from twenty replicate cycles performed in presence of 5 mmol L^{-1} of $K_3Fe(CN)_6/K_4Fe(CN)_6$ prepared in a 0.1 mol L^{-1} KCl solution, at a scanning rate of 50 mV s^{-1}.

characteristics of the electrochemical switching behavior between conducting and insulating states. Herein, the thiophene-SPE and the chemically-unmodified screen-printed carbon electrode were submitted to a CV technique in the presence of 5 mmol L^{-1} of $K_3Fe(CN)_6/K_4Fe(CN)_6$ prepared in 0.1 mol L^{-1} of KCl solution, at a 0.1 V s^{-1} scan rate and potential ranging from −0.6 V to 1.0 V (Fig. 2). The incorporation of the thiophene into the carbon ink resulted in an increase of approximately 40% of the current density. This behavior tell that the thiophene makes considerable contribution to higher charge transfer, improving the technical performance of carbon ink electrode.

The stability of the thiophene-SPE was also evaluated by setting the chemically- modified electrode to successive CVs. After 20 cycles performed in presence of 5 mmol L^{-1} of $K_3Fe(CN)_6/K_4Fe(CN)_6$ prepared in a 0.1 mol L^{-1} KCl electrolyte, at 0.1 V s^{-1} scanning rate and a potential ranging from −0.6 V to1.0 V, the redox peaks were practically constant. It was obtained a coefficient of variation of approximately 3.4% that is much more stable than the electrode without thiophene (9.2% coefficient of variation) (Fig. 3).

3.2. Effect of thiophene concentration

The influence of thiophene concentration on the electrode performance were performed by using CV in presence of $K_3Fe(CN)_6/K_4Fe(CN)_6$ as redox probe. The concentrations of thiophene varied from 0.5% to 10%, were analyzed according to maximal amplitude of the produced redox peaks. It was found that the redox peaks increased with the thiophene concentration, achieving

a plateau at 2.5% (m/v) thiophene. The use of 2.5% of thiophene resulted conductivities two times greater than for non-modified electrodes (Fig. 4) Thus, this concentration was used in all remaining experiments.

3.3. Fourier transform infra-red (FTIR) spectroscopy

FTIR spectra were used to investigate the modification of the carbon ink with thiophene. The FTIR spectra of the carbon ink layer without thiophene are shown in Fig. 5. Typical spectra for several concentrations of carbon black (ink component) are shown in Fig. 5(a). A band at 1634 cm^{-1} is probably a high conjugated C=O. O'Reilly and Mosher [23] discuss the assignment of the 1600 cm^{-1} band in carbon black and they attributed to aromatic ring stretching frequencies whose intensity is enhanced by the presence of oxygen atoms as phenol or ether groups. Two peaks are required in the 1400 cm^{-1} to1200 cm^{-1} region to reproduce the experimental curve. A band at 1400 cm^{-1} to 1450 cm^{-1} is assumed to be the C–O stretching frequency of the carboxylic acid groupand a band at 1120 cm^{-1} to 1190 cm^{-1}, probably due to the coupled C–O stretching frequency and OH bending modes of COOH and possibly the C–O stretching modes of ethers.

After the incorporation of thiophene in the carbon ink, the spectral analysis showed functional groups of the thiophene (Fig. 5(b)). Two bands at 2920 cm^{-1} and 2850 cm^{-1} corresponding to the C–H stretching; at cm^{-1} to the C=C stretching, at 1250 cm^{-1} to the CH2 stretching, at 1116 cm^{-1} to the bending vibrating peak of C–H, and 572 cm^{-1} to the feature peak of S. Also was observed at 1116 cm^{-1} and 1012 cm^{-1} peaks in the spectra attributed to S–O and S–phenyl bonds of sulfonic acid. Peaks of C,

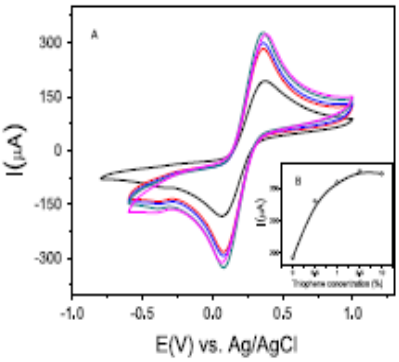

Fig. 4. Effect of the concentration of the thiophene monomer in the presence of 5 mmol L^{-1} of $K_3Fe(CN)_6/K_4Fe(CN)_6$ at a scanning rate of 50 mV s^{-1}.

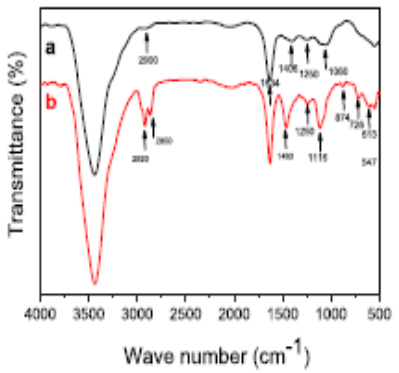

Fig. 5. ATR-FTIR spectra of the SPE–(a) without thiophene; and (b) with thiophene.

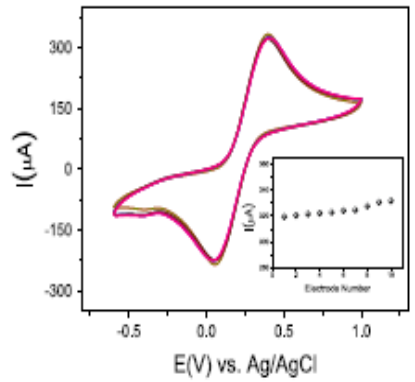

Fig. 6. Study of the reproducibility and stability of printed electrodes modified with thiophene. Ten screen-printed electrodes were tested in the presence of 5 mmol L^{-1} of $K_3Fe(CN)_6/K_4Fe(CN)_6$ at a scanning rate of 50 mV s^{-1}.

C–C, and C–S bonds in the thiophene backbone at 1463 cm^{-1}, 874 cm^{-1}, and 726 cm^{-1}, respectively, was also indicated [24]. Focusing on the 1450 cm^{-1} to1370 cm^{-1} range, the band at 1434 cm^{-1} is observed together with three other weak bands at 1418 cm^{-1}, 1408 cm^{-1}, and 1400 cm^{-1}, that are typically indicative of the thiophene in the carbon ink.

3.4. Reproducibility and stability of the thiophene-SPE

SPE not only answers the criterion of cost effectiveness, but also it satisfy the previously much sought after criteria of being highly reproducible and offering sensitive methods of detection towards target analytes, whilst maintaining low cost production through scales of economy. The adaptability of SPE is also of great benefit, due to mainly its ability to easily modify the electrode through different inks or chemical compounds allows for highly specific and finely calibrated electrode to be produced for specific target analytes [25,26]. To evaluate the reproducibility of the SPE, a series often electrodes were prepared (Fig. 6a). The relative standard deviation (RSD) of the measurements for the ten electrodes was 1.28%, suggesting an acceptable precision and reproducibility. These good results should be attributed to the use of ink with a thiophene Fig. 6). The electrodes from one series not only have the same sensitivities, but also nearly the same standard potentials, which is especially important in the case of disposable sensors.

3.5. Scan rate study

Information involving the electrochemical mechanisms can often be obtained by the relationship between the cathodic/anodic current peak and scanning rate of CV [27]. Fig. 7 shows the CVs of thiophene-SPEs at different scanning rates ranging from 10 mV s^{-1} to 100 mV s^{-1}, performed in 5 mmol L^{-1} of $K_3Fe(CN)_6/K_4Fe(CN)_6$ prepared in 0.1 mol L^{-1} of KCl solution, with potential ranging from −0.6 V to 1.0 V.

According to Fig. 7b, by increasing the scanning rates from 10 mV s^{-1} to 100 mV s^{-1}, the CVs of all redox couples showed a pair of symmetric peaks with a gradually increasing peak current. The currents of both the anodic and cathodic peaks increased linearly with the square root of the scanning rate, thus indicating that the process is controlled by diffusion. There was proportionality between the cathodic peak currents and the square root of the scanning rate, which shows that the charge transfer occurred reversibly. The electron transfer rate constant (ks) was calculated employing the Laviron equation [28]:

$ks = \alpha nFv/RT;$

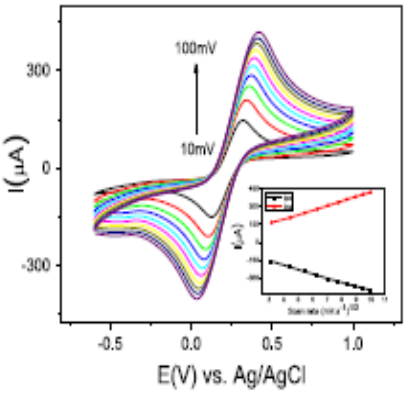

Fig. 7. (a) Cyclic voltammograms of the immunosensor in 5 mmol L^{-1} of $K_3Fe(CN)_6/K_4Fe(CN)_6$ at scanning rates (from inner to outer) of: 10 mV s^{-1}, 20 mV s^{-1}, 30 mV s^{-1}, 40 mV s^{-1}, 50 mV s^{-1}, 60 mV s^{-1}, 70 mV s^{-1}, 80 mV s^{-1}, 90 mV s^{-1}, and 100 mV s^{-1}; (b) Plots of current peak as a function of the square root of the scanning rate.

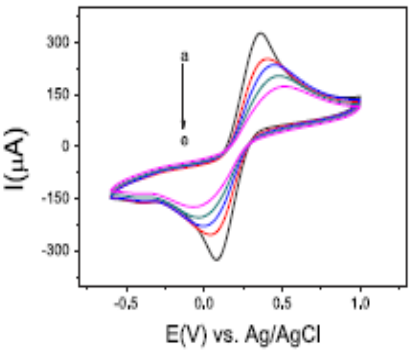

Fig. 8. Cyclic voltammograms of the immunosensor in each step of immobilization: (a) bare thiophene-SPE; (b) AuNP–Ptn-A/thiophene-SPE; (c) anti-NS1/AuNP–Ptn-A/thiophene-SPE; (d) glycine/anti-NS1/AuNP–Ptn-A/thiophene-SPE and (e) NS1/glycine/anti-NS1/AuNP–Ptn-A/thiophene-SPE. Scans were performed in 5 mmol L^{-1} of $K_3Fe(CN)_6/K_4Fe(CN)_6$, at a scanning rate of 0.1 V s^{-1}.

where α is the electron transfer coefficient, n is the number of electrons transferred, F is the Faraday constant, v is the scanning rate, R is the gas constant and T is the temperature. The ks was estimated to be 1.2×10^4 s^{-1}.

3.6. Immobilization of the anti-NS1

CV is a very versatile electrochemical technique which allows probing of the mechanics of redox reactions and transport properties of a system in solution. When well defined redox mediators are used, CV can be utilized to characterize the stepwise modifications of the occurred at the interface of electrode surface by changes on conductivity/reactivity properties. As shown at Fig. 8, when the thiophene-SPE was coated with gold-conjugated protein A film, a decrease of the anodic and cathodic peaks was observed. Although the presence of AuNP on the electrode surface increase the electroactive area, producing a nanostructured regions, the insulating nature of protein A is probably responsible by hindering the electronic transfer [19]. According to the area of the redox peaks, a decrease of electroactive area at approximately 23% was observed. Also was observed a decrease of redox peaks after anti-NS1 antibodies immobilization and glycine blocking as expected [16].

The role of nanogold layer onto the thiophene-modified screen printed electrode was not only to increase the amount of immobilized anti-NS1 antibodies [6], but also promote an oriented immobilization of antibodies by their Fc terminal. Therefhore, this simple strategy improves the sensitivity and selectivity of the immunosensor [29,30].

3.7. Analytical response of the immunosensor

Under optimized experimental conditions, the calibration curve of the immunosensor was obtained. The electrodes were incubated in different concentrations of NS1 and submitted to CV measurements in presence of $K_3[Fe(CN)_6]/K_4[Fe(CN)_6]$ (5 mmol L^{-1}) in KCL (0.1 mmol L^{-1}). The results show that the anodic peak current decreased with the increase of NS1 concentration in the incubation solution (Fig. 9a). Linearity in the calibration curve was obtained over

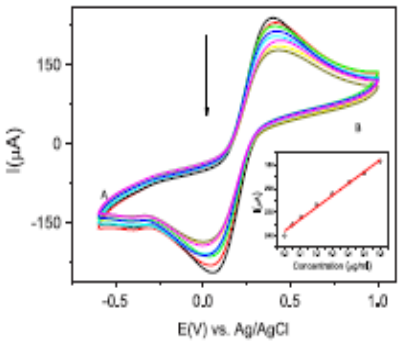

Fig. 9. (a) Cyclic voltammograms of the immunosensor in different NS1 concentrations (b) Calibration curve obtained by the anodic peaks from three replicated measurements.

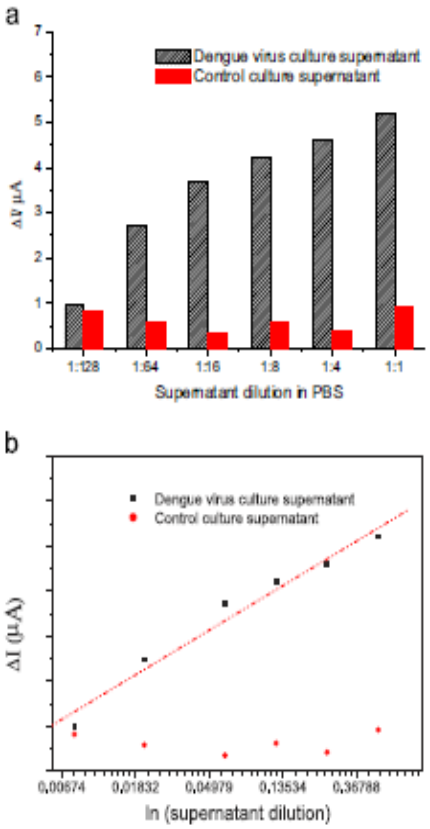

Fig. 10. (a) Analytical responses of thiophene-SPEs to the NS1 native protein f from dengue virus and control (CD4 cells) culture supernatant at serial dilutions. (b) Linear fit obtained by natural logarithm of supernatants dilutions. The amperometric responses obtained by DDP in 5 mmol L^{-1} of $K_3Fe(CN)_6/K_4Fe(CN)_6$.

the range of 0.05 g mL^{-1} to 0.6 g mL^{-1} of NS1 (r=0.991). The limit of detection (LOD) defined as three times the blank standard deviation signal was found to be 0.015 μg mL^{-1}, which was much lower than the other methods used to detect the NS1 antigen [16,31,32]. Alcon et al. [7] reported that the NS1 antigen was found circulating from the first day after onset of the illness up until the 9th day. In primary infections, NS1 levels range from 0.05 μg mL^{-1} to 0.6 μg mL^{-1} in serum samples of patients in the acute phase of the disease (up to 7 days). These clinical range for dengue diagnostic are matched with values detected by the gold nanoparticle thiophene-SPE developed.

3.8. Determination of NS1 in real samples

The proposed immunosensor was tested against real NS1 samples through culture supernatant collected on the 5th day after inoculation in C6/36 cell monolayers, period which the NS1 native protein reach maximal production [7]. The immunoelectrodes were incubated with 10 μL of a serial two-fold dilution of dengue virus culture supernatants in PBS for 30 min, at room temperature and specific responses were obtained regarding control supernatant (C6/36 cell culture). Immunosensor responses for all serial dilutions of the control culture (1:128, 1:64, 1:32, 1:16, 1:8, 1:4 to 1:1) were practically constant and similar to 1:128 dilution of control culture supernatants, whereas dengue virus supernatant responses increased inversely proportional to serial dilutions (Fig. 10a). Linear fit obtained by natural logarithm from curve shown in Fig. 9A, shows a correlation coefficient of 0.996 (n=6, p < <0,01) that is indicative of a good linearity (Fig. 10b). This label-free immunosensor is more practical than ELISA and also provide quantitative responses contrary to RDTs [33].

4. Conclusions

Thiophene monomers incorporated into the carbon ink resulted in more stable, sensible and reproducible screen printed electrodes. Moreover, nanolayer formed by gold conjugated to protein A resulted more antibodies immobilized on the electrode surface and non-random linkage, this encouraging results indicate that this chemically-modified carbon-based can be used to specific NS1 detection. Moreover, this developed immunosensor can easily become a point-of-care testing for early diagnostic of acute-phase.

Acknowledgements

The authors thank the National Council of Scientific and Technological Development (CNPq, Brazil) and the Pernambuco Research Foundation (FACEPE, PE, Brazil) for financial support.

References

[1] J.L. Kyle, E. Harris, Annu. Rev. Microbiol. 62 (2008) 71–92.
[2] A.T.A. Mairuhu, J. Wagenaar, D.P.M. Brandjes, E.C.M. van Gorp, Eur. J. Clin. Microbiol. Infect. Dis. (2004) 425–433.
[3] S.D. Blacksell, R.G. Jarman, R.V. Gibbons, A. Tanganuchitcharncha, M. P. Mammen, A. Nisalak, S. Kalayanarooj, M.S. Bailey, R. Premaratna, H.J. de Silva, N.P.J. Day, D.G. Lalloo, Clin. Vaccine Immunol. 19 (2012) 804–810.
[4] WHO, Special Programme for Research, Training in Tropical Diseases, Dengue: guidelines for diagnosis, treatment, prevention and control, World Health, 2009.
[5] M.L. Moi, T. Omatsu, S. Tajima, C.-K. Lim, A. Kotaki, M. Ikeda, F. Harada, M. Ito, M. Saijo, I. Kurane, T. Takasaki, J. Travel Med. 20 (2013) 185–193.
[6] S.D. Blacksell, J. Biomed. Biotechnol. (2012) 1–12 (Article ID 151967).
[7] S. Alcon, A. Talarmin, M. Debruyne, A. Falconar, V. Deubel, M. Flamand, J. Clin. Microbiol. 40 (2002) 376–381.
[8] S.R. Fry, M. Meyer, M.G. Semple, C.P. Simmons, S.D. Sekaran, J.X. Huang, C. McElnea, C.-Y. Huang, A. Valks, P.R. Young, M.A. Cooper, PLoS Negl.Trop. Dis. 5 (2011) e1199.
[9] G.-J. Zhang, L. Zhang, M.J. Huang, Z.H.H. Luo, G.K.I. Tay, E.-J.A. Lim, T.G. Kang, Y. Chen, Sens. Actuators, B 146 (2010) 138–144.
[10] T.Q. Huy, N.T.H. Hanh, N.T. Thuy, P. Van Chung, P.T. Nga, M.A. Tuan, Talanta 86 (2011) 271–277.
[11] S.D. Blacksell, R.G. Jarman, M.S. Bailey, A. Tanganuchitcharnchai, K. Jenjaroen, R.V. Gibbons, D.H. Paris, R. Premaratna, H.J. de Silva, D.G. Lalloo, N.P.J. Day, Clin. Vaccine Immunol. 18 (2011) 2095–2101.
[12] F. Ricci, G. Adornetto, G. Palleschi, Electrochim. Acta 84 (2012) 74–83.
[13] V. Somerset, J. Leaner, R. Mason, E. Iwuoha, A. Morrin, Electrochim. Acta 55 (2010) 4240–4246.
[14] A.C.M.S. Dias, S.L.R. Gomes-Filho, M.M.S. Silva, R.F. Dutra, Biosens. Bioelectron. 44 (2013) 216–221.
[15] O.D. Renedo, M.A. Alonso-Lomillo, M.J.A. Martínez, Talanta 73 (2007) 202–219.
[16] Y. Yoshioka, G.E. Jabbour, Synth. Met. 156 (2006) 779–783.
[17] J.E.N. Dolatabadi, M. Guardiah, Anal. Methods 6 (2014) 3891–3900.
[18] I.T. Cavalcanti, M.I.F. Guedes, M.D.P.T. Sotomayor, H. Yamanaka, R.F. Dutra, Biochem. Eng. J. 67 (2012) 225–230.
[19] T.H. Sisson, C.W. Castor, J. Immunol. Methods 127 (1990) 215–220.
[20] R.S. Lanciotti, C.H. Calisher, D.J. Gubler, G.J.Chang, A.V. Vorndam, J. Clin. Microbiol. 30 (1992) 545–551.
[21] M.A. Alonso-Lomillo, O. Domínguez-Renedo, L. Ferreira-Gonçalves, M.J. Arcos-Martínez, Biosens. Bioelectron. 25 (2010) 1333–1337.
[22] N.R. Stradiotto, H. Yamanaka, M.V.B. Zanoni, J. Braz. Chem. Soc. 14 (2003) 159–173.
[23] J.M. O'Reilly, R.A. Mosher, Carbon N. Y. 21 (1981) 47–51.
[24] Z. Wu, C. Li, Z. Wei, P. Ying, Q. Xin, J. Phys. Chem. B 106 (2002) 979–987.
[25] J.P. Metters, R.O. Kadara, C.E. Banks, Analyst 136 (2011) 1067–1076.
[26] R. Koncki, M. Mascini, Anal. Chim. Acta 351 (1997) 143–149.
[27] S.L.R. Gomes-Filho, A.C.M.S. Dias, M.M.S. Silva, B.V.M. Silva, R.F. Dutra, Microchem. J. 109 (2013) 10–15.
[28] E. Laviron, J. Electroanal. Chem. Interfacial Electrochem. 101 (1979) 19–28.
[29] Z. Pei, H. Anderson, A. Myrskog, G. Dunér, B. Ingemarsson, T. Aastrup, Anal. Biochem. 398 (2010) 161–168.
[30] S. Bahadır, P. Pivarnik, S. Letcher, A.G. Rand, Biosens. Bioelectron. 15 (2000) 11–12.
[31] S. Datta, C. Wattal, Indian J. Med. Microbiol. 28 (2010) 107–110.
[32] D.H. Libraty, P.R. Young, D. Pickering, T.P. Endy, S. Kalayanarooj, S. Green, D. W. Vaughn, A. Nisalak, F.A. Ennis, A.L. Rothman, J. Infect. Dis. 186 (2002) 1165–1168.
[33] V.T. Hang, N.M. Nguyet, D.T. Trung, V. Tricou, S. Yoksan, N.M. Dung, T. Van Ngoc, T.T. Hien, J. Farrar, B. Wills, C.P. Simmons, PLoS Negl. Trop. Dis. 3 (1) (2009) e360.

7. Conclusão

Diante dos resultados apresentados, conclui-se que:

1) Foi possível a obtenção de imunossensores para detecção da proteína NS1 empregando nanomateriais com limite de detecção de 0.04µg/mL^{1} a 2.5 µg/mL^{1}

2) O emprego da PAH combinado aos NTC possibilitou a imobilização e orientação dos anticorpos Anti-NS1 e melhorou o limite de detecção visto na curva de calibração.

3) O sucesso do primeiro imunossensor levou a continuidade do projeto a partir da troca do dispositivo transdutor para um eletrodo impresso modificado com o monômero condutor Tiofeno,

4) O uso do monômero tiofeno na tinta de carbono aumenta em 70% a condutividade do sensor em relação ao eletrodo não modificado.

5) Os estudos dos Eis de carbono modificados com tiofenos foram bem sucedidos, mostrando reprodutibilidade, obtendo-se, como esperado, uma sensibilidade necessária para aplicação em imunossensores.

6) Foi possível detectar concentrações de NS1 na ordem de ng.mL-1 nos Eis,

7) Foi alcançado no primeiro trabalho um limite de detecção de 0.035 µg/mL^{1} e 0.015 µg mL^{-1} para o segundo trabalho. Observou-se significante melhora do sinal e do ajuste da curva analítica com a utilização do usando dos Eis.

8. Apêndice

Biosensors and Bioelectronics 44 (2013) 216–221

Contents lists available at SciVerse ScienceDirect

Biosensors and Bioelectronics

journal homepage: www.elsevier.com/locate/bios

A sensor tip based on carbon nanotube-ink printed electrode for the dengue virus NS1 protein

Ana Carolina M.S. Dias, Sérgio L.R. Gomes-Filho, Mízia M.S. Silva, Rosa F. Dutra*

Biomedical Engineering Laboratory, Federal University of Pernambuco, Av. Prof. Moraes Rego, 1235, Campus da Saúde, 50670-901 Recife, Brazil

ARTICLE INFO

Article history:
Received 5 November 2012
Received in revised form
18 December 2012
Accepted 18 December 2012
Available online 2 January 2013

Keywords:
Immunosensor
Screen-printed electrode
Carbon nanotubes
Dengue virus
NS1

ABSTRACT

An immunosensor for the non-structural protein 1 (NS1) of the dengue virus based on carbon nanotube-screen printed electrodes (CNT-SPE) was successfully developed. A homogeneous mixture containing carboxylated carbon nanotubes was dispersed in carbon ink to prepare a screen printed working electrode. Anti-NS1 antibodies were covalently linked to CNT-SPE by an ethylenediamine film strategy. Amperometrical responses were generated at −0.5 V vs. Ag/AgCl by hydrogen peroxide reaction with peroxidase (HRP) conjugated to the anti-NS1. An excellent detection limit (in the order of 12 ng mL^{-1}) and a sensitivity of 85.59 μA mM^{-1} cm^{-2} were achieved permitting dengue diagnostic according to the clinical range required. The matrix effect, as well as the performance of the assays, was successfully evaluated using spiked blood serum sample obtaining excellent recovery values in the results. Carbon nanotubes incorporated to the carbon ink improved the reproducibility and sensitivity of the CNT-SPE immunosensor. This point-of-care approach represents a great potential value for use in epidemic situations and can facilitate the early screening of patients in acute phase of dengue virus.

1. Introduction

Dengue is considered a major public health problem in tropical and subtropical regions of the world and is endemically prevalent in approximately 112 countries (Gurugama et al., 2010). It is a self-limiting, non-specific illness characterized by fever, headache, myalgia, and constitutional symptoms. Its severe forms (hemorrhagic fever and shock syndrome) may lead to multisystem involvement and death, mostly amongst children. The incidence of this disease has increased over the last 50 years with 2.5 billion people living in areas where dengue is endemic (Smith et al., 2009). In view of the high mortality rate and to reduce the disease burden, it is desirable to have a rapid and practical diagnostic method for early detection of dengue virus (Singhi et al., 2007). The major laboratorial methods currently available for diagnosis of the disease are viral culture (Samuel and Tiyagi, 2006), viral RNA detection by reverse transcriptase PCR (RT-PCR) (Huhtamo et al., 2010) and serological tests such as an immunoglobulin M (IgM) capture enzyme-linked immunosorbent assay (MAC-ELISA). The first two assays have restricted scope as a routine diagnostic procedure due to its requirement of highly skilled personnel, laborious procedure and time consumption (Huy et al., 2011). The MAC-ELISA, which is a commonly used assay, has a low sensitivity in the first four days of illness (Alcon et al., 2002). Therefore, early dengue diagnosis still remains a problem, as all these mentioned assays have their own pitfalls.

Dengue virus is an enveloped positive-sense RNA virus. The genomic RNA is approximately 11 kb in length and is composed of three structural protein genes that encode for nucleocapsid or core protein, a membrane-associated protein, an envelope protein and seven non-structural protein genes including NS1 protein (Shrivastava et al., 2011). Recently, ELISA assays specific to NS1 protein have been carried out showing that NS1 secretory protein is found at high concentrations during the early clinical phase of the disease, suggesting it as a predictive marker for dengue diagnosis and responsive to four serotypes (Lapphra et al., 2008). By aiming to achieve a practical diagnostic, rapid, immunochromatographic tests (RDTs) to NS1 detection have been proposed; however, they are limited due to their instability to provide qualitative responses and poor sensitivity on admission samples (Blacksell et al., 2006). Compared with RT-PCR analyzers and RDTs, biosensors present numerous advantages such as simpler management, easier miniaturization, faster and quantitative responses and, moreover, they can permit on-site monitoring (Dai et al., 2011). So far, only a few immunosensors have been developed to detect NS1 antigen and non-commercial approaches are available. Oliveira et al. (2011) developed a biosensor based on concanavalin A lectin as a bioreceptor; however, it is limited in the detection of NS1 due to its interaction with carbohydrates and

* Corresponding author. Tel./fax: +55 81 21268200.
E-mail addresses: rosa.dutra@ufpe.br, rfiremandutra@yahoo.com.br (R.F. Dutra).

0956-5663/$ - see front matter © 2012 Elsevier B.V. All rights reserved.
http://dx.doi.org/10.1016/j.bios.2012.12.033

glycoproteins that are present in the acute phase of dengue disease, including the cytokines, IFNα and others. Su et al. (2003) developed a quartz crystal microbalance immunosensor to simultaneously detect NS1 and envelope proteins in 1:10 diluted serum with 500 μg mL^{-1}. Although some progresses have been achieved, new attempts to obtain a practical and selective NS1 biosensor are required for diagnostic of dengue virus in acute phase.

Different types of transduction can be employed in a biosensor, after the analyte recognition through the sensing biomolecules. Although optical and piezoelectric transduction by using surface plasmon resonance (Dutra and Kubota, 2007) and quartz crystal microbalance (Mattos et al., 2012), respectively, have been more commonly employed for immunoassay, electrochemical transduction has received great attention, especially by using the screen printed electrodes (SPEs) (Kumbhat et al., 2010). SPEs have been shown to be more attractive since they combine a good strategy to accomplish disposable, safe and quantitative point-of-care testing (Silva et al., 2010). They are constructed by printing a conductive ink onto a solid support with significant advantages, like the feasibility to obtain printed electrodes in different sizes and designs, as well as the facility to incorporate diverse compounds in order to change their nature and electrochemical properties (Gornall et al., 2009). It is possible to develop SPEs with high performance, low background current and improved electron transfer kinetic, by simply adding conductive modifiers (Mohamed et al., 2010).

Nowadays, the important role that the carbon nanotubes play in the performance of electrochemical biosensors is well-known (Laschi et al., 2008). Due to their extraordinary chemical and physical properties, such as high electrical conductivity and good chemical stability, it is possible to obtain nanostructured electrodes with faster electron transfer reactions (Tam and Hieu, 2011). In addition, the carbon nanotubes can be functionalized with reactive groups to purposely attach biomolecules and other compounds (Li et al., 2010; Leng et al., 2011). Herein, caboxylated carbon nanotubes were incorporated into the carbon ink to produce SPEs with enhanced sensitivity and stability. A thin film containing amine groups was deposited on the caboxylated carbon nanotube-screen printed electrode (CNT-SPE) in order to perform a covalent and oriented immobilization of the anti-NS1 antibodies. This immunosensor showed to be an innovative electrochemical method for diagnosis of early clinical phase of dengue infection.

2. Experimental

2.1. Materials and reagents

Electrodag PF-407 C carbon ink was acquired from Acheson Henkel Corporation (USA). COOH-functionalized multi-walled carbon nanotubes (COOH-MWCNT), 95% purity degree, were obtained from Dropsens (Oviedo, SPA). Mouse monoclonal antibodies against NS1 glycoprotein of dengue virus (Anti-NS1) and Dengue Virus NS1 glycoprotein were purchased from Abcam (Cambridge, UK). Ethylenediamine (EDA) was acquired from Sigma-Aldrich (St. Louis, USA). Dimethylformamide (DMF) and hydrogen peroxide (H_2O_2) (30% w/v) were obtained from F. Maia (Cotia, BRA). Anti-NS1 antibody was labeled with horseradish peroxidase (HRP) according to Avrameas (1969). For the coupling of HRP to the anti-NS1, 12 mg of peroxidase was dissolved in 1 mL of 0.1 M phosphate buffer (pH 6.8) containing 5 mg of anti-NS1 antibody. While the solution was gently stirred, 0.05 mL of a 1% aqueous solution of glutaraldehyde was added. The mixture was allowed to stand at room temperature (approximately 25 °C) for 2 h and then twice dialyzed against 5 L of PBS at 4 °C overnight. The precipitate was removed by centrifugation for 30 min at 20,000 rpm. This stock solution of peroxidase labeled-antibody was kept at +4 °C until used.

The pool of blood samples used in this work consisted of five serum samples from voluntary donors, kindly provided by Oswaldo Cruz Hospital of the Pernambuco University, according to the ethics committee's recommendations. All voluntary donors were found negative for dengue virus. The serum samples were collected from venous blood and immediately centrifuged for 120 s at 3000*g* and stored at −20 °C. The positive pool was spiked with NS1 fixing with a same volume at concentrations similar to those detected in the viremic dengue patients (Alcon et al., 2002).

Unless indicated, all the antibodies and antigen solutions was prepared in 0.01 mmol L^{-1} phosphate buffer saline (PBS) at pH 7.0. Ultrapure water (18 MΩ cm) used to prepare all solutions was obtained from a Milli-Q water purification system (Millipore Inc., Billerica, USA).

2.2. Apparatus

All the electrochemical experiments were performed in an Ivium Compact Stat potentiostat/galvanostat from Ivium Technologies (Eindhoven, The Netherlands) interfaced with a microcomputer and controlled by Ivium Soft software. A three-electrode system consisting of the CNT-SPE as the working electrode (4 mm diameter), an Ag/AgCl electrode as the reference electrode and a helical platinum wire as the counter electrode was used. The electrodes were set up in a glassy electrochemical cell with 5 mL volume.

The experiments to characterize the assembling of the CNT-SPE were conducted by using cyclic voltammetry in 5 mmol L^{-1} $K_3Fe(CN)_6/K_4Fe(CN)_6$ prepared in 0.1 mol L^{-1} KCl solution, at 0.1 V s^{-1} scan rate and potential ranging from −0.6 to 1.0 V.

The atomic force microscopy (AFM) technique was used for morphological and topographic characterization of the CNT-SPE. The micrographs were obtained using a WITec Alpha 300S AFM microscope (WITec Instruments, Ulm, Germany) operating in contact mode with a silicon tip at 0.2 N/m constant force.

2.3. Preparation of the CNT-SPE

The CNT-SPEs were obtained from a mixture containing carbon ink and COOH-MWCNT. Prior to mixing, 1 mg COOH-MWCNT was dispersed in 1 mL DMF solvent and sonicated in an ultrasonic batch for 2 h. After that, the CNT-SPEs were manufactured by squeezing the mixture over the adhesive plastic mold fixed on the rectangular support of polyethylene terephtalate (Fig. S1, supplementary information). Afterwards, the electrodes were cured at 60 °C for 20 min and finally, the adhesive plastic mold was removed. The circular area of the working electrode (approximately 4 mm of diameter) was delimited using adhesive tape resistant to chemical (electroplating and anodizing vinyl tape 470 supplied from 3M Co., USA). After they were ready, the CNT-SPEs were pretreated by cyclic voltammetry using 30 cycles at a scan rate of 0.1 V s^{-1}, potential ranging from −2.0 to 2.0 V and 2.44 mV step potential in 0.1 mol L^{-1} KCl solution as supporting electrolyte (Alonso-Lomillo et al., 2009).

2.4. Immobilization of the anti-NS1

Anti-NS1 antibodies were immobilized via EDA film deposited on the electrode surface. The pretreated CNT-SPEs were immersed in a 10% (v/v) EDA aqueous solution for 1 h and dried at room temperature (~25 °C) by forming EDA film. Afterwards, 10 μL of anti-NS1 (1 μg mL^{-1}) prepared in PBS was incubated on the

electrode surface for 1 h. Anti-NS1 antibodies non-covalently linked, i.e. simply adsorbed on the electrode surface were removed with 50 mmol L^{-1} NaCl solution. Non-specific bindings were blocked by incubating the electrode surface, with 50 mmol L^{-1} glycine solution for 1 h. For preservation of the anti-NS1, the immobilized CNT-SPEs were stored in a refrigerator (approximately at +4 °C) in a moist chamber.

2.5. Immunosensor performance

The analytical responses of the immunosensor were evaluated by the following procedure: the CNT-SPEs were incubated with 10 µL of NS1 samples for 30 min followed by exhaustive PBS washings. Subsequently, the CNT-SPEs were incubated with 10 µL of anti-NS1–HRP (1 µg mL^{-1}) in PBS for 30 min and then with PBS washings. Electrochemical responses were obtained by catalytic reaction of the H_2O_2 with the peroxidase conjugated to anti-NS1 and measured by chronoamperometry applying a fixed potential of −0.5 V vs. Ag/AgCl for 120 s.

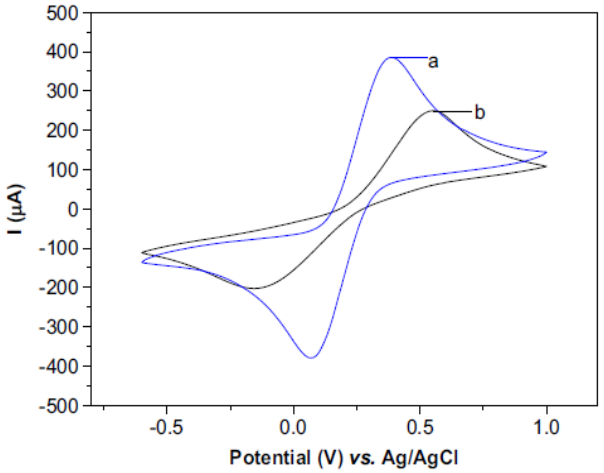

Fig. 1. Cyclic voltammograms profile of the carbon ink-printed electrode with CNT (a) and without CNT (b). Scans performed in 5 mmol L^{-1} $K_3Fe(CN)_6/K_4Fe(CN)_6$, at 0.1 V s^{-1} scan rate.

3. Results and discussion

3.1. Preparation of the CNT-SPE

CNTs have raised considerable interest in electrochemistry due to their ability to increase the electron transfer kinetics, to enlarge the electroactive surface area and to enhance the sensitivity of sensors (Taurino et al., 2012). However the electrocatalytic properties of the CNTs are strongly influenced by many factors. Herein, the incorporation of the CNT in carbon ink resulted in an increase of 190% of the electroactive surface area, as can be seen in the cyclic voltammograms in Fig. 1. Regarding the stability parameter, a synergic effect between CNT and carbon ink was observed. After 20 cycles in the presence of 5 mmol L^{-1} $K_3Fe(CN)_6/K_4Fe(CN)_6$ prepared in 0.1 mol L^{-1} KCl solution, at 0.1 V s^{-1} scan rate and potential ranging from −0.6 to 1.0 V, the voltammograms kept the redox peaks practically constant (3.4% of variation coefficient), i.e. more stable than the electrode without CNT (9.2% of the variation coefficient) (data not shown).

The functionalization of the sensing surface by introducing reactive groups for an oriented immobilization of the antibodies is a crucial step to obtain an immunosensor with a high performance (Cavalcanti et al., 2012). Herein, the EDA film containing amine groups was used to covalently bind the anti-NS1 by its Fc portion. On the other hand, the remaining amine groups of the EDA film were also utilized to form amide bonds with carboxyl groups of the CNT-SPE surface (Fig. 2). The EDA film acted as a bifunctional linker since the amide bonds were formed between the anti-NS1 and the carboxylated electrode surface. This assembly resulted in a stable and oriented matrix of immobilized antibodies.

Optimizing the EDA concentration for a maximal immunosensor response, cyclic voltammograms were obtained using a redox probe. Electrodes with EDA films in different concentrations were analyzed according to the maximal amplitude of the redox peaks (Fig. S2, supplementary information). It was found that the redox peaks increased with the EDA concentration, achieving a plateau at 10% (v/v) EDA. Thus, this concentration was used in all remaining experiments.

3.2. AFM analysis of the CNT-SPE surface

The morphology of the CNT-SPE surfaces was studied in three different steps using the AFM on contact mode. The topographic images of stepwise modification on the electrode surface are

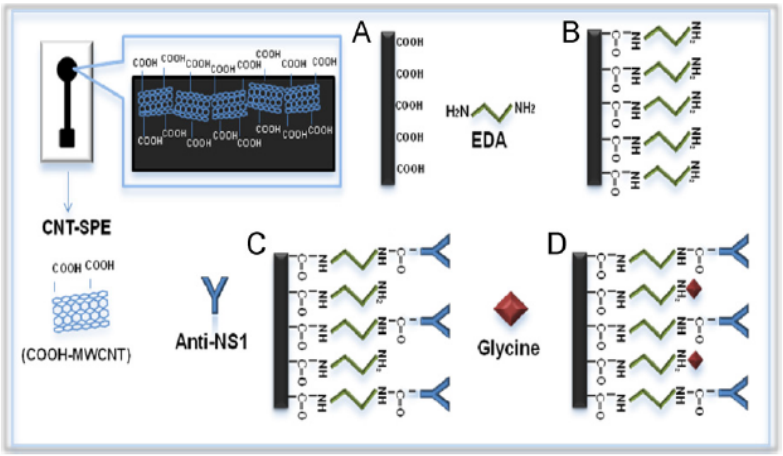

Fig. 2. Schematic illustration of the stepwise preparation of the immunosensor: (a) bare CNT-SPE, (b) EDA film formation, (c) anti-NS1 immobilization, and (d) blocking with glycine.

exhibited in Fig. 3. The CNT-SPE surface became flatter after EDA modification, by decreasing the roughness (R) from approximately 376 nm to 190 nm, probably attributed to filling up of the interstices in the electrode surface. After incubation with the anti-NS1, an agglomerate of globular structures was observed ($R \cong 240$ nm), confirming that the anti-NS1 was attached to the EDA film.

3.3. Electrochemical characterization

Quantitative analysis of the coverage with EDA film can be calculated by cyclic voltammetric investigations (Campuzano et al., 2006). The area of the redox peaks can be used in the characterization of the layers with respect to their degree of coverage and stability. Fig. 1b shows cyclic voltammograms using 5 mmol L^{-1} $K_3Fe(CN)_6/K_4Fe(CN)_6$ prepared in 0.1 mol L^{-1} KCl solution as a redox probe. When the electrode surface was modified by the EDA film, the electron transfer kinetic of $Fe(CN)_6^{3-/4-}$ was enhanced. As shown in Fig. 4, the stepwise assembly of the EDA on the electrode is accompanied by increase in the amplitude of the redox peaks. The current increase can be attributed to formation of the positively charged film on the electrode attracting the hexacyanoferrate that is negatively charged, which is consistent with the enhanced electron transfer. According to the area of the redox peaks, an increase of approximately 16%, with increase of the electroactive area was observed. The electrochemical nature of EDA layer implies in an increase of the catalytic activity, which can be confirmed by the increase in the redox peaks between the bare electrode and EDA modified electrode. Alternatively, a decrease in the current redox peaks was observed after incubation with anti-NS1. This decrease in the area of the redox peaks was expected due to insulating nature of the antibodies (Yun et al., 2007). Similar behavior was also observed after the blocking step of the non-specific bindings with incubation of the electrode in 5 mmol L^{-1} glycine solution.

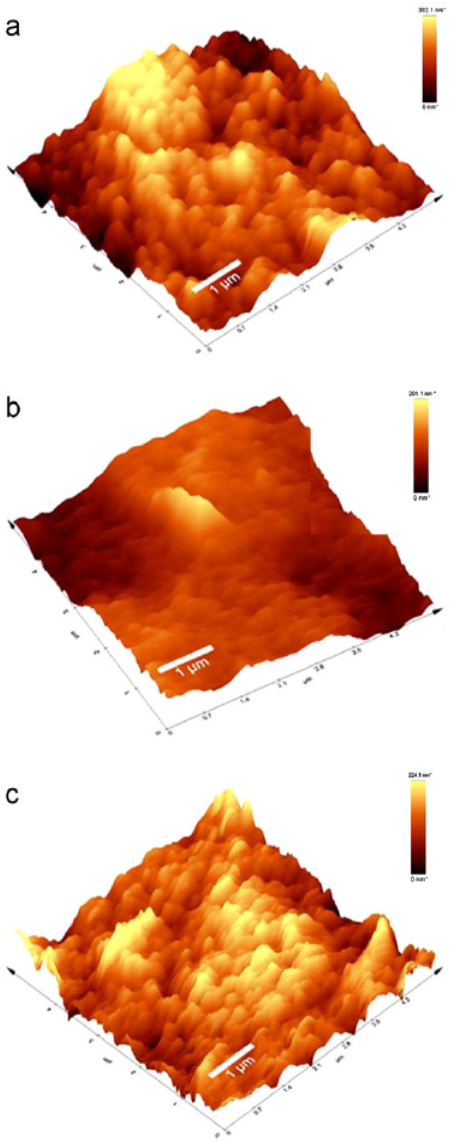

Fig. 3. AFM images: (a) bare CNT-SPE; (b) CNT-SPE modified by EDA and (c) CNT-SPE with immobilized anti-NS1.

3.4. Optimization of the experimental conditions

Since the maximum loading amount directly influences the immunoassay sensitivity, the antibody concentration of the sensing interface must be optimized (Zhang et al., 2008). Different concentrations of anti-NS1 (from 0.1 to 5 µg mL^{-1}) prepared in PBS were immobilized on the electrode surface using the same concentration of the NS1 measured (0.5 µg mL^{-1}). The immunosensor response showed a maximal concentration at 1 µg mL^{-1} anti-NS1, as a result of the antigen–antibody equilibrium required (Fig. S3, supplementary information). Thus, this concentration was chosen for the remaining experiments.

The activity of the enzyme used as electroactive species in the sandwich immunoassay is influenced by the pH of the solution. Most of these enzymes have an optimum activity in a limited range of pH (Liu et al., 2006). It is well known that at relatively high pH, the activity of the enzyme is inhibited (Darain et al., 2003). Thus, a study of the pH effect (from 5.5 to 8.0) on the immunosensor response was carried out in which the optimum catalytic activity of the enzyme was obtained at PBS pH 7.0 (Fig. S4(a), supplementary information). Several studies of immunoreactions exhibit optimal binding at this pH and hence it was adopted in all studies.

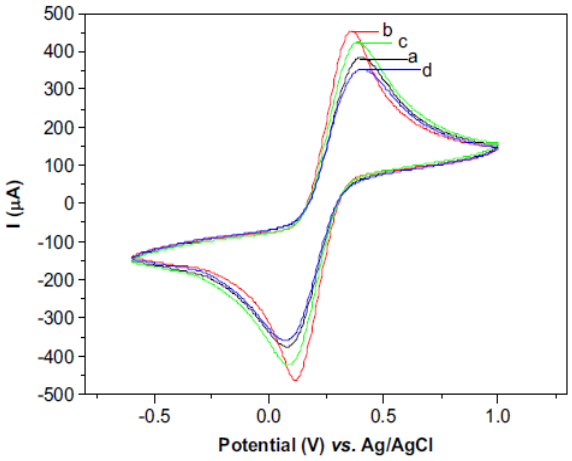

Fig. 4. Cyclic voltammograms of the immunosensor in each step of immobilization: (a) bare CNT-SPE; (b) EDA/CNT-SPE; (c) anti-NS1/EDA/CNT-SPE and (d) glycine/anti-NS1/EDA/CNT-SPE. Scans performed in 5 mmol L^{-1} $K_3Fe(CN)_6/K_4Fe(CN)_6$, at 0.1 V s^{-1} scan rate.

Incubation time exerts an important influence on the analytical performance of the immunosensor (Mao et al., 2010). Studies of the incubation time effect were carried out with the electrode surface incubated in NS1 solution (1 μg mL^{-1} in PBS) for 10, 20, 30, 45 and 60 min. The analytical response of the CNT-SPE increased with the incubation time reaching a plateau at 30 min, which was chosen for subsequent experiments (Fig. S4(b), supplementary information).

3.5. Analytical response of the immunosensor

Calibration curve was obtained by using the chronoamperometry technique. The analytical response of the CNT-SPE incubated in different concentrations of NS1 antigen prepared in PBS was generated by the catalytic reaction between H_2O_2 and HRP conjugated to anti-NS1, at −0.5 V fixed potential. This working potential was chosen based on the potential of the cathodic peaks exhibited in cyclic voltammograms due to anti-NS1–HRP response to the substrate (hydrogen peroxide). The results showed an increase of the current proportional to the NS1 concentrations. A linear range between 40 ng mL^{-1} and 2 μg mL^{-1} NS1 was obtained, indicating a good analytical performance (r=0.996, n=8) with a sensitivity of 85.59 μA mM^{-1} cm^{-2} (Fig. 5). Limit of detection (LOD) calculated according to IUPAC was found to be approximately 12 ng mL^{-1} for the NS1, being much lower than LOD previously described for the validated quartz crystal microbalance immunosensor developed to detect NS1 and envelope protein (LOD approximately 3 μg mL^{-1}) (Su et al., 2003). The linear range and LOD can be compared to sandwich ELISA kit (Dussart et al., 2003). Alcon et al. (2002) reported that the NS1 antigen was found circulating from the first day after the illness onset up to the 9th day. In primary infections, NS1 levels range from 0.04 to 2 μg mL^{-1} in serum samples of patients in the disease acute phase (up to 7 days). These levels match with the detected levels by the CNT-SPE developed in this work. Thus, this immunosensor presents as a real potential for dengue diagnosis, with the advantage to easily become a point-of-care testing.

3.6. Precision and accuracy studies

The reproducibility of the immunosensor response was evaluated by using six different electrodes incubated with a fixed NS1 concentration of 0.5 μg mL^{-1}. An excellent reproducibility was obtained (coefficient of variation CV=3.4%). The proposed immunosensor also showed good repeatability by measuring 10 replicated from the same CNT-SPE with 0.5 μg mL^{-1} NS1 concentration (CV=4%).

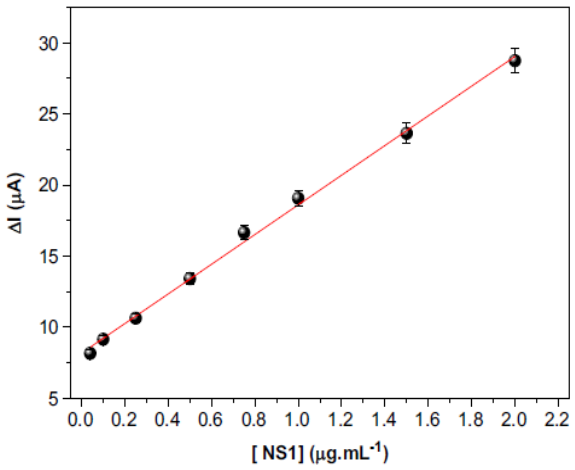

Fig. 5. Calibration curve of the immunosensor for NS1 protein of dengue virus.

Table 1
Recovery values in spiked PBS and serum samples based on the immunosensor. In all cases, n=3.

Concentration (ng mL^{-1})	PBS		Serum	
	Found concentration (ng mL^{-1})	Recovery (%)	Found concentration (ng mL^{-1})	Recovery (%)
0.10	0.104	104.0	0.116	116.0
0.50	0.510	102.0	0.512	102.4
1.00	1.030	103.0	1.010	101.0
1.50	1.480	98.7	1.470	98.0

Attempting to make use of this NS1 immunosensor in blood, recovery studies were done spiking serum samples negative to dengue with different NS1 protein concentrations. Herein, both PBS and serum samples were submitted to the same procedures and measured by the immunosensor. The recovery values are presented in Table 1, showing excellent results for the PBS and serum samples detection methodologies, with average recovery values of 101.9% and 104.4%, respectively.

The analytical accuracy of the immunosensor in PBS was better than in blood serum especially when the NS1 is measured in much lower concentrations. This result is attributed to the complexity of the blood sample that contains substances that alter the measurable concentration of the analyte or the antibody binding capacity. Approximately 40% of the serum samples contain non-analyte antibody binding substances, with 15% interference in non-blocked assays (Tate and Ward, 2004). Based on results obtained from serum sample, the immunosensor also showed effective surface-blocked assays.

4. Conclusions

A screen printed electrode specific to NS1 protein detection based on CNTs was successfully developed. The incorporation of the CNTs into carbon ink to prepare the CNT-SPE promoted an increase of the electroactive area, as well as improved the kinetic electron transfer, besides enhancing stability, reproducibility and sensitivity of the tip sensor. Due to the performance of the immunosensor presented in this work, this strategy can be suitable for the rapid, on-site and screen-out analysis of the NS1 protein. Additionally, this technology is attractive for mass production, with the advantage of being cheaper and more practical than RT-PCR and ELISA test, opening new ways for an early diagnosis of the acute dengue infection.

Acknowledgments

The authors thank the National Council of Scientific and Technological Development—CNPq for financial support and Centre of Strategic Technologies of Northeast for performing AFM imaging. A.C.M.S. Dias thanks FACEPE for its scholarship during this work.

Appendix A. Supporting information

Supplementary data associated with this article can be found in the online version at http://dx.doi.org/10.1016/j.bios.2012.12.033.

References

Alcon, S., Talarmin, A., Debruyne, M., Falconar, A., Deubel, V., Flamand, M.J., 2002. Journal of Clinical Microbiology 40 (2), 376–381.

Alonso-Lomillo, M.A., Domínguez-Renedo, O., Matos, P., Arcos-Martínez, M.J., 2009. Bioelectrochemistry 74, 306–309.

Avrameas, S., 1969. Immunochemistry 6 (1), 43–52.

Blacksell, S.D., Newton, P.N., Bell, D., Kelley, J., Mammen, M.P., Vaughn, D.W., Wuthiekanun, V., Sungkakum, A., Nisalak, A., Day, N.P.J., 2006. Clinical Infectious Diseases 42, 1127–1134.

Campuzano, S., Pedrero, M., Montemayor, C., Fatás, E., Pingarrón, J.M., 2006. Journal of Electroanalytical Chemistry 586, 112–121.

Cavalcanti, I.T., Silva, B.V.M., Peres, N.G., Moura, P., Sotomayor, M.D.P.T., Guedes, M.I.F., Dutra, R.F., 2012. Talanta 91, 41–46.

Dai, Y., Cai, Y., Zhao, Y., Wu, D., Liu, B., Li, R., Yang, M., Wei, Q., Du, B., Li, H., 2011. Biosensors and Bioelectronics 28, 112–116.

Darain, F., Park, S.-U., Shim, Y.-B., 2003. Biosensors and Bioelectronics 18, 773–780.

Dussart, P., Labeau, B., Lagathu, G., Louis, P., Nunes, M.R.T., Rodrigues, D.G., Storck-Herrmann, C., Cesaire, R., Morvan, J., Flamand, M., Baril, L., 2003. Clinical and Vaccine Immunology 13, 1185–1189.

Dutra, R.F., Kubota, L.T., 2007. Clinica Chimica Acta 376, 114–120.

Gornall, D.D., Collyer, S.D., Higson, S.P.J., 2009. Sensors and Actuators B: Chemical. 141, 581–591.

Gurugama, P., Garg, P., Perera, J., Wijewickrama, A., Seneviratne, S.L., 2010. Indian Journal of Dermatology 55, 68–78.

Huhtamo, E., Hasu, E., Uzcátegui, N.Y., Erra, E., Nikkari, S., Kantele, A., Vapalahti, O., Piiparinen, H., 2010. Journal of Clinical Virology 47 (1), 49–53.

Huy, T.Q., Hanh, N.T.H., Thuy, N.T., Chung, P.V., Nga, P.T., Tuan, M.A., 2011. Talanta 86, 271–277.

Kumbhat, S., Sharma, K., Gehlot, R., Solanki, A., Joshi, V., 2010. Journal of Pharmaceutical and Biomedical Analysis 52, 255–259.

Lapphra, K., Sangcharaswichai, A., Chokephaibulkit, K., Tiengrim, S., Piriyakarnsakul, W., Chakorn, T., Yoksan, S., Wattanamongkolsil, L., Thamlikitkul, V., 2008. Diagnostic Microbiology and Infectious Disease 60 (4), 387–391.

Laschi, S., Bulukin, E., Palchetti, I., Cristea, C., Mascini, M., 2008. ITBM-RBM 29, 202–207.

Leng, C., Wu, J., Xu, Q., Lai, G., Ju, H., Yan, F., 2011. Biosensors and Bioelectronics 27, 71–76.

Li, N., Xu, Q., Zhou, M., Xia, W., Chen, X., Bron, M., Schuhmann, W., Muhler, M., 2010. Electrochemistry Communications 12, 939–943.

Liu, Y., Qin, Z., Wu, X., Jiang., H., 2006. Biochemical Engineering Journal 32, 211–217.

Mao, L., Yuan, R., Chai, Y., Zhuo, Y., Yang, X., 2010. Sensors and Actuators B: Chemical 149, 226–232.

Mattos, A.B., Freitas, T.A., Silva, V.L., Dutra, R.F., 2012. Sensors and Actuators B: Chemical 3, 439–446.

Mohamed, G.G., Ali, T.A., El-Shahat, M.F., Al-Sabagh, A.M., Migahed, M.A., Khaled, E., 2010. Analytica Chimica Acta 673, 79–87.

Oliveira, M.D.L., Nogueira, M.L., Correia, M.T.S., Coelho, L.C.B.B., Andrade, C.A.S., 2011. Sensors and Actuators B: Chemical. 155, 789–795.

Samuel, P.P., Tiyagi, B.K., 2006. Indian Journal of Medical Research 123, 615–628.

Shrivastava, A., Dash, P.K., Sahni, A.K., Gopalan, N., Lakshmana Rao, P.V., 2011. Indian Journal of Medical Microbiology 29 (2011), 51–55.

Silva, B.V.M., Cavalcanti, I.T., Mattos, A.B., Moura, P., Sotomayor, M.P.T., Dutra, R.F., 2010. Biosensors and Bioelectronics 26 (3), 1062–1067.

Singhi, S., Kissoon, N., Bansal, A., 2007. Journal of Pediatrics 83, 22–35.

Smith, A.W., Chen, L.H., Massad, E., Wilson, M.E.T., 2009. Emerging Infectious Diseases 15, 8–11.

Su, C.C., Wu, T.Z., Chen, L.K., Yang, H.H., Tai, D.F., 2003. Analytica Chimica Acta 479, 117–123.

Tam, P.D., Hieu, N.V., 2011. Applied Surface Science 257, 9817–9824.

Taurino, I., Carrara, S., Giorcelli, M., Tagliaferro, A., Micheli, G., 2012. Surface Science 606, 156–160.

Tate, J., Ward, G., 2004. ClinicalBiochemist Reviews 25 (2), 105–120.

Yun, Y., Bange, A., Heineman, W.R., Halsall, H.B., Shanov, V.N., Dong, Z., Pixley, S., Behbehani, M., Jazieh, A., Tu, Y., 2007. Sensors and Actuators B: Chemical 123, 177–182.

Zhang, S., Zheng, F., Wu, Z., Shen, G., Yu, R., 2008. Biosensors and Bioelectronics 24, 129–135.

Talanta 117 (2013) 431–437

Contents lists available at ScienceDirect

Talanta

journal homepage: www.elsevier.com/locate/talanta

A carbon nanotube screen-printed electrode for label-free detection of the human cardiac troponin T

Bárbara V.M. Silva, Igor T. Cavalcanti, Mízia M.S. Silva, Rosa F. Dutra*

Biomedical Engineering Laboratory, Federal University of Pernambuco, Av. Prof. Moraes Rego, 1235-Cidade Universitária, 50670-901 Recife, Pernambuco, Brazil

ARTICLE INFO

Article history:
Received 15 March 2013
Received in revised form
28 August 2013
Accepted 30 August 2013
Available online 6 September 2013

Keywords:
Immunosensor
Screen-printed electrode
Carbon nanotube
Human cardiac troponin T
Point-of-care testing

ABSTRACT

Label-free immunosensor based on amine-functionalized carbon nanotubes screen-printed electrode is described for detection of the cardiac troponin T, an important marker of acute myocardial infarction. The disposable sensor was fabricated by tightly squeezing an adhesive carbon ink containing carbon nanotubes onto a polyethylene terephthalate substrate forming a thin film. The use of carbon nanotubes increased the reproducibility and stability of the sensor, and the amine groups permitted nonrandom immobilization of antibodies against cardiac troponin T. Amperometric responses were obtained by differential pulse voltammetry in presence of a ferrocyanide/ferricyanide redox probe after troponin T incubation. The calibration curve indicated a linear response of troponin T between 0.0025 ng mL^{-1} and 0.5 ng mL^{-1}, with a good correlation coefficient (r=0.995; $p < 0.0001$, n=7). The limit of detection (0.0035 ng mL^{-1} cardiac troponin T) was lower than any previously described by immunosensors and was comparable with conventional analytical methods. The high reproducibility and clinical range obtained using this immunosensor support its utility as a potential tool for point-of-care acute myocardial infarction diagnostic testing.

1. Introduction

Human cardiac troponin T (cTnT) is a sensitive and specific marker of cardiac injury that is regarded as the gold standard marker in the diagnosis of acute myocardial infarction (AMI). The detection of ultra-low levels of cTnT during early stages of cardiac disease facilitates the risk stratification and prognosis of the heart damage. The blood cTnT concentration rises rapidly within 3–4 h after AMI onset [1–3] and can be analyzed in the laboratory using several well-established enzymatic immunoassays based on reactions with chromogenic [4] and chemiluminescent substrates [5]. Point-of-care testing for cTnT could provide a potential analytical tool to reduce the turnaround time for assay compared with currently methods. Immunosensor technology offers a practical and simple immunoassay method for the determination of cTnT in the emergency departments.

Although immunosensors based on optic [6–9] and piezoelectric [10–12] transductions have been widely described for label-free cTnT detection, they are not suitable for point-of-care testing because they require more complex instrumentations and laborious manufacturing procedures, besides they are more expensive and difficult to miniaturize. Electrochemical transducers employing screen-printed electrodes (SPEs) have emerged as appropriate for point-of-care testing. These transducers are easily adaptable for in mass production, disposable and interchangeable with other biosensors, such as popular enzymatic glucometers [13,14]. Another advantage exhibited by the SPEs is their versatility to obtain electrodes with modifications in size and thickness by simple changing squeezing pressure, resulting in electrodes more sensitive and exhibiting improved electrochemical proprieties.

The cTnT detection in human serum by using electrochemical immunosensors has been possible by some authors [15–18]. However, the requirement of the electroactive species like the peroxidase enzyme that are dependent on Michaelis–Menten kinetic limits the immunosensor sensitivity. Moreover, the necessity for additional biochemical steps, including conjugated antibody incubations and reactions with specific substrates, increases the analysis time [19]. Recently reports have described label-free immunosensors that use voltammetric techniques, such as differential pulse voltammetry (DPV) [20,21]. This technique measures current by generating successive and regular voltage pulses superimposed on the potential linear sweep or stair steps. The current in an immunosensor is changed by antigen–antibody coupling on the electrode surface altering the mass transfer (i.e., electronic diffusion). At high potentials, DPV is limited by the high background current that hinders mass transfer and leads to a reduction in the accuracy of the amperometric response [22]. In attempting to overcome these difficulties some nanomaterials have been

*Corresponding author. Tel./fax: +55 81 2126 8000.
E-mail addresses: rosa.dutra@ufpe.br, rfiremandutra@yahoo.com.br (R.F. Dutra).

0039-9140/$ - see front matter © 2013 Elsevier B.V. All rights reserved.
http://dx.doi.org/10.1016/j.talanta.2013.08.059

proposed increasing the accuracy of immunosensors. Carbon nanotubes (CNTs) have attracted considerable attention due to their extraordinary properties, including their ability to mediate the electron-transfer reactions and to increase electrode surface area [23]. Gomes-Filho et al. [17] have proposed CNTs as alternative suggestion for the detection of serum cTnT with low limit of detection (LOD), although the conjugation of peroxidase to anti-cTnT was necessary to obtain the amperometric signal.

CNTs have been commonly deposited onto an electrode surface by simple adsorption [24] or assembled on a polymeric film [17]. However, these strategies are associated with instabilities in the response because the CNTs can leach during the measurement process. When the CNTs are incorporated into the sensor matrix (i.e., by forming nanocomposites), it is easier to control the amount of the CNTs used and to minimize their loss. Additionally, this procedure has advantage to be a one-step preparation method [25] and to dispense the use of electron-transfer mediators [26], beside CNTs act as anchors for an optimal biomolecules immobilization. Due to their facility to be functionalized with amine groups antibodies should be immobilized by Fc portion in order to expose the Fab sites to the epitopes [27]. In this study, amine functionalized CNTs were incorporated into the ink printing used to fabricate SPEs (CNT-SPE). A stable and oriented immobilization of antibodies combined with the electrochemical advantages of the CNTs allowed a rapid detection of cTnT. No labels were necessary when the antigen–antibody interactions were measured by applying DPV. The method described herein involves a straightforward preparation process and represents an advancement in the adaptation of SPEs point-of-care testing.

2. Materials and methods

2.1. Reagents and patient samples

Native cTnT purified from human cardiac muscle tissue was obtained from Calbiochem (Darmstadt, Germany). Mouse monoclonal anti-cTnT was purchased from Abcam (Cambridge, England). Amine-functionalized, multi-walled, 95% pure CNTs (NH_2-CNTs), were obtained from DropSens (Oviedo, Spain). Potassium ferricyanide ($K_3[Fe(CN)_6]$), potassium ferrocyanide ($K_4[Fe(CN)_6]$), *N*-hydroxysuccinimide (NHS), *N*-ethyl-*N*′-(3-dimethylaminopropyl) carbodiimide (EDC), dimethylformamide (DMF), and glycine were acquired from Sigma-Aldrich (St. Louis, MO, USA). Carbon ink (Electrodag PF-407C) was purchased from Acheson (Port Huron, MI, USA) for the fabrication of the CNT-SPEs. Phosphate-buffered saline (PBS) (10 mmol L^{-1}, pH 7.4) used in all experiments was prepared by dissolving 0.2 g KCl, 8.0 g NaCl, 0.24 g KH_2PO_4, and 1.44 g Na_2HPO_4 in 1000 mL of deionized Milli-Q water (from Millipore, units (Bedford, MA, USA). All chemicals were analytical grade.

Blood serum samples were collected from patients with AMI who were admitted to the Cardiac Emergency Hospital of Pernambuco—PROCAPE (Recife, Brazil). An automatic Elecsys 2010 Immunoassay Analyzer (Roche Diagnostics) was used to quantify cTnT via an electrochemical chemiluminescence immunoassay (ECLIA). Samples were stored at −20 °C while not in use during the electrochemical measurements.

2.2. Apparatus

Electrochemical measurements were performed using an Ivium CompactStat potentiostat obtained from Ivium Technologies (Eindhoven, Netherlands) that was interfaced to a computer system and controlled by Ivium software. All electrochemical measurements were made using a three-electrode system comprised of the CNT-SPE as working electrode, a helical platinum wire as auxiliary electrode, and an Ag/AgCl electrode as reference. All potentials given in this work were determined relative to the Ag/AgCl reference electrode. Electrochemical analyses were carried out using an electrochemical cell (10 mL) at room temperature (at approximately 24 °C).

Fourier transform infrared (FT-IR) spectroscopy was performed to chemically characterize the CNT-SPE. FT-IR measurements were performed in attenuated total reflectance (ATR) mode using an IFS-66 FTIR (scans=50, energy scanning from 400 cm^{-1} to 4000 cm^{-1}) acquired from Bruker (Karlsruhe, Germany).

Atomic force microscopy (AFM) was performed to characterize the morphology and topography of the CNT-SPE using an alpha300S AFM obtained from WITec (Ulm, Germany). Images were acquired in tapping mode using silicon tips at 0.2 N m^{-1} constant force.

2.3. CNT-SPE manufacturing

The CNT-SPE was fabricated by tightly squeezing an adhesive carbon ink containing NH_2-CNTs onto a polyethylene terephthalate (PET) rectangular surface to form a thin film. Prior to carbon ink incorporation, the NH_2-CNTs (5 mg) were dispersed in 1 mL of DMF and were immersed in an ultrasonic bath for 4 h until a black homogeneous suspension was obtained. A plastic mold was affixed to the rectangular PET surface (0.4 cm × 1.0 cm) to ensure SPEs with equal printed areas. After fabrication, the electrodes were cured at 60 °C for 20 min [22]. The manufactured CNT-SPE consisted of a circular area (Ø=4 mm) joined to a rectangular area (1 mm × 15 mm), which was used as an electrical contact. Prior to use, the CNT-SPE was cleaned rigorously by electrochemical pretreatment with 40 scans, in a potential between 2.0 V and −2.0 V in KCl (100 mmol L^{-1}) [28].

2.4. Anti-cTnT immobilization

Prior to immobilization, the carboxylic groups of anti-cTnT antibodies (5 μg mL^{-1}) were activated for 90 min in a solution of NHS (5 mmol L^{-1}) and EDC (2 mmol L^{-1}) prepared in PBS (10 mmol L^{-1}, pH 7.4). Afterwards, an aliquot (10 μL) of activated anti-cTnT antibodies was pipetted onto the CNT-SPE. The anti-cTnT incubation was maintained in a moist chamber at room temperature for 60 min. Finally, a glycine solution (50 mmol L^{-1}) prepared in PBS (10 mmol L^{-1}, pH 7.4) to block non-specific bindings was pipetted on the electrode for 45 min (Fig. 1a).

2.5. Electrochemical immunoassay

Antigen–antibody interactions at the interface of the CNT-SPE were monitored by DPV in real-time (Fig. 1b). DPV measurements were recorded from 0 V to 0.8 V with a pulse amplitude of 0.025 V, a width of 0.05 s, and a step potential of 0.05 V. The analytical response to cTnT was obtained taking into account the difference between the peak current (ΔI) of the CNT-SPE with cTnT and the blank (i.e. without cTnT). The current signals were registered at a fixed potential (+0.25 V).

Immunosensor preparation was characterized by cyclic voltammetry (CV) and electrochemical impedance spectroscopy (EIS) analyses. CVs were scanned from 1.0 V to −0.6 V at 50 mV s^{-1}. AC impedance measurements were performed in the frequency range from 1×10^{-2} Hz to 6.5×10^{4} Hz in a given open circuit voltage with an amplitude of 10 mV. All electrochemical measurements were conducted in $K_3[Fe(CN)_6]/K_4[Fe(CN)_6]$ (5 mmol L^{-1}) prepared in PBS (10 mmol L^{-1}, pH 7.4).

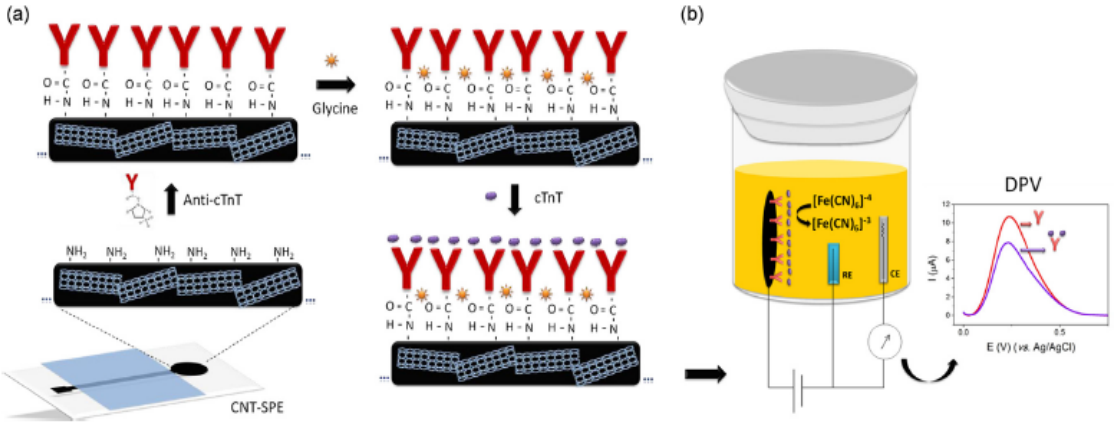

Fig. 1. Schematic representation of the (a) immunosensor fabrication and (b) electrochemical principle of detection.

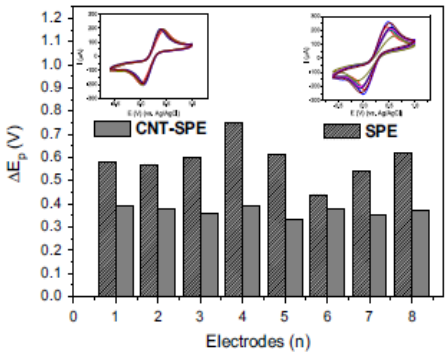

Fig. 2. ΔEp of the eight SPEs with and without NH_2-CNT. *Inset*: CVs of the electrodes with and without NH_2-CNT in presence of the $K_3[Fe(CN)_6]/K_4[Fe(CN)_6]$ (5 mmol L^{-1}) prepared in PBS (10 mmol L^{-1}, pH 7.4) at 50 mV s^{-1} scan rate.

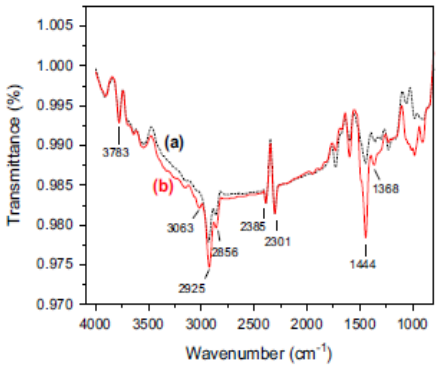

Fig. 3. ATR FT-IR spectra of the SPE (a) without NH_2-CNT and (b) with NH_2-CNT.

3. Results and discussion

3.1. Effect of NH_2-CNTs on the SPE

The electrochemical profile of the SPE with and without NH_2-CNTs incorporated into the carbon ink matrix was investigated initially using CVs. The influence of NH_2-CNTs on the redox peak-to-peak separation (ΔEp) is shown in Fig. 2. SPEs with NH_2-CNT exhibited a lower ΔEp (0.38 V) than those without NH_2-CNTs (0.58 V), suggesting greater electron transfer. A lower relative standard deviation (RSD) was observed in SPEs with NH_2-CNTs (2.1%) in comparison to without NH_2-CNTs (8.7%), indicating an increased reproducibility. Additionally, a higher reversibility of the redox peaks was obtained with NH_2-CNTs, suggesting improved homogeneity and regularity of the carbon ink film on the electrode surface [29,27].

FT-IR spectra were used to investigate the modification of the carbon ink with NH_2-CNTs (5 mg mL^{-1}). The FT-IR spectra of the carbon ink layer without NH_2-CNTs are shown in Fig. 3a. The peak at 3783 cm^{-1} corresponds to the band of hydroxyl groups. The peaks at 2925 cm^{-1} and 2856 cm^{-1} reveal asymmetric and symmetric stretches corresponding to methyl and methylene groups, respectively. These bands are attributed to the ethylene glycol ether present in the ink [30]. The peaks at 2385 cm^{-1} and 2301 cm^{-1} are attributed to C–H stretching vibrations of alkyne groups. After incorporation of the NH_2-CNTs in the carbon ink (Fig. 3b), two peaks were observed at 2925 cm^{-1} and 2856 cm^{-1} corresponding to methyl and methylene groups, respectively [31]. It was also observed the presence of peaks corresponding to amino groups at 1444 cm^{-1} and 1368 cm^{-1} that could be attributed to the presence of NH_2-CNTs in the carbon ink [21].

AFM was used to characterize the morphology of the CNT-SPEs. The topographic surface of the CNT-SPE was characterized by amorphous structures typical of polymeric films with an average roughness of 272.5 nm (Fig. 4a). After electrochemical pretreatment, the average roughness decreased to 124.4 nm (Fig. 4b) due to the removal of impurities and organic contaminants on the sensor surface. When anti-cTnT antibodies were pipetted onto the electrode surface (10 μL, 5 μg mL^{-1}) and incubated for 60 min, the average roughness increased to 273.1 nm, confirming that the anti-cTnT antibodies had been successfully immobilized (Fig. 4c).

3.2. Immobilization of the anti-cTnT

The amine groups of the CNTs were used to promote a covalent immobilization of the anti-cTnT antibodies via amide bonds. For this procedure, the Fc terminal of the anti-cTnT antibodies were activated by EDC/NHS mixing. EDC reacts with the carboxyl groups of the antibodies to form amine-reactive *o*-acylisourea intermediates. Addition of NHS stabilizes the amine-reactive intermediate and increases the efficiency of EDC-mediated coupling reactions. In situ activation of anti-cTnT antibodies yields NHS-ester-terminated Fc regions that are susceptible to nucleophilic attack from amines on the electrode surface to form stable amide bonds [32]. Oriented anti-cTnT immobilization by Fc terminal improves the sensitivity and selectivity of the immunosensor by exposing the Fabs, which exhibit a high affinity towards epitopes of the cTnT antigens.

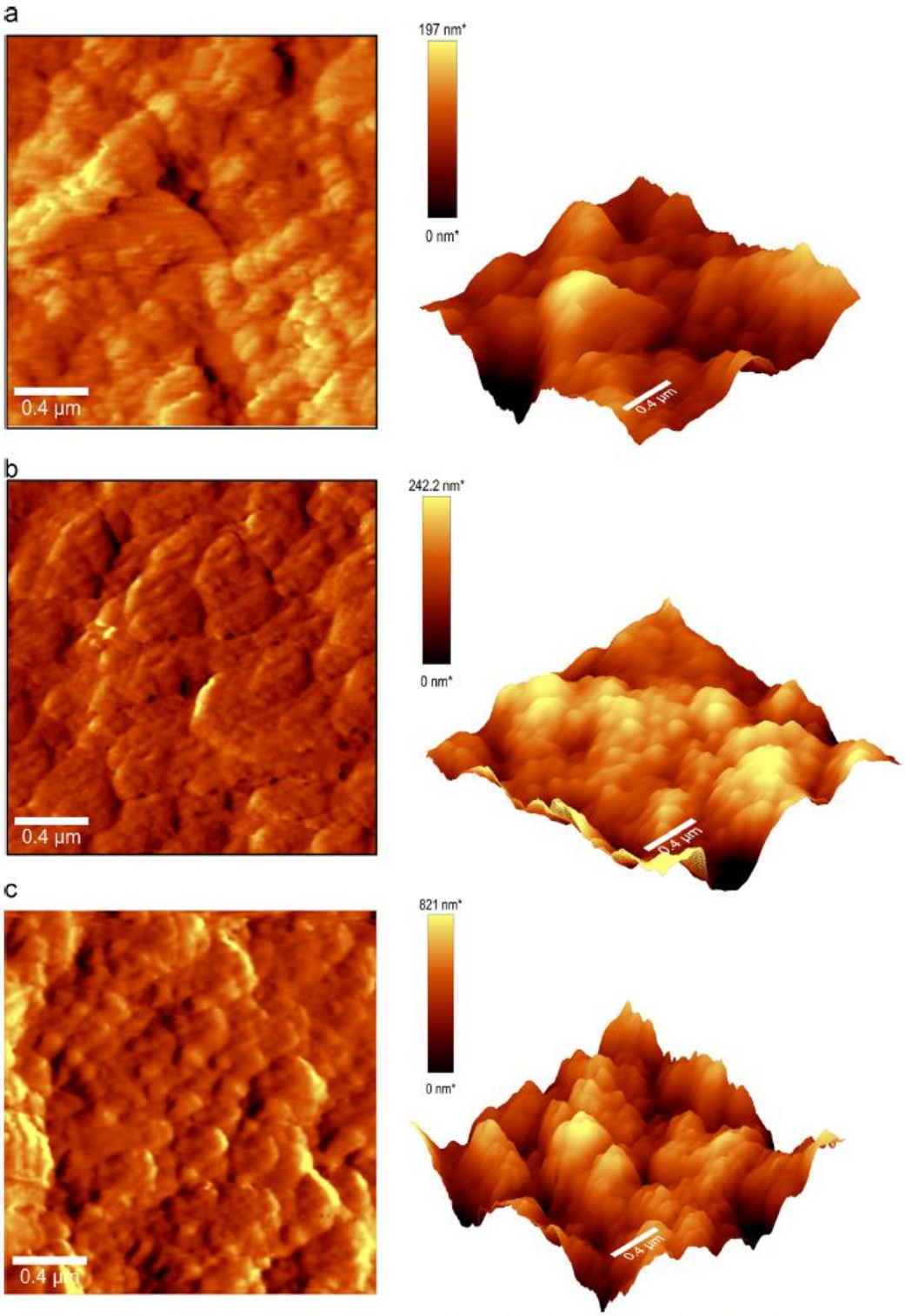

Fig. 4. 2D and 3D AFM images of the CNT-SPE (a) as manufactured, (b) after electrochemical pretreatment and (c) after anti-cTnT immobilization.

The amount of antibody immobilized on the electrode surface also affects the sensitivity of the immunosensor. In order to obtain a maximal efficiency on the attached anti-cTnT to electrode surface, the exposure time to the EDC/NHS by anti-cTnT was optimized. Herein, the exposure time ranged from 15 min to 120 min with anti-cTnT at 5 $\mu g\ mL^{-1}$. It was observed an increase of the exposure time with increase of the DPV peaks, reaching a plateau at 90 min (Fig. S1—Supplementary data). In this instant, a maximal amount of anti-cTnT Fc portions were activated resulting in more amide bonds with the NH_2-CNTs.

3.3. Assembling the SPE

In Fig. 5a, the CV of the CNT-SPE as manufactured shows a ΔE_p of 0.68 V (curve I). After electrochemical pretreatment (curve II), the ΔE_p decreased to 0.38 V, which illustrates a decrease of electron transfer resistance by removing of organic contaminants or impurities from the electrode surface. On the other hand, when the anti-cTnT was pipetted on the CNT-SPE it was, observed a decrease in the redox peaks as a result of electron-transfer inhibition due to the insulating nature of the antibody (curve III). The blocking effect to non-specific binding was observed after incubation with glycine (50 mmol L^{-1}) (curve IV). The negatively charged glycine acts by hindering the electron transfer between the anionic species of the electrolyte and the electrode surface, as demonstrated by a slight reduction in redox peaks.

CNT-SPE assembly also was evaluated by EIS. The electrodes were submitted to an electrochemical cell with $K_3[Fe(CN)_6]/K_4[Fe(CN)_6]$ (5 mmol L^{-1}) prepared in PBS (10 mmol L^{-1}, pH 7.4). According to the Nyquist plot showed in Fig. 5b, it was observed, after electrochemical pretreatment a reduction in the charge-transfer resistance (R_{ct}) from 5805 Ω (curve I) to 665 Ω (curve II), by decreasing the diameter of the semicircles. Immobilization of the anti-cTnTs were confirmed by an increase in the R_{ct} (768 Ω, curve III), due to their insulating nature. Glycine, the blocking agent, also was linked on the electrode surface as confirmed by an increase in the diameter of the semicircle (R_{ct}=966 Ω, curve IV). These results are in accordance with those obtained using CV.

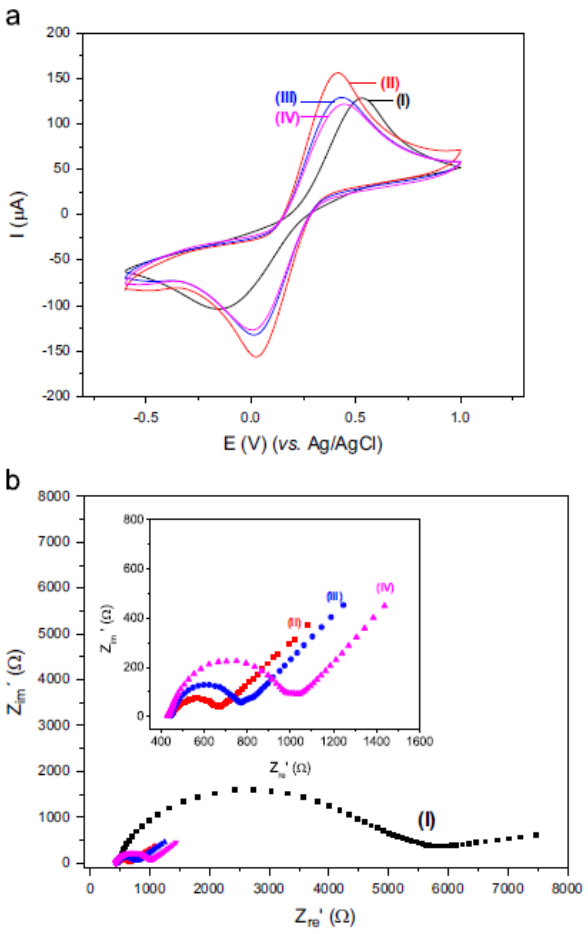

Fig. 5. Stepwise the CNT-SPE preparation: (curve I) as manufactured, (curve II) after electrochemical pretreatment, (curve III) anti-cTnT/CNT-SPE, (curve IV) glycine/anti-cTnT/CNT-SPE (a) CVs and (b) Nyquist plots in $K_3[Fe(CN)_6]/K_4[Fe(CN)_6]$ (5 mmol L^{-1}) prepared in PBS (10 mmol L^{-1}, pH 7.4).

In order to study electron diffusion at the sensor interface, glycine/anti-cTnT/CNT-SPEs were submitted to different scan rates. The electrodes were immersed in an electrochemical cell containing $K_3[Fe(CN)_6]/K_4[Fe(CN)_6]$ (5 mmol L^{-1}) in PBS (10 mmol L^{-1}, pH 7.4) as the redox probe, and voltammograms were registered (Fig. S2—Supplementary data). The currents of the anodic peak (I_{pa}) and the cathodic peak (I_{pc}) increased linearly with the square root of the scan rate (Fig. S2—Supplementary data, inset). The following linear regression equations then were calculated: $I_{pa}=14.857\nu^{1/2}+21.502$ ($r=0.999$) and $I_{pc}=-14.035\nu^{1/2}-33.578$ ($r=0.996$). These equations suggested a diffusion-controlled process. The electroactive surface area of the glycine/anti-cTnT/CNT-SPE was calculated according to the Randles–Sevcik equation [22] to be 0.047 cm^2.

3.4. Experimental conditions

Optimal experimental conditions for immunosensor detection were investigated according to the pH and ionic strength of the buffer (PBS). Electrostatic intermolecular forces of the electrolyte can affect electron transfer on the electrode surface [33]. The pH of PBS (10 mmol L^{-1}) was varied from 5.5 to 8.0; the current increased proportionately with the pH achieving a maximal current peak at pH 6.5 (Fig. S3a—Supplementary data). Therefore, pH 6.5 was adopted for all remaining measurements. The ionic strength was varied from 0.01 mmol L^{-1} to 10 mmol L^{-1}, and steady state was achieved at 5 mmol L^{-1} (Fig. S3b—Supplementary data).

Additional parameters affecting immunosensor performance include the immobilized antibody load and the incubation time of the cTnT. The anti-cTnT antibody concentration was varied from 0.01 μg mL^{-1} to 10 μg mL^{-1}. The current response to a fixed concentration of cTnT (0.05 ng mL^{-1}) in PBS was proportional to the anti-cTnT concentration with a plateau at approximately 5 μg mL^{-1} anti-cTnT (Fig. S4a—Supplementary data). At this anti-cTnT concentration, a 40 min incubation time was optimal as demonstrated by a plateau in the curve (Fig. S4b—Supplementary data), which suggested maximal antigen–antibody interaction.

3.5. Analytical response to the cTnT

Under optimized experimental conditions, the calibration curve of the immunosensor was obtained. The electrodes were incubated in various concentrations of cTnT for 40 min and then were submitted to DPV measurements in the presence of $K_3[Fe(CN)_6]/K_4[Fe(CN)_6]$ (5 mmol L^{-1}) in PBS (5 mmol L^{-1}, pH 6.5). The calibration curve indicated a gradual decrease in DPV current peaks with increased cTnT concentrations (Fig. 6a). When the data were adjusted to a linear regression equation, $\Delta I=3.25*C_{cTnT}+4.2$, a correlation coefficient of 0.995 ($p<0.0001$, $n=7$) and a low relative error ($\ll 1\%$) were obtained (Fig. 6a, inset). Based on the RSD of the blank and the slope of the calibration curve, the LOD was calculated as: LOD=3(RSD/slope) [34]. CNT-SPEs exhibited a lower LOD (0.0035 ng mL^{-1}) than previously described for cTnT electrochemical immunosensors [15–18]. One of limitations encountered for these labeled immunosensors is associated with the interaction or passivation of the electrode by requirement of an enzyme substrate or chemical mediator [35]. Moreover, limitations related to Michaelis–Menten kinetic imply an increase in the analyses time and a reduced sensitivity.

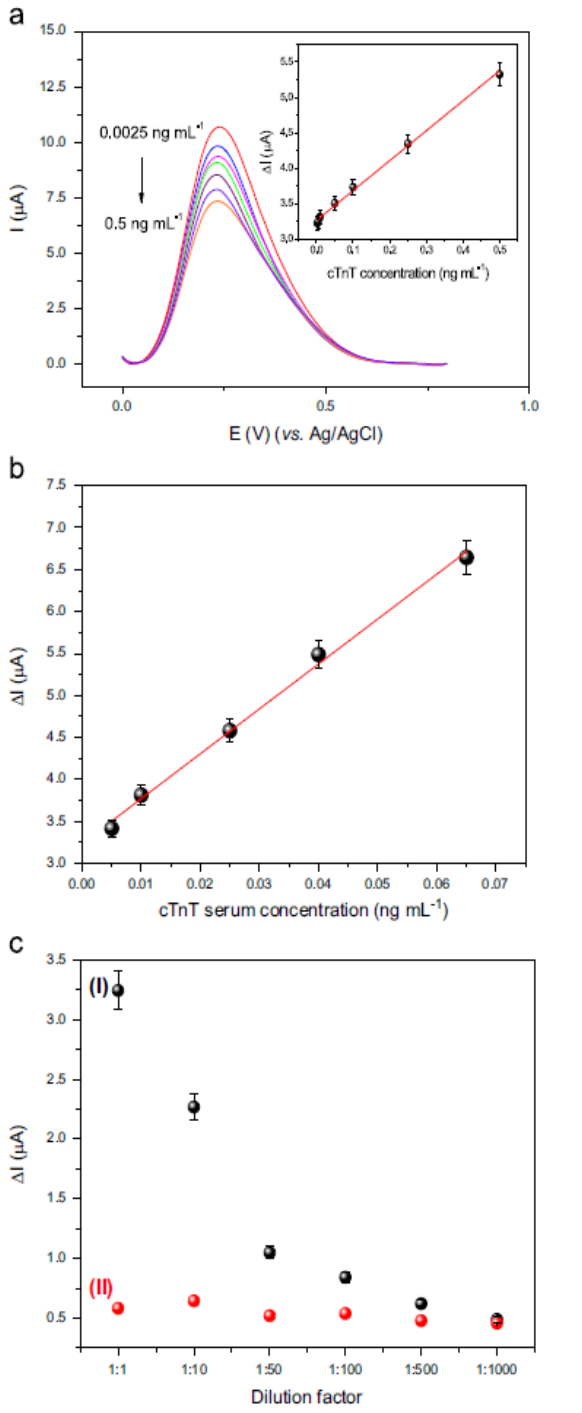

Fig. 6. (a) DPVs of immunosensor response to different the cTnT concentrations (0.0025 to 0.5 ng mL^{-1}) in presence of $K_3[Fe(CN)_6]/K_4[Fe(CN)_6]$ (5 mmol L^{-1}) in PBS (5 mmol L^{-1}, pH 6.5). *Inset*: linear fit of the calibration curve. (b) Analytical CNT-SPE responses to the cTnT measured in serum samples and (c) matrix effect study performed by successive serum dilution of samples from (curve I) myocardial infarcted and (curve II) non-myocardial infarcted patients. Error bars are based on the standard deviation of three replicates.

3.6. Repeatability and reproducibility

The repeatability of the CNT-SPE was evaluated by replicate measurements of a single electrode in response to 0.05 ng mL^{-1} cTnT under optimized experimental conditions. An RSD value of 3.2% was found for five successive determinations corresponding to a good repeatability of the immunosensor. The reproducibility was also evaluated using ten CNT-SPEs manufactured on different days and measured in response to 0.05 ng mL^{-1} cTnT. The obtained RSD was 3.8%, which implies a good reproducibility and repeatability in the fabrication procedures.

3.7. Determination of cTnT in serum samples

Fig. 6b shows the amperometric responses of the CNT-SPEs to cTnT serum samples. The immunosensor measurements were compared with those using ECLIA. The results showed good agreement with ECLIA at a 95% confidence level when the paired *t*-test was applied. The calibration plot exhibited a good linear correlation (r=0.990, p< 0.0001), and a linear range of detection was observed between 0.005 ng mL^{-1} and 0.065 ng mL^{-1} cTnT. This range is comparable to the clinical range, which is associated with a cutoff of 0.01 ng mL^{-1} cTnT [36]. The LOD of CNT-SPEs for cTnT in serum samples was found to be approximately 0.007 ng mL^{-1}.

The matrix effect on the analytical response of CNT-SPEs also was evaluated (Fig. 6c). Blood serum from a non-myocardial infarction subject was diluted 1:1, 1:10, 1:50, 1:100, 1:500, and 1:1000 and then was compared to a myocardial infarction subject's serum, containing 0.01 ng mL^{-1} cTnT. All dilutions were carried out using PBS (10 mmol L^{-1}, pH 7.4). The serum dilution curve obtained from the non-myocardial infarction subject (curve I) was maintained practically constant, showing a non-matrix effect. This proposed label-free immunosensor is simpler, more rapid, and more practical for cTnT detection in blood serum and can be carried out by one-step manufacturing in addition to low cost requirements.

4. Conclusions

A disposable CNT-SPE was developed for the measurement of cTnT in blood serum. The incorporation of NH_2-CNT into the carbon ink enabled a more stable measurement and an oriented anti-cTnT immobilization leading to a high sensitivity. Additionally, the platform dispensed chemical mediators, compounds or polymers to anchor the CNTs. The CNT-SPE described in this study achieved a high sensitivity and a low LOD (0.0035 ng mL^{-1}) of cTnT compared to others electrochemical immunosensors. The linear range was obtained within cTnT clinical levels for AMI diagnostics, although further validation studies with real samples are required before clinical use.

Acknowledgements

This work was supported by the National Council for Scientific and Technological Development (CNPq) agency from Brazil. Bárbara V.M. Silva thanks to Coordination for Enhancement of Higher Education Personnel (CAPES), Brazil foundation, for the scholarship during this work. The assistance of the Northeast Center for Strategic Technologies (Recife, Brazil) and Central Analytical of Federal University of Pernambuco (Recife, Brazil) are also acknowledged.

Appendix A. Supplementary material

Supplementary data associated with this article can be found in the online version at http://dx.doi.org/10.1016/j.talanta.2013.08.059.

References

[1] J.S. Alpert, K. Thygesen, E. Antman, J.P. Bassand, J. Am. Coll. Cardiol. 36 (2000) 959–969.
[2] K. Thygesen, J.S. Alpert, H.D. White, Eur. Heart J. 28 (2007) 2525–2538.
[3] S. Mendis, K. Thygesen, K. Kuulasmaa, S. Giampaoli, M. Mahonen, K Ngu Blackett, L. Lisheng, Int. J. Epidemiol. 40 (2011) 139–146.
[4] H.A. Katus, A. Remppis, S. Looser, K. Hallermeier, T. Scheffold, W. Kubler, Mol. Cell. Cardiol. 21 (1989) 1349–1353.
[5] G. Klein, M. Kampmann, H. Baum, T. Rauscher, T. Vukovic, K. Hallermayer, H. Rehner, M. Müller-Bardorff, H.A. Katus, Wien. Klin. Wochenschr. 110 (1998) 40–51.
[6] R.F. Dutra, R.K. Mendes, V. Lins da Silva, L.T. Kubota, J. Pharm. Biomed. Anal. 43 (2007) 1744–1750.
[7] R.F. Dutra, L.T. Kubota, Clin. Chim. Acta 376 (2007) 114–120.
[8] H. Andersson, B. Kågedal, C.-F. Mandenius, Anal. Bioanal. Chem. 398 (2010) 1395–1402.
[9] J.T. Liu, C.J. Chen, T. Ikoma, T. Yoshioka, J.S. Cross, S.J. Chang, J.Z. Tsai, J. Tanaka, Anal. Chim. Acta 703 (2011) 80–86.
[10] K. Wong-ek, O. Chailapakul, N. Nuntawong, K. Jaruwongrungsee, A. Tuantranont, Biomed. Tech. (Berlin) 55 (2010) 279–284.
[11] R.A. Fonseca, J. Ramos-Jesus, L.T. Kubota, R.F. Dutra, A Nanostructured, Sensors 11 (2011) 10785–10797.
[12] A.B. Mattos, T.A. Freitas, V. Lins da Silva, R.F. Dutra, Sens. Actuators, B 161 (2012) 439–446.
[13] J. Wang, Chem. Rev. 108 (2008) 814–825.
[14] V. Gubala, L.F. Harris, A.J. Ricco, M.X. Tan, D.E. Williams, Anal. Chem. 84 (2012) 487–515.
[15] B.M.V. Silva, I.T. Cavalcanti, A.B. Mattos, P. Moura, M. del, P. Sotomayor, R. F. Dutra, Biosens. Bioelectron. 26 (2010) 1062–1067.
[16] B. Esteban-Fernández de Ávila, V. Escamilla-Gomez, S. Campuzano, M. Pedrero, J.M. Pingarrón, Electroanalysis 24 (2012) 1–8.
[17] S.L.R. Gomes-Filho, A.C.M.S. Dias, M.M.S. Silva, B.V.M. Silva, R.F. Dutra, Microchem. J. 109 (2013) 10–15.
[18] A.B. Mattos, T.A. Freitas, L.T. Kubota, R.F. Dutra, Biochem. Eng. J. 71 (2013) 97–104.
[19] B.E. Rapp, F.J. Gruhl, K. Länge, Anal. Bioanal. Chem. 398 (2010) 2403–2412.
[20] J. Lin, Z. Wei, H. Zhang, M. Shao, Biosens. Bioelectron. 41 (2013) 342–347.
[21] K.-J. Huang, D.-J. Niu, J.-Y. Sun, J.-J. Zhu, J. Electroanal. Chem. 656 (2011) 72–77.
[22] A.J. Bard, L.R. Faulkner, Electrochemical Methods: Fundamentals and Applications, John Wiley & Sons, New York, 2000.
[23] P. Yáñez-Sedeño, J.M. Pingarrón, Trends Analyst Chem. 29 (2010) 938–953.
[24] P.J. Lamas-Ardisana, P. Queipo, P. Fanjul-Bolado, A. Costa-Garcia, Anal. Chim. Acta 615 (2008) 30–38.
[25] M. Pumera, A. Merkoci, S. Algeret, Sens. Actuators, B 113 (2006) 617–622.
[26] C. Lynam, N. Gilmartin, A.I. Minett, R. O'Kennedy, G. Wallace, Carbon 47 (2009) 2337–2343.
[27] S. Puertas, M.G. Villa, E. Mendoza, C. Jiménez-Jorquera, J.M. Fuente, C. Fernández-Sánchez, V. Grazu, Biosens. Bioelectron. 43 (2013) 274–280.
[28] M.A. Alonso-Lomillo, O. Domínguez-Renedo, L.D.T.D. Román, M.J. Arcos-Martínez, Anal. Chim. Acta 688 (2011) 49–53.
[29] F. Valentini, A. Amine, S. Orlanducci, M.L. Terranova, G. Palleschi, Anal. Chem. 75 (2003) 5413–5421.
[30] T.T. Nguyen, M. Raupach, L.J. Janik, Clays Clay Miner. 35 (1987) 60–67.
[31] P. Griffiths, J.A.D. Haseth, Fourier Transform Infrared Spectrometry, John Wiley & Sons, New York, 2007.
[32] Z. Pei, H. Anderson, A. Myrskog, G. Dunér, B. Ingemarsson, T. Aastrup, Anal. Biochem. 398 (2010) 161–168.
[33] V. Dugas, A. Elaissari, Y. Chevalier, Surface Sensitization techniques and recognition receptors immobilization on biosensors and microarrays, in: M. Zourob (Ed.), Recognition Receptors in Biosensors, Springer, New York, 2010, pp. 47–134.
[34] G.L. Long, J.D. Winefordner, Anal. Chem. 55 (1983) 713A–724A.
[35] F. Ricci, G. Adornetto, G. Palleschi, Electrochim. Acta 84 (2012) 74–83.
[36] M.P. Hudson, C.M. O'Connor, W.A. Gattis, G. Tasissa, V. Hasselblad, C. M. Holleman, L.H. Gaulden, F. Sedor, E. Magnus Ohman, Am. Heart J. 147 (2004) 546–552.

Microchemical Journal 109 (2013) 10–15

Contents lists available at SciVerse ScienceDirect

Microchemical Journal

journal homepage: www.elsevier.com/locate/microc

A carbon nanotube-based electrochemical immunosensor for cardiac troponin T

S.L.R. Gomes-Filho, A.C.M.S. Dias, M.M.S. Silva, B.V.M. Silva, R.F. Dutra *

Biomedical Engineering Laboratory, Federal University of Pernambuco, Av. Prof. Moraes Rego, 1235, Cidade Universitária, 50670-901, Recife, Brazil

ARTICLE INFO

Article history:
Received 1 December 2011
Received in revised form 26 May 2012
Accepted 28 May 2012
Available online 31 May 2012

Keywords:
Cardiac troponin T
Immunosensor
Carbon nanotubes
Polyethyleneimine

ABSTRACT

A nanostructured immunosensor based on carbon nanotubes supported by a conductive polymer film was developed for detection of cardiac Troponin T (cTnT), an important cardiac marker for acute myocardial infarction. Carboxylated carbon nanotubes were covalently bound to the electrode surface via polyethyleneimine. The functionalized nanostructured surface was used to bind anti-cTnT monoclonal antibodies. Stepwise modification of the electrode was characterized by cyclic voltammetry studies. The immunosensor achieved a low limit of detection (0.033 ng mL^{-1}) and a linear range between 0.1 and 10 ng mL^{-1} cTnT), significant for acute myocardial infarction diagnosis. Good reproducibility and repeatability were obtained by the proposed immunosensor supported by a coefficient of variation of 3.7% and 2.6%, respectively.

1. Introduction

Acute myocardial infarction (AMI) is considered one of the major causes of mortality in the world population. According to the World Health Organization, diagnosis of AMI is based on the following criteria: clinical history of ischemic chest discomfort, changes in the electrocardiogram and alterations in the quantity of markers of myocardial necrosis [1,2]. Cardiac Troponin T (cTnT) has been used as a clinical marker for myocardial damage associated with acute infarction [3]. It is more reliable because it is released in the blood more rapidly than creatine kinase (CK)-MB, its concentration in blood increases quickly within 3 to 4 h after onset of the AMI [4,5]. Thus, the development of a rapid and practical immunosensor for cTnT measurements is desirable due to its roles in cardiospecific diagnosis, risk stratification, prognostic risk assessment and therapeutic choices.

Immunoassays for cTnT detection such as Electrochemiluminescence Immunoassay (ECLIA) and Enzyme-linked Immunosorbent Assay (ELISA) have been widely used for AMI diagnosis [6]. However, they are not practical, involve skilled personnel and are not easily miniaturized, hindering a rapid diagnostic in the cardiac emergence [7,8]. Alternatively, an ideal immunosensor device is capable of overcoming all these difficulties. Although some progresses have been reached in detection of the cTnT by immunosensors, either in the transducers type or in relation to process of the antibodies immobilization, some limitations are highlighted. Mattos et al. [9] developed a dual quartz crystal microbalance system with a lower detection limit; Vasconcelos et al. [10] constructed a simplified capacitive transducer; Dittmer et al. [11], an optomagnetic biosensor and some authors have developed transduction based on Kretschmann configuration using the surface plasmon resonance technique [12–14]. Despite that all these methods support quantitative and non-time consuming analysis, they are not practical, economical and are not compatible with the most used transduction technology of the well-established enzymatic glucometers [15,16]. Thus, immunosensor based on amperometric transduction compared with all those previously described has been considered attractive for analytical approaches especially due to its versatility, adaptability to previous portable systems and its possibility of becoming a point-of-care testing [17,18]. These transducers can be configured as a screen printed electrode, profitable if in mass produced and ideal to dispose after use, allowing safe and reliable analysis, and ideal for practical trials and care-management of the AMI.

Chemical mediators in the amperometric biosensors have been widely described [19,20]. These resonant compounds shuttle the electrons between the active site of the enzymes and the electrode surface, in order to amplify the analytical response. However, the use of mediators can cause damage or passivation on the electrode surface, reducing its life-time. On the other hand, when mediators are incorporated to carbon paste or conductive ink, they can be release into the bulk solution leading to irregular response. Recently, new strategies for enhancement amperometric transduction based on nanomaterials have been employed [21]. Carbon nanotubes (CNT) have become the focus of intensive research by analytical chemists for use as electrodes that transmit electrical signals or as sensors to detect concentrations of chemicals or biological materials. The structure of CNT can be described as a rolled-up tubular shell of graphite sheet with the carbon atoms covalently bound to their neighbours. Physical and chemical properties such as electrical conductance, high mechanical stiffness and the possibilities to functionalize CNTs in order to change their intrinsic properties are reasons why they are used in biosensors [22]. Furthermore, they promote a rapid electron transfer, increasing the reaction rate of many electroactive species and then decreasing the electrode response

* Corresponding author. Tel.: +55 81 21268200; fax: +55 81 21268000.
E-mail addresses: rosa.dutra@ufpe.br, rosa.dutra@pq.cnpq.br (R.F. Dutra).

0026-265X/$ – see front matter © 2012 Published by Elsevier B.V.
doi:10.1016/j.microc.2012.05.033

time [23,24]. These fascinating properties are the reasons why the CNT electrodes can achieve high sensitivity with low detection limits. In addition, CNTs increase the electroactive area by forming a nanostructured surface that promotes a greater amount of immobilized biomolecules.

Polymers have exerted an important role for CNTs bond on the electrode surface due to they act as true anchors resulting in more regular biosensors response. A new class of polymers known as intrinsically conducting polymers or electroactive conjugated polymers has recently emerged in the electrochemical sensors. They are commonly deposited on the electrode surface area operating as an electron promoter between the polymer film and electrolyte solution [25]. Herein, the polyethyleneimine (PEI) in the branched form, which has a higher density of amine groups [26,27], was used to bind carboxylated CNTs (COOH–CNT). A nanostructured surface was obtained in order to increase the immunoreactive electrode area and to achieve a more sensitive and reliable response.

2. Experimental

2.1. Materials

cTnT was obtained from Calbiochem (San Diego, USA). Anti-cTnT-HRP and anti-cTnT antibodies were purchased from Abcam (Cambridge, USA). COOH functionalized multi-walled carbon nanotubes (COOH–CNT) were obtained from DropSens (Oviedo, Spain). 50% (w/v) polyethyleneimine solution in water, 1-ethyl-3-(3-dimethylaminopropyl) carbodiimide hydrochloride (EDC), *N*-hydroxysuccinimide (NHS) and horseradish peroxidase (HRP) enzyme were acquired from Sigma-Aldrich (St. Louis, USA). 30% (v/v) H_2O_2 was provided by Labsynth (São Paulo, Brazil). Phosphate buffer saline (PBS) (0.01 mol L^{-1}, pH 7.4) used in all experiments was prepared by dissolving 0.2 g KCl, 8.0 g NaCl, 0.24 g KH_2PO_4 and 1.44 g Na_2HPO_4 in 1000 mL of Milli-Q water. All other chemicals were of analytical reagents grade and used without further purification. The water used to prepare of the solutions was obtained from a Milli-Q water purification system from Millipore Inc. (Billerica, USA).

2.2. Apparatus and measurements

The electrochemical experiments were carried out using the Autolab PGSTAT12 potentiostat/galvanostat (Eco Chemie, The Netherlands) coupled with the microcomputer and controlled by GPES 4.9 software. A three-electrode system comprising of a gold electrode as the working electrode, a platinum wire as the auxiliary electrode, and an Ag/AgCl electrode as the reference, was employed for all electrochemical experiments.

Cyclic voltammetry experiments were carried out on an electrochemical cell (10 mL) at room temperature (24 °C). The voltammetry measurements ranged from −0.1 to 0.6 V in 4 mmol L^{-1} $K_3Fe(CN)_6$ solution.

2.3. Dispersion and activation of COOH–CNT

3 mg of COOH–CNT was dispersed in 1 mL of DMF and sonicated for 2 h to form a COOH–CNT homogeneous solution. Then, the dispersed COOH–CNT was activated with a 1:1 mixture of 8 mmol L^{-1} EDC and 20 mmol L^{-1} NHS, which was left to react for 1 h at room temperature [24].

2.4. Self-assembling of the immunosensor

Prior to use, the gold electrode with geometric area of approximately 0.2 mm^2 was cleaned with a freshly prepared nitric acid solution (4 mmol L^{-1}) for 10 min, then exhaustively rinsed in an ultrasonic bath in water and ethanol. The cleaning procedure of the electrode was confirmed by cyclic voltammograms. Afterwards, the electrodes were coated with 5 μL of 5% (v/v) PEI in ethanol and dried at 45 °C for 10 min, in order to form a uniform polymer film. Then, 5 μL of previously activated COOH–CNT was deposited on the electrode surface and dried at 50 °C for 20 min. Elapsed time of the solvent drying, the electrode was then washed to remove the excess of unbound COOH–CNT. Then, an aliquot of 5 μL anti-cTnT (1 μg mL^{-1}) was pipetted on the nanostructured surface COOH–CNT/PEI/Au and incubated for 60 min at 4 °C. In order to block remaining active sites and avoid non-specific binding, the electrode surface was incubated with 0.05 mol L^{-1} glycine solution for 60 min. An illustrative scheme of the stepwise construction process of the immunosensor is shown in Fig. 1.

2.5. Measurements principle of immunosensor

Initially, the anti-cTnT coated electrode was incubated with 5 μL of cTnT solution prepared in PBS (0.01 mol L^{-1}, pH 7.4), for 30 min. Subsequently, an aliquot of anti-cTnT-HRP (1 μg mL^{-1}) was pipetted on the sensor surface and incubated for 30 min. After each step of immunoassay, the electrode surface was washed with PBS.

All the amperometric signals were generated by H_2O_2 reaction with enzyme conjugated to anti-cTnT. Then, an H_2O_2 solution (5 mmol L^{-1}) prepared in PBS (0.01 mol L^{-1},pH 7.0) was filled in an electrochemical cell (10 mL) to generate the amperometric signal.

3. Results and discussion

3.1. Electrochemical characterization of the modified electrodes

The use of polymers as anchors for CNT has been justified [28]. In this work, gold surface was coated with PEI, a highly cationic polymer. Its film contains a large number of amine groups that bind to the COOH–CNT by an amide linkage [29], allowing a covalent binding between the antibodies and COOH–CNT. Concerning the COOH–CNT interaction to PEI, when the electrode was prepared without PEI film, there was not a stable COOH–CNT binding to the electrode surface. In order to quantitatively determine the stability of the COOH–CNT binding to the electrode surface, cyclic voltammograms were performed with three electrodes immersed in the electrochemical cell in the presence of a 4 mmol L^{-1} $K_3Fe(CN)_6$ solution. The coefficient of variation of the redox peaks were 95.9% and 0.4% in five cycles, for the electrode prepared without and with PEI film, respectively. The COOH–CNT was probably released from the electrode surface.

All assembly process of Anti-cTnT/COOH–CNT/PEI on the gold electrode was monitored by cyclic voltammetry in 4 mmol L^{-1} $K_3Fe(CN)_6$ solution (Fig. 2). Based on the voltammograms (curves a and b), it was possible to calculate the (Γ) of the PEI film on the bare electrode surface through Eq. (1):

$$\Gamma^i bf = 1 - Qclean/QPEI \quad (1)$$

where, Q_{PEI} load (obtained by integrating the area of redox peaks of the PEI/Au electrode) and Q_{clean} load (obtained by integrating the area of redox peaks of the bare electrode). The degree of coverage achieved was 19%, indicative of a good volume ration.

Cyclic voltammogram of the COOH–CNT/PEI modified electrode presented an increase in the pair of reversible redox peaks in $E_{pa} = 0.29$ V and $E_{pc} = 0.16$ V (see also in Fig. 2). This behavior confirms the attachment of the CNTs on the electrode surface that lead to an enhancement in the conductivity and a higher electron transfer to the electroactive area (curve c) [30]. When the anti-cTnT was immobilized, the voltammetry showed a slight decrease in the amplitude of the redox peaks (curve d). This behavior can be attributed to reduction in the electron-transfer kinetics on the electrode surface, resulting from the addition of the biological insulating material that prevents the load diffusion to the electrode surface [31].

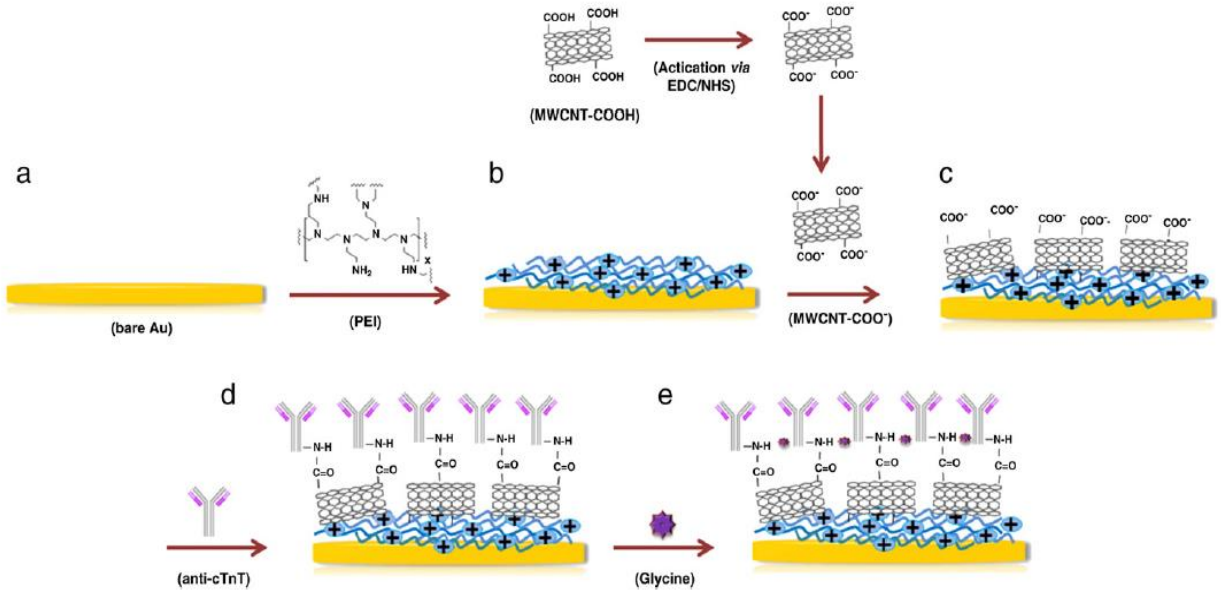

Fig. 1. Schematic diagram of the immunosensor in the successive steps. (a) Bare Au , (b) formation of the PEI film, (c) assembly of the COOH–CNT, (d) immobilization of anti-cTnT, (e) blocking with glycine.

3.1.1. Effect of the PEI concentration

In order to determine the dependence of concentration of PEI on the electrochemical response of the immunosensor, solutions containing different concentrations of PEI were prepared. The concentration of PEI was changed from 0.5% to 10% (w/v) and voltammograms were performed with different electrodes. To compensate the variations among them, the difference between the cathodic peak currents (Δi), obtained in $K_3Fe(CN)_6$ solution was calculated. According to Fig. 3, the cathodic peak current enhanced with the increasing of the PEI concentration reaching a plateau at 5.0% (v/v). Thus, the concentration of PEI 5.0% (v/v) was chosen for all remaining experiments.

3.1.2. Effect of the CNT concentration

The size of the electroactive area depends on the amount of COOH–CNT attached to PEI film. The cathodic peaks current reached a plateau at 1.5 mg mL^{-1} COOH–CNT (Fig. 4). After this point, the excess of the COOH–CNT can cause aggregation phenomena, and unleashing the CNTs from electrode surface. On the other hand, it is not as easy to obtain a homogenous dispersion when higher CNT concentrations are employed, consequently resulting in a non-regular COOH–CNT solution that can block the electron transfer to the electrode surface.

The repeatability of the nanostructured electrode was also evaluated by performing successive cyclic voltammograms (30 cycles) in 4 mmol L^{-1} $K_3Fe(CN)_6$ solution. A low coefficient of variation was obtained (CV = 0.31%) indicating a stable nanostructured platform for the electrochemical immunosensor.

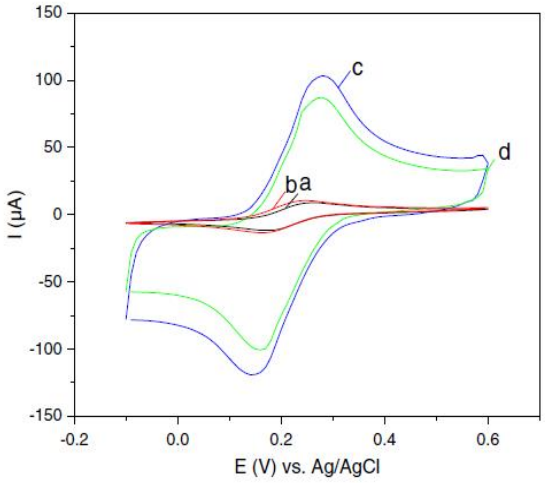

Fig. 2. Cyclic voltammograms of the immunosensor in each step of immobilization: (a) bare Au, (b) PEI/Au, (c) CNT/PEI/Au, (d) anti-cTnT/CNT/PEI/Au, in the presence of 4 mmol L^{-1} $K_3Fe(CN)_6$ under scan rate of 100 mV s^{-1}.

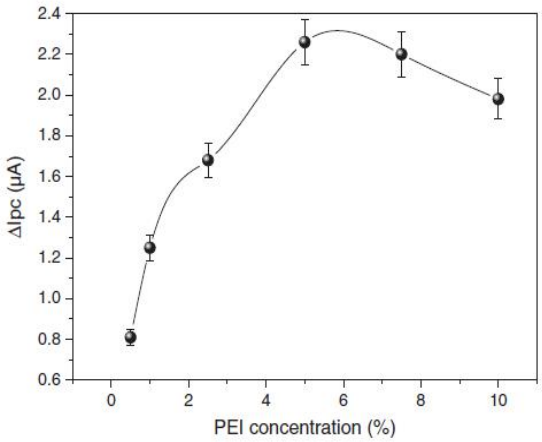

Fig. 3. Effect of the PEI concentration on the immunosensor response. Measurements were conducted by CV in a solution of H_2O_2 5 mmol L^{-1} diluted in PBS 10 mmol L^{-1}, pH 7.0.

3.1.3. Scan rate study

Information involving the electrochemical mechanisms can often be obtained by relationship between the cathodic/anodic current peak and scan rate [32]. Cyclic voltammograms under different scan rates (5 to 250 mV s^{-1}) were performed with the Anti-cTnT-HRP/cTnT/Glycine/Anti-cTnT/COOH–CNT/PEI/Au electrode in 10 mL 4 mmol L−1 $K_3Fe(CN)_6$ solution. It was found that the peaks of anodic and cathodic currents were modified with the scan rate (Fig. 5a). According to Fig. 5b, the currents of both anodic and cathodic peaks increased linearly with the square root of the scan rate indicating that the process was controlled by diffusion. There was proportionality between the cathodic peak currents and the square root of the scan rate, showing that the charge transfer occurred reversibly. The electron transfer rate constant (*ks*) was calculated employing the Laviron equation [33]:

$$ks = \alpha n F v / RT \quad (2)$$

where, α is the electron transfer coefficient, n is the number of electrons transferred, F is the Faraday constant, v is the scan rate, R is the gas constant and T is the temperature. The *ks* were estimated to be 1.2×10^4 s^{-1}.

3.2. Analytical response of the immunosensor

3.2.1. Effect of pH

The enzyme activity used as electroactive species in immunosensor is strongly influenced by the medium pH. Fig. 6 shows the difference in the cathodic current peak in a constant potential of −0.2 V at different pH values. In this study it can be observed that the current peak increased gradually until it attained the maximum at pH 7.0, then it decreased. Thus, pH 7.0 was chosen as the optimum pH value.

3.2.2. Effect of PBS concentration

In order to obtain the best PBS concentration for immunosensor response, electrochemical measurements of the Anti-cTnT-HRP/cTnT/Glycine/Anti-cTnT/COOH–CNT/PEI/Au electrode were performed in 5 mmol L^{-1} H_2O_2 diluted in PBS (0.01, 0.1, 1, 2.5, 5, 7.5, 10, 12.5, 15, 17.5 and 20 mmol L^{-1}). The curve of cathodic currents in a constant potential of −0.2 V showed that the optimum concentration was achieved at 10 mmol L^{-1} (Fig. 7). Thus, the PBS concentration of 10 mmol L^{-1} was selected for all remaining experiments.

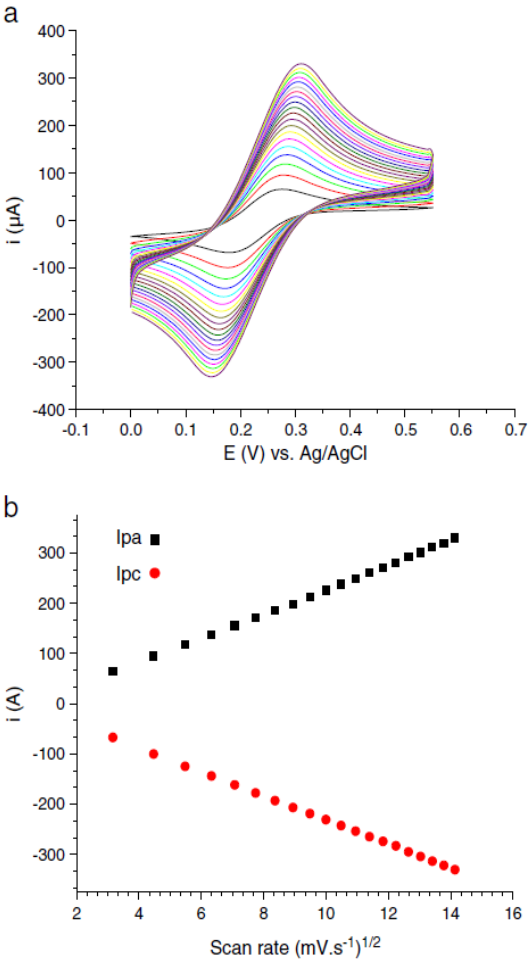

Fig. 5. (a) Cyclic voltammograms of the immunosensor in the 4 mmol L^{-1} $K_3Fe(CN)_6$, at scan rate (from inner to outer): 10, 20, 30, 40, 50, 60, 70, 80, 90, 100, 110, 120, 130, 140, 150, 160, 170, 180, 190, 200 mV s^{-1} (b) Plots of currents peak as a function of square root of scan rate.

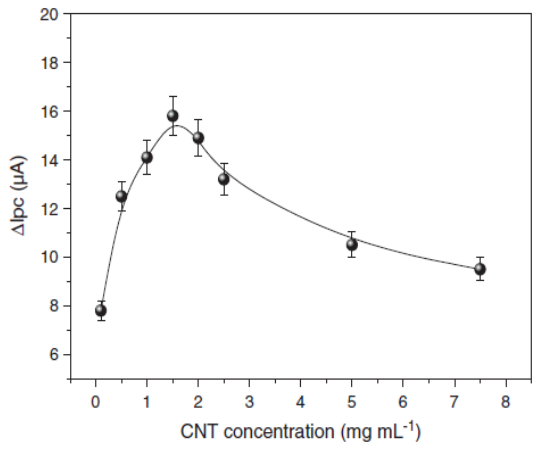

Fig. 4. Influence of the CNT concentration on the cathodic peak current. CVs were conducted in a solution of 4 mmol L^{-1} $K_3Fe(CN)_6$.

3.3. Reproducibility and repeatability of the immunosensor

The reproducibility of the proposed immunosensor was studied under established conditions performed on the Anti-cTnT-HRP/cTnT/Glycine/Anti-cTnT/COOH–CNT/PEI/Au electrode with cTnT concentration at 1 ng mL^{-1}. All scans were conducted in a solution of H_2O_2 5 mmol L^{-1} diluted in PBS 10 mmol L^{-1}, pH 7.0, at a scan rate of 100 mV s^{-1}. After measurements of the cathodic current peaks were taken, it was observed that the immunosensor showed good reproducibility, with a coefficient of variation of 3.7%; a value similar to the ones described by conventional laboratory tests for troponin T, such as enzyme immunoassays (ELISA and ECLIA) [34,35]. Meanwhile, the repeatability of the immunosensor was evaluated by 10 replicates of cTnT (1 ng mL^{-1}) from one same electrode. A satisfactory coefficient of variation equal to 2.6% was obtained (Fig. 8).

3.4. Calibration curve

As shown in Fig. 9, the calibration plot exhibited a good linear correlation ($r = 0.996$, $p << 0.001$, $n = 7$) with cTnT concentration varying

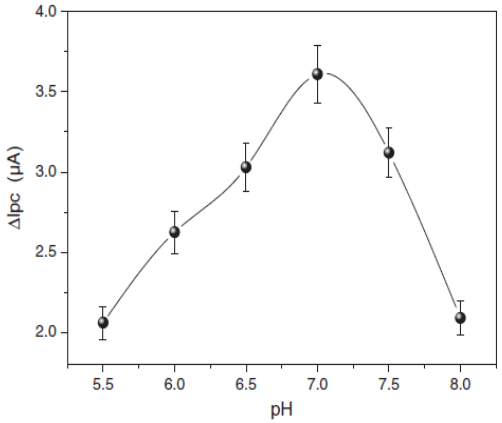

Fig. 6. pH effect on the immunosensor response. The amperometry measurement was carried out in H_2O_2 5 mmol L^{-1}.

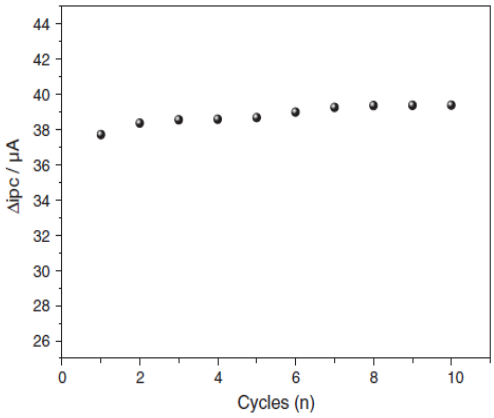

Fig. 8. Repeatability of the immunosensor in ten replicate measurements.

from 0.1 to 10 ng mL^{-1}. In this proposed immunosensor, the detection limit was established at 0.033 ng mL^{-1} cTnT being comparable to the ECLIA method which presents a limit of detection of 0.01 ng/mL according to the manufacturer (Elecsys® Troponin T STAT Immunoassay in the Cobas E601 analyzer, Roche Diagnostics Mannheim, Germany) [10,15]. This immunosensor showed itself capable of evaluating cTnT in the range of the cardiac infarction myocardial based on the WHO criteria from the 1970s which the cutoff value for cTnT is 0.1 ng/mL. Regarding the simplicity of this sensor, the PEI/CNT joint resulted in a highly sensitive immunosensor in which the use of chemical mediators was not necessary in obtaining amperometric response.

3.5. Immunosensor response to the human serum samples

To accomplish the cTnT calibration plot in real samples, 10 μL human serum was pipetted on the electrode surface and the electrochemical measurements were done. In order to prevent fluctuations on the electrochemical responses resulting from evaporation of samples, a moist chamber was used in all incubation procedures. The amount of cTnT in the serum samples was previously measured by a Roche Elecsys 2010 Immunoassay Analyzer, which is based on ECLIA method. The cTnT measurements of this immunosensor were performed with 1:100 diluted serum samples. The measurements showed a good agreement with the ECLIA methods at 95% confident level when the paired *t*-test was applied. As shown in Fig. 10, the calibration plot exhibited a good linear correlation between 0.02 and 0.32 ng mL^{-1} cTnT ($r=0.987$, $n=5$, $p<0.0001$). This method has the advantage of being more practical, more easily portable and does not require chemical mediators to obtain the response.

4. Conclusion

In the development of the proposed nanostructured immunosensor, the combined use of PEI film and CNT provided important advantages for obtaining a highly sensitive analytical method for cTnT with relevant clinical range for acute myocardial infarction detection. Additionally, in this electrochemical approach, the use of CNTs could exempt the use of chemical mediators since that satisfactory electron transfer was obtained. The results indicated that the concentration of cTnT detectable by use of the proposed immunosensor meets the requirements for AMI diagnosis.

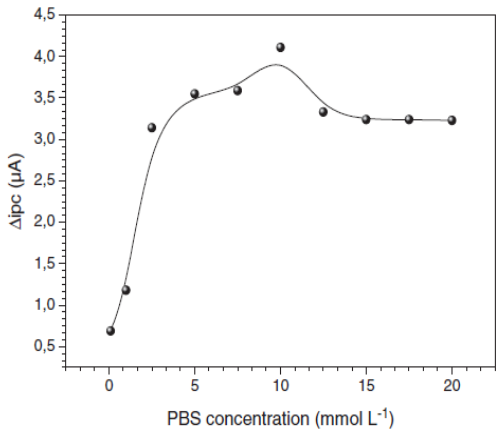

Fig. 7. Effect of PBS concentration on the immunosensor response. The amperometry measurement was carried out in the H_2O_2 5 mmol L^{-1} (pH 7.0).

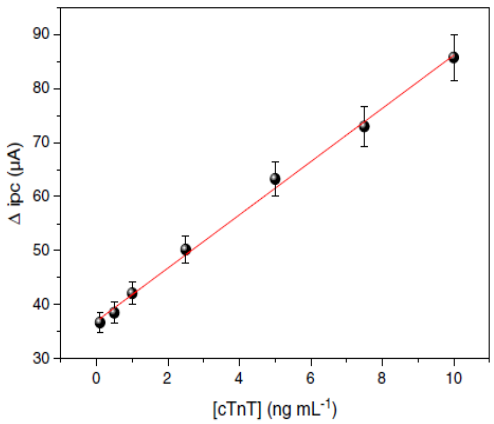

Fig. 9. Calibration curve of the immunosensor. The amperometry measurement was carried out in the H_2O_2 5 mmol L^{-1} diluted in PBS 10 mmol L^{-1}, pH 7.0.

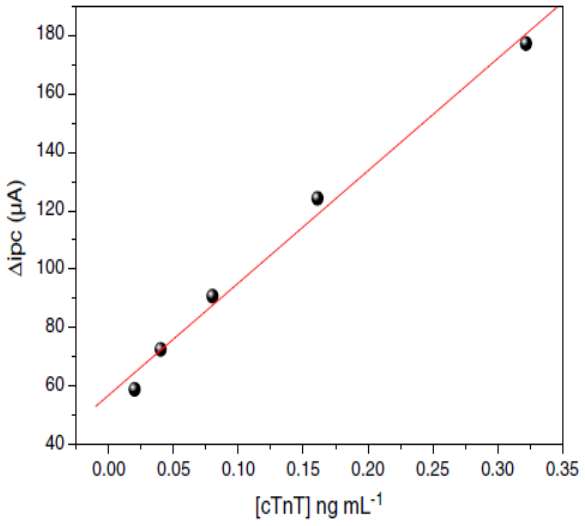

Fig. 10. Linear response of immunosensor to the serum samples in different concentrations of cTnT measured by ECLIA methods.

References

[1] OPAS—Organização pan-americana da saúde, Doenças Crônicas degenerativas e obesidade: Estratégia Mundial sobre alimentação saudável, atividade física e saúde, Second ed. World Health Organization, Brasília, 2003.

[2] H.D. White, D.P. Chew, Acute myocardial infarction, Lancet 372 (2008) 570–584.

[3] F.Z. Asumda, P.B. Chase, Nuclear cardiac troponin and tropomyos in are expressed early in cardiac differentiation of rat mesenchymal stem cells, Differentiation 83 (2012) 106–115.

[4] W. Shen, D. Tian, H. Cui, D. Yang, Z. Bian, Nanoparticle-based electrochemiluminescence immunosensor with enhanced sensitivity for cardiac troponin I using N-(aminobutyl)-N- (ethylisoluminol)-functionalized gold nanoparticles as labels, Biosens. Bioelectron. 27 (2011) 18–24.

[5] Z. Yang, D.M. Zhou, Cardiac markers and their point-of-care testing for diagnosis of acute myocardial infarction, Clin. Biochem. 39 (2006) 771–780.

[6] S.S. Kallempudi, Y. Gurbuz, A nanostructured-nickel based interdigitated capacitive transducer for biosensor applications, Sens. Actuators B 160 (2011) 891–898.

[7] M.I. Prodromidis, Impedimetric immunosensors—a review, Electrochim. Acta 55 (2010) 4227–4233.

[8] X. Liu, J. Wei, D. Song, Z. Zhang, H. Zhang, G. Luo, Determination of affinities and antigenic epitopes of bovine cardiac troponin I (cTnI) with monoclonal antibodies by surface plasmon resonance biossensor, Anal. Biochem. 314 (2003) 301–309.

[9] A.B. Mattos, T.A. Freitas, V.L. Silva, R.F. Dutra, A dual quartz crystal microbalance for human cardiac troponin T in real time detection, Sens. Actuators B 161 (2012) 439–446.

[10] E.A. Vasconcelos, N.G. Peres, C.O. Pereira, V.L. Silva, E.F. Silva Jr., R.F. Dutra, Potential of a simplified measurement scheme and device structure for a low cost label-free point-of-care capacitive biosensor, Biosens. Bioelectron. 25 (2009) 870–876.

[11] W.U. Dittmer, T.H. Evers, W.M. Hardeman, W. Huijnen, R. Kamps, P. Kievit, J.H.M. Neijzen, J.H. Nieuwenhuis, M.J.J. Sijbers, D.W.C. Dekkers, M.H. Hefti, M.F.W.C. Martens, Rapid, high sensitivity, point-of-care test for cardiac troponin based on optomagnetic biossensor, Clin. Chim. Acta 411 (2010) 868–873.

[12] R.F. Dutra, R.K. Mendes, V.L. Silva, L.T. Kubota, Surface plasmon resonance immunosensor for human cardiac troponin T based on self-assembled monolayer, J. Pharm. Biomed. Anal. 43 (2007) 1744–1750.

[13] R.F. Dutra, L.T. Kubota, An SPR immunosensor for human cardiac troponin T using specific binding avidin to biotin at carboxymethyldextran-modified gold chip, Clin. Chim. Acta 376 (2007) 114–120.

[14] J.T. Liu, C.J. Chenb, T. Ikomac, T. Yoshiokac, J.S. Crossd, S.J. Changa, J.Z. Tsaib, J. Tanaka, Surface plasmon resonance biosensor with high anti-fouling ability for the detection of cardiac marker troponin T, Anal. Chim. Acta 703 (2011) 80–86.

[15] S. Park, H. Boo, T.D. Chung, Electrochemical non-enzymatic glucose sensors, Anal. Chim. Acta 556 (2006) 46–57.

[16] C. Loncaric, Y. Tang, C. Ho, M.A. Parameswaran, H.-Z. Yu, A USB-based electrochemical biosensor prototype for point-of-care diagnosis, Sens. Actuators B 161 (2012) 908–913.

[17] B.V.M. Silva, I.T. Cavalcanti, A.B. Mattos, P. Moura, M.D.P.T. Sotomayor, R.F. Dutra, Disposable immunosensor for human cardiac troponin T based on streptavidin-microsphere modified screen-printed electrode, Biosens. Bioelectron. 26 (2010) 1062–1067.

[18] B.Y. Zhao, Q. Wei, C. Xu, H. Li, D. Wu, Y. Cai, K. Mao, Z. Cui, B. Du, Label-free electrochemical immunosensor for sensitive detection of kanamycin, Sens. Actuators B 155 (2011) 618–625.

[19] M. Senel, E. Cevik, M.F. Abasıyanık, Amperometric hydrogen peroxide biosensor based on covalent immobilization of horseradish peroxidase on ferrocene containing polymeric mediator, Sens. Actuators B 145 (2010) 444–450.

[20] J. Liu, S. Sun, C. Liu, S. Wei, An amperometric glucose biosensor based on a screen-printed electrode and Os-complex mediator for flow injection analysis, Measurement 44 (2011) 1878–1883.

[21] T.Ahuja Rajesh, D. Kumar, Recent progress in the development of nano-structured conducting polymers/nanocomposites for sensor applications, Sens. Actuators B 136 (2009) 275–286.

[22] Y.H. Yun, Z. Dong, V. Shanov, W.R. Heineman, H.B. Halsall, A. Bhattacharya, L. Conforti, R.K. Narayan, W.S. Ball, M.J. Schulz, Nanotube electrodes and biosensors, Nanotoday 2 (2007) 30–37.

[23] S. Laschi, E. Bulukin, I. Palchetti, C. Cristea, M. Mascini, Disposable electrodes modified with multi-wall carbon nanotubes for biosensor applications, ITBM-RBM 29 (2008) 202–207.

[24] B.C. Janegitz, R. Pauliukaite, M.E. Ghica, C.M.A. Brett, O. Fatibello-Filho, Direct electron transfer of glucose oxidase at glassy carbon electrode modified with functionalized carbon nanotubes within a dihexadecyl phosphate film, Sens. Actuators B 18 (2011) 411–417.

[25] M.S. Belluzo, M.É. Ribone, C.M. Lagier, Assembling amperometric biosensors for clinical diagnostics, Sensors 8 (2008) 1366–1399.

[26] X. Liu, X. Qu, H. Fan, S. Ai, R. Han, Electrochemical detection of DNA hybridization using a water-soluble branched polyethyleneimine–cobalt(III)–phenanthroline indicator and PNA probe on Au electrodes, Electrochim. Acta 55 (2010) 6491–6495.

[27] H. Hong, S. Lee, T. Kim, M. Chung, C. Choi, Surface modification of the polyethyleneimine layer on silicone oxide film via UV radiation, Appl. Surf. Sci. 255 (2009) 6103–6106.

[28] J.J. Sun, H.Z. Zhao, Q.Z. Yang, J. Song, A. Xue, A novel layer-by-layer self-assembled carbon nanotube-based anode: preparation, characterization, and application in microbial fuel cell, Electrochim. Acta 55 (2010) 3041–3047.

[29] M. Shen, S.H. Wang, X. Shi, X. Chen, Q. Huang, E.J. Petersen, R.A. Pinto, J.R. Baker Jr., W.J. Weber Jr., Polyethyleneimine-mediated functionalization of multiwalled carbon nanotubes: synthesis, characterization, and in vitro toxicity assay, J. Phys. Chem. C 113 (2009) 3150–3156.

[30] B. Zeng, S. Wei, F. Xiao, F. Zhao, Voltammetric behavior and determination of rutin at a single-walled carbon nanotubes modified gold electrode, Sens. Actuators B 115 (2006) 240–246.

[31] Y.H. Yun, A. Bange, W.R. Heineman, H.B. Halsall, V.N. Shanov, Z. Dong, S. Pixley, M. Behbehani, A. Jazieh, Y. Tu, D.K.Y. Wong, A. Bhattacharya, M.J. Schulz, A nanotube array immunosensor for direct electrochemical detection of antigen–antibody binding, Sens. Actuators B 123 (2007) 177–182.

[32] K.J. Huang, D.J. Niu, W.Z. Xie, W. Wang, A disposable electrochemical immunosensor for carcinoembryonic antigen based on nano-Au/multi-walled carbon nanotubes–chitosans nanocomposite film modified glassy carbon electrode, Anal. Chim. Acta 659 (2010) 102–108.

[33] E. Laviron, General expression of the linear potential sweep voltammogram in the case of diffusion less electrochemical systems, J. Electroanal. Chem. Interfacial Electrochem. 101 (1979) 19–28.

[34] P. Venge, N. Johnston, B. Lindahl, S. James, Normal plasma levels of cardiac troponin I measured by the high-sensitivity cardiac troponin I access prototype assay and the impact on the diagnosis of myocardial ischemia, J. Am. Coll. Cardiol. 54 (2009).

[35] C. Meune, S. Zuily, K. Wahbi, Y.E. Claessens, S. Weber, C.C. Gobeaux, Combination of copeptin and high-sensitivity cardiac troponin T assay in unstable angina and non-ST-segment elevation myocardial infarction: a pilot study, Arch. Cardiovasc. Dis. 104 (2011) 4–10.